12-13-2002

Modeling of Evaporation and Condensation Pressure-Drop in Micro-Fin Tubes

Meng-Onn Tan

MODELING OF EVAPORATION AND CONDENSATION PRESSURE-DROP IN MICRO-FIN TUBES

By

Meng-Onn Tan

A Thesis
Submitted to the Faculty of
Mississippi State University
in Partial Fulfillment of the Requirements
for the Degree of Master of Science
in Mechanical Engineering
in the Department of Mechanical Engineering

Mississippi State, Mississippi

December 2002

MODELING OF EVAPORATION AND CONDENSATION PRESSURE-DROP IN MICRO-FIN TUBES

By

Meng-Onn Tan

Approved:

Louay M. Chamra Associate Professor of Mechanical Engineering (Major Professor)	Rogelio Luck Associate Professor and Graduate Coordinator of Department of Mechanical Engineering
B. Keith Hodge Professor of Mechanical Engineering (Committee Member)	Carl A. James Assistant Research Professor of Mechanical Engineering (Committee Member)

A. Wayne Bennett
Dean of the College of Engineering

Name: Meng-Onn Tan

Date of Degree: Dec 13, 2002

Institution: Mississippi State University

Major Field: Mechanical Engineering

Major Professor: Dr. Louay M. Chamra

Title of Study: MODELING OF EVAPORATION AND CONDENSATION PRESSURE-DROP IN MICRO-FIN TUBES

Pages in Study: 108

Candidate for Degree of Master in Science

Three existing pressure-drop models are validated and analyzed with experimental data compiled from the research database. From the analysis, it was found that the pressure-drop prediction results from the models are not very accurate and not consistent with all experimental datasets. A new pressure-drop model was consequently created based on the findings from the study, and experimental data from the database were used to validate the model to produce more accurate and consistent predictions. The new pressure-drop model was tested on experimental datasets that were in the database and also with experimental datasets that were not in the database. Good and consistent results were achieved, and the new model proved capable of predicting pressure drops for different pure refrigerants and refrigerant mixtures flowing inside different configurations of micro-fin tubes for both condensation and evaporation.

ACKNOWLEGDEMENTS

I would like to express my gratitude towards the people who guided me in the writing of this thesis. Dr. Louay M. Chamra provided guidance and absolute support towards my entire masters program and my thesis preparation process. Sincere appreciation is also directed to my thesis committee members, Dr. B. Keith Hodge and Dr. Carl A. James, for their precious advice and assistance.

DEDICATION

I would like to dedicate this research to my parents, Eric Tan and Sandra Yeo, my sister, Meng-Fuan and my brother, Meng-Kheng, for their endless support and guidance.

TABLE OF CONTENTS

Page

APPENDIX

LIST OF TABLES

TABLE Page

LIST OF FIGURES

FIGURE Page

FIGURE Page

FIGURE Page

NOMENCLATURE

A	Cavallini et al. (1999) roughness factor constant / Friedel (1979) constant
A1, A2, A3	Friedel (1979) empirical constants
A_c	Cross-sectional flow area (m^2)
C_o	Flow distribution parameter
Coef	Number of Coefficients (empirical constants)
d	Tube diameter (m)
d_h	Hydraulic diameter (m)
e	Fin height (m)
e_r	Cavallini et al. (1999) roughness factor
E	Friedel (1979) parameter
f	Single-phase friction factor
f_N	Choi et al. (1999) friction factor
F_f	Friedel (1979) parameter
Fr	Froude number
g	Gravitational acceleration (m/s^2)
G	Total mass flux (kg/m^2-s)
H	Phase change number
i_{fg}	Specific enthalpy of vaporization (J/kg)

K_f	Bo Pierre's boiling number
L	Length of test section (m)
MAD	Mean Absolute Deviation (%)
n_f	Number of micro-fins
N	Total number of data points
p	Pressure (Pa)
PF	Pressure-drop penalty factor introduced by Christoffersen (1993)
Re	Reynolds number
S_p	Perimeter of one fin and channel taken perpendicular to axis of the fin (m)
SER	Standard error of regression function introduced by Montgomery and Peck (1992)
th	Tube wall thickness (m)
T	Temperature (^oC)
v	Specific volume (m^3/kg)
We	Weber number
x	Average vapor quality
X_{tt}	Martinelli parameter

Greek Symbols

β	Micro-fin apex angle (^{o}, degree)
ΔP	Pressure-drop (Pa)
Δx	Quality change over test section

ε	Void fraction
γ	Micro-fin helix angle (^{o}, degree)
μ	Dynamic viscosity (N-s/m^2)
ν	Kinematic viscosity (m^2/s)
Φ_{LO}^2	Friedel (1979) two-phase frictional multiplier
ϕ_{LO}^2	Souza and Pimenta (1995) two-phase frictional multiplier
ϕ	Inclination angle (^{o}, degree)
ρ	Density (kg/m^3)
σ	Surface tension (N/m)
Γ	Physical property index

Subscripts

a	Acceleration
acc	Acceleration
BP	Bo Pierre
exp	Experimental
f	Friction
g	Gravitational
GO	Vapor only flow
i	Inside / inlet
l	Liquid phase

LO	Liquid only flow
m	mean
o	Outside / outlet
sat	Saturation
tp	Two phase
tt	Turbulent-turbulent
v	Vapor phase

CHAPTER I

INTRODUCTION

The refrigeration and air conditioning industry is developing more compact machinery with higher energy efficiency in system operation, and subsequent heat transfer procedures require heat exchangers with enhanced surfaces to accommodate high heat fluxes. Micro-fin tubes are commonly used as enhanced surfaces in heat exchangers and represent a technology that has been able to beneficially enhance heat transfer in both single-phase and two-phase applications without causing drastic increases in pressure-drop.

Typical micro-fin tubes available for industrial applications are made of copper and have an outside diameter around 10 mm, 50-70 spiral fins with spiral angle, 10 to 35^{o}, fin height, from 0.075 to 0.4 mm, and triangular or trapezoidal cross-sections. Apex angles range between 30 to 60^{o}; however, only a few investigators report this parameter. Another type of enhanced tubing are internally finned tubes. These tubes have fewer than 30 fins and fin heights greater than 0.4 mm.

In general, two parameters are of primary interest in refrigerant heat transfer: pressure-drop and heat transfer. The goal of heat-transfer-enhancement research and development work is to maximize heat transfer while minimizing pressure-drop. Newell and Shah (2001) reported that increases in pressure-drop in micro-fin tubes are generally

less than 1.5 times the smooth-tube pressure-drop. There are some exceptions, however, in studies where taller fins are investigated. A general observation is that pressure-drop is affected by the fin height. Newell and Shah (2001) concluded that a fin would increase pressure-drop most significantly when the fin is large relative to the average liquid film thickness. When fins protrude through the liquid film layer, surface tension effects between the fins and the liquid phase may have important wetting characteristics. When fins are below the liquid phase surface, they are buried within the liquid phase where surface tension effects lose significance. In horizontal tubing, both conditions may exist with a relatively deep liquid layer at the tube bottom and a relatively thin liquid film layer at the top of the tube. Various factors affect the liquid film profile. Higher mass fluxes, lower vapor densities, and smaller tube diameters tend to make the film thickness more uniform around the tube circumference for both condensation and evaporation. A thinner liquid film will induce an increase in pressure-drop in horizontal micro-fin tubes. Newell and Shah (2001) also reported that fin heights of less than 0.2 mm have relatively small pressure-drop effects when compared with smooth tubes.

The helix angle also appears to be a significant factor in pressure drops in horizontal micro-fin tubes. Small helix angles have lower pressure drops than larger helix angles. As the helix angle is increased, micro-fins appear to begin acting as roughness structures that add additional momentum dissipation effects. Ito and Kimura (1979) reported that tubes with helix angles greater than 70^{o} were found to act as fully roughened pipes.

The main purpose of this research is to review available horizontal micro-fin tube pressure-drop correlations that are applicable to both pure refrigerant and refrigerant mixtures. A new pressure-drop model, capable of predicting pressure drops for both condensation and evaporation for different refrigerants, including pure refrigerants and refrigerant mixtures, will be developed for micro-fin tubes.

CHAPTER II

LITERATURE SURVEY

Most two-phase flow pressure-drop correlations are generally divided into empirical correlations and models based on actual flow-field configuration. Correlations for pressure drops using graphical methods are also available, but are cumbersome and less practical compared to equation-based methods. More progress has been made in the prediction of flow regimes in smooth tubes than prediction of flow regimes in micro-fin tubes as flow visualization studies for enhanced tubes are still not widely available. The ability of a micro-fin to delay or promote the transition to a particular flow regime adds an extra dimension to the complications of predicting flow regimes.

More empirical correlations than flow-field configuration models are available for two-phase pressure-drop predictions in enhanced tubes. At present, empirical correlations for enhanced tubes that rely on extensions to models developed for smooth tubes are available. For this review, three empirical pressure-drop correlations were chosen for analysis. Cavallini et al. (1999) and the Souza and Pimenta (1995) each presented two pressure-drop correlations based on the separated flow model. These two correlations will be discussed in this review. A pressure-drop correlation by Choi et al. (1999) that is based on the homogenous model will also be analyzed. All three correlations discussed

in this review are applicable to refrigerant pressure-drop in an evaporation or condensation environment.

The total pressure-drop for two-phase flow in tubes consists of frictional, acceleration and gravitational components. Two principal types of flow models are used in developing frictional pressure-drop: the homogenous model and the separated flow model [Tong (1967) and Wallis (1969)]. In the first, the flow of both liquid and vapor phases are assumed to be in equilibrium, and the liquid and vapor velocities are assumed equal. The frictional pressure-drop is computed as if the flow were a single-phase flow. In the separated flow model, the two phases are considered separate and the velocities may differ. Equation (2.1), which is obtained from the two-phase flow momentum equation, shows the total pressure-drop for two-phase flow in tubes.

$$\left(\frac{dp}{dz}\right)=\left(\frac{dp}{dz}\right)_f+\left(\frac{dp}{dz}\right)_g+\left(\frac{dp}{dz}\right)_a \tag{2.1}$$

The first term is the frictional pressure gradient, the second term is the gravitational pressure-drop gradient, and the third term is the acceleration pressure gradient. The expressions for all three terms are:

$$\Delta P_f = \Phi_{LO}{}^2 \cdot 2 \cdot f_{LO} \cdot \frac{G^2}{d_i \cdot \rho_l} \tag{2.2}$$

$$\Delta P_g = g \cdot \left(\varepsilon \cdot \rho_v + (1-\varepsilon) \cdot \rho_l\right) \cdot \sin(\phi) \tag{2.3}$$

$$\Delta P_a = G^2 \cdot \left[\frac{x^2}{\rho_v \cdot \varepsilon} + \frac{(1-x)^2}{[\rho_l \cdot (1-\varepsilon)]}\right] \tag{2.4}$$

Souza and Pimenta (1995) and Cavallini et al. (1999) concentrated their

analysis on the frictional pressure gradient as this represents the bulk of the total pressure-drop in the general pressure-drop correlation. In fully-developed flow, acceleration effects are minimal and the pressure-drop is predominantly due to friction. The separated flow model was used by both papers in the frictional pressure gradient development. Gravitational effects are due to gravitational forces acting on the liquid and vapor phases and are dependent on the inclination angle of the tube. In horizontal tubes, the inclination angle is zero. The gravitational pressure-drop component is, thus, relevant only for long vertical tubes and is negligible for horizontal tubes. The acceleration pressure-drop is primarily due to the difference in densities between the liquid and vapor phases. The vapor void fraction, ε, and average refrigerant quality are taken into account as well. The summation of the frictional, gravitational, and acceleration components gives the total pressure-drop over an axial length.

The computation of the frictional pressure gradient based on the separated flow model requires the calculation of the two-phase frictional multiplier, Φ_{LO}^2.

Cavallini et al. (1999) recommends the use of the Friedel (1979) correlation as the two-phase frictional multiplier for gas/liquid flow in smooth tubes. The Friedel (1979) correlation was obtained by the curve-fitting of an equation for Φ_{LO}^2 using a large database of two-phase pressure measurements in a smooth tube. The equation for Φ_{LO}^2 is shown below

$$\Phi_{LO} = \sqrt{E + \frac{3.24 \cdot Ff \cdot H}{Fr^{0.045} \cdot We^{0.035}}} \tag{2.5}$$

where

$$E = (1-x)^2 + x^2 \cdot \frac{(\rho_l \cdot f_{GO})}{(\rho_v \cdot f_{LO})} \tag{2.6}$$

$$Ff = x^{0.78} \cdot (1-x)^{0.224} \tag{2.7}$$

$$H = \left(\frac{\rho_l}{\rho_v}\right)^{0.91} \cdot \left(\frac{\mu_v}{\mu_l}\right)^{0.19} \cdot \left(1-\frac{\mu_v}{\mu_l}\right)^{0.7} \tag{2.8}$$

$$Fr = \frac{G^2}{g \cdot d_i \cdot \rho_m^2} \tag{2.9}$$

$$We = \frac{G^2 \cdot d_i}{\rho_m \cdot \sigma} \tag{2.10}$$

$$\rho_m = \frac{\rho_l \cdot \rho_v}{[x \cdot \rho_l + (1-x) \cdot \rho_v]} \tag{2.11}$$

f_{GO} and f_{LO} are the smooth tube single phase friction factors calculated from the Blausius equation and are presented in Equations (2.12) and (2.13). Different friction factor expressions are used for laminar flow or turbulent flow in the smooth tube.

$$f_{LO} = 0.079 \cdot \left(\frac{G \cdot d_i}{\mu_l}\right)^{-0.25} \qquad f_{GO} = 0.079 \cdot \left(\frac{G \cdot d_i}{\mu_v}\right)^{-0.25} \quad \text{Turbulent flow} \tag{2.12}$$

$$f_{LO} = \frac{16}{\left(\frac{G \cdot d_i}{\mu_l}\right)} \qquad f_{GO} = \frac{16}{\left(\frac{G \cdot d_i}{\mu_v}\right)} \quad \text{Laminar flow} \tag{2.13}$$

Turbulent flow is assumed for a Reynolds number above 2000, and laminar flow for Reynolds numbers below 2000. The liquid Reynolds number is calculated as ($G*d_i/\mu_l$), while the vapor Reynolds number is calculated as ($G*d_i/\mu_v$).

Cavallini et al. (1999) adapted the smooth tube Friedel (1979) correlation for use with micro-fin tubes by using an alternative way to calculate the single-phase friction factors, f_{LO} and f_{GO}, that accounts for single-phase pressure losses inside micro-fin tubes. Cavallini et al. (1999) referenced Ito and Kimura (1979) and noted that the single-phase friction factor for micro-fin tubes is equivalent to the value for smooth tubes at low Reynolds numbers. At high Reynolds numbers, the single-phase friction factor depends on the ratio of fin height to tube diameter and the fins spiral angle. Cavallini et al. (1999) suggested that the single-phase friction factor used in the micro-fin tubes frictional pressure-drop calculation should be taken as the higher value of that obtained from the Blausius equation for smooth tubes and that estimated from the Moody diagram under fully-developed turbulent flow (at high Reynolds numbers) and at the relative roughness e_r. The relative roughness is determined as follows:

$$e_r = \frac{A \cdot (e)}{(0.1 + \cos\gamma)} \tag{2.14}$$

where e is the micro-fin height and γ is the helix angle of the micro-fins.

Cavallini et al. (1999) suggested different values for the constant A for condensation pressure-drop and for evaporation pressure-drop. An A value of 0.18 is used for condensation, while 0.30 is used for evaporation.

The friction factor expressions that tend to fully-developed turbulent flow (at high Reynolds numbers) and uses the relative roughness e_r are:

$$(4 \cdot f_{LO})^{0.5} = 1.74 - 2 \cdot \log_{10}\left(2 \cdot \frac{e_r}{d_i}\right) \tag{2.15}$$

$$\left(4\cdot f_{GO}\right)^{0.5} = 1.74 - 2\cdot\log_{10}\left(2\cdot\frac{e_r}{d_i}\right) \tag{2.16}$$

The friction factors, f_{LO} and f_{GO}, used in the two-phase multiplier and frictional pressure-drop calculation for micro-fin tubes are then taken as the higher value between the calculated values in equation (2.12) and (2.13) and equations (2.15) and (2.16). The calculated Φ_{LO}^2 is then used as a two-phase multiplier for the frictional pressure gradient.

The acceleration pressure-drop component requires the calculation of the void fraction, ε. Cavallini et al. (1999) used the Rouhani (1969) model to evaluate the void fraction ε

$$\varepsilon = \frac{\left(x\cdot\rho_l\right)}{\left[\left(C_o\right)\cdot\left[x\cdot\rho_l + \left(1-x\right)\cdot\rho_v\right] + \frac{\left(\rho_l\cdot\rho_v\cdot\mu_G\right)}{G}\right]} \tag{2.17}$$

where

$$C_o = 1 + 0.2\cdot\left(1-x\right)\cdot\left[\frac{\left[g\cdot\left(d_i\cdot\rho_l\right)^2\right]}{G^2}\right]^{\frac{1}{4}} \qquad for \quad \varepsilon > 0.1$$

$$C_o = 0 \qquad for \quad \varepsilon \to 0 \tag{2.18}$$

and

$$\mu_G = 1.18\cdot\left(1-x\right)\cdot\left[\sigma\cdot g\cdot\frac{\left(\rho_l-\rho_v\right)}{\rho_l^{\,2}}\right]^{\frac{1}{4}} \tag{2.19}$$

Cavallini et al. (1999) also recommend the usage of the void fraction, ε, by Rouhani (1969) for the calculation of gravitational pressure gradient in vertical tubes.

Cavallini et al. (1999) compared their model against experimental data that consisted of condensation and evaporation of pure refrigerants, R12, R22, R32, and R502, and refrigerant mixtures, R407A, R407C, R404A, and R410A. The accuracy for condensation was found to be 24.3% and for evaporation the accuracy was 22.6%.

Souza and Pimenta (1995) developed a two-phase multiplier, ϕ_{LO}^2, based on the Lockhart-Martinelli parameter, X_{tt}, and the property index, Γ. Souza and Pimenta (1995) carried out a regression analysis on 160 experimental data points for R-134a, R-22, R-12, MP-39, and R32/125 in the development of the two-phase multiplier ϕ_{LO}^2 that is applicable to smooth tubes.

The correlation for the smooth tube two-phase multiplier ϕ_{LO}^2 proposed by Souza and Pimenta (1995) is

$$\phi_{LO}^{\ 2} = 1 + \left(\Gamma^2 - 1\right) x^{1.75} \left(1 + 0.9524 \cdot \Gamma \cdot X_{tt}^{\ 0.4126}\right) \tag{2.20}$$

The parameter X_{tt} was developed by Lockhart-Martinelli (1949) and Martinelli-Nelson (1949) by assuming turbulent flows for both liquid and vapor phases. The parameter, X_{tt}, and the property index, Γ, are shown below.

$$X_{tt} = \left(\frac{1-x}{x}\right)^{0.875} \left(\frac{\rho_v}{\rho_l}\right)^{0.5} \left(\frac{\mu_l}{\mu_v}\right)^{0.125} \tag{2.21}$$

$$\Gamma = \left(\frac{\rho_l}{\rho_v}\right)^{0.5} \left(\frac{\mu_v}{\mu_l}\right)^{0.125} \tag{2.22}$$

The two-phase multiplier, ϕ_{LO}^2, is multiplied with the single-phase frictional pressure-drop gradient to obtain the two-phase frictional pressure-drop gradient, similar to equation (2.2). f_{LO} is a single-phase friction factor calculated from the Blausius equation.

$$\Delta P_f = \phi_{LO}^{\ 2} \cdot 2 \cdot f_{LO} \cdot \frac{G^2}{d_i \cdot \rho_l} \tag{2.23}$$

Souza and Pimenta (1995) compare the predictions obtained from their correlation with smooth tube evaporation experimental data for refrigerants R134a, R12, R22, MP-39, and R32/125. The mean absolute deviation was found to be within ± 20%.

Newell and Shah (2001) suggested the usage of the pressure-drop penalty factor *PF*, described by Christoffersen et al. (1993), as a multiplier to the Souza and Pimenta (1995) smooth-tube frictional pressure-drop correlation. The penalty factor, *PF*, is the ratio of the enhanced tube pressure-drop to that of a smooth tube with the same root diameter d_i and is a function of refrigerant properties without significant dependence on mass flux or quality. The ratio of refrigerant vapor density to liquid density is used to determine the value of the penalty factor, *PF*. In their studies, Christoffersen et al (1993) used a micro-fin tube with 18^o helix angle and a fin height of 0.19 mm. The penalty factor can be determined from equation (2.24).

$$\begin{aligned} PF &= 1.55 && when && \left(\rho_v / \rho_l\right) < 0.01 \\ PF &= 1.71 - 17.5 \cdot \left(\rho_v / \rho_l\right) && when && 0.01 \le \left(\rho_v / \rho_l\right) \le 0.03 \\ PF &= 1.19 && when && \left(\rho_v / \rho_l\right) > 0.03 \end{aligned} \tag{2.24}$$

The penalty factor *PF* is inserted into the frictional pressure-drop gradient as follows:

$$\Delta P_f = \phi_{LO}{}^2 \cdot 2 \cdot f_{LO} \cdot \frac{G^2}{d_i \cdot \rho_l} \cdot PF \tag{2.25}$$

Souza and Pimenta (1995) used the void fraction, ε, in the calculation of acceleration pressure-drop. Souza and Pimenta (1995) recommended the Zivi (1964) equation, which was developed using the concept of minimum entropy production, for the calculation of void fraction. The Zivi (1964) equation shown in equation (2.26).

$$\varepsilon = \frac{1}{1 + \left[1 - x \middle/ x\right] \left\langle \rho_v \middle/ \rho_l \right\rangle^{0.67}} \tag{2.26}$$

The void fraction, ε, is used in a momentum equation developed by Souza et al. (1993) to compute the acceleration pressure-drop component. The acceleration pressure-drop equation by Souza et al. (1993) is

$$\Delta P_a = G^2 \left[\left| \left(\frac{x_o^2}{\rho_v \varepsilon_o} \right) + \frac{\left[1 - x_o\right]^2}{\rho_l \left[1 - \varepsilon_o\right]} \right| - \left| \frac{x_i^2}{\rho_v \varepsilon_i} + \frac{\left[1 - x_i\right]^2}{\rho_l \left[1 - \varepsilon_i\right]} \right| \right] \tag{2.27}$$

Souza and Pimenta (1995) did not discuss the gravitational pressure-drop component as their research focused only on horizontal two-phase flows. Gravitational pressure-drop is relevant only for long vertical tubes and is negligible for horizontal tubes.

Choi et al. (1999) used the Pierre (1964) correlation as the basis of their correlation. The Pierre correlation (1964) assumed a homogenous model where the flow

of both liquid and vapor phases are in equilibrium, and the liquid and vapor velocities are equal. The Pierre correlation (1964) was developed for the prediction of evaporation pressure-drop for R12 in 12-mm and 18-mm, horizontal, smooth tubes. The correlation is presented in equation (2.28).

$$\Delta P_{BP} = \left[f_{BP} + \frac{(x_o - x_i)d_i}{x \cdot L} \right] \frac{G^2 \cdot x \cdot \nu_v \cdot L}{d_i} \tag{2.28}$$

The two-phase friction factor for pure refrigerants, f_{BP}, and Pierre's boiling number K_f are as follows:

$$f_{BP} = 0.0185 \left(\frac{K_f}{\mathrm{Re}} \right)^{0.25} \tag{2.29}$$

$$K_f = \frac{\Delta x \cdot i_{fg}}{L \cdot g} \tag{2.30}$$

Choi et al. (1999) modified Pierre's two-phase friction factor, f_{BP}, to accommodate two-phase pressure-drop data from NIST. The inside diameter, d_i, was also changed to the hydraulic diameter, d_h, to account for micro-fins. The Choi et al. (1999) correlation is shown as equation (2.31).

$$\Delta P_{tp} = \Delta P_{friction} + \Delta P_{acceleration} = \left[\frac{\left[f_N \cdot L \cdot (\nu_o + \nu_i) \right]}{d_h} + (\nu_o + \nu_i) \right] \cdot G^2 \tag{2.31}$$

The friction factor, f_N, is calculated in terms of the liquid Reynolds number, Re_{fo}, and the two-phase number, K_f. The friction factor, f_N, was correlated with NIST two-phase, micro-fin pressure-drop data. Kedzierski and Goncalves (1999) recommended the use of the hydraulic diameter in place of the inside tube diameter for micro-fin tubes.

Equations (2.32), (2.33), and (2.34) present the friction factor equation, the liquid Reynolds number, Re_{fo}, equation, and the hydraulic diameter equation, respectively.

$$f_N = 0.00506 \cdot \mathrm{Re}_{FO}^{-0.0951} \cdot K_f^{0.1554} \tag{2.32}$$

$$\mathrm{Re}_{FO} = \frac{G \cdot d_h}{\upsilon_l} \tag{2.33}$$

$$d_h = \frac{4 \cdot A_c \cdot \cos(\gamma)}{N \cdot S_p} \tag{2.34}$$

Choi et al. (1999) recommended the use of the model for both smooth tubes and micro-fin tubes for both condensation pressure-drop and evaporation pressure-drop. In smooth-tube predictions, the inside diameter, d_i, will be used instead of the hydraulic diameter, d_h.

Choi et al. compared the predictions obtained by the model with NIST experimental pressure-drop data for condensation in refrigerants R32, R125, R134a, R410A and for evaporation in refrigerants R32, R125, R134a, R410A, R22, R407c, R32/134a. The NIST experimental data are predicted within an accuracy of 10.8%.

CHAPTER III

MODEL VALIDATION

Three correlations for micro-fin tubes discussed in the previous chapter are further evaluated in this chapter. The three correlations are the Cavallini et al. (1999) model, the Souza and Pimenta (1995) model, and the Choi et al. (1999) model. These three models are validated using available experimental datasets.

Experimental Database

A database is established using the available experimental data for pure refrigerants and refrigerant mixtures flowing inside micro-fin tubes. These experimental data are used in the validation process of the pressure-drop models. Tables 3.1 and 3.3 show the flow conditions of the experimental data for pure refrigerants and refrigerant mixtures in evaporation and condensation environment. The properties shown are the saturation temperature and pressure, T_{sat} and P_{sat}, the range of mass fluxes, G, and the mean vapor quality, x. Table 3.2 and 3.4 present the tube geometries: the outside tube diameter, d_o, the tube wall thickness, th, the fin height, e, the number of micro-fins, n_f, the micro-fin helix angle, γ, and the length of the test section, L.

Table 3.1. Flow conditions for pure refrigerants and refrigerant mixtures flowing inside micro-fin tubes in an evaporation environment.

Reference	Runs	Fluid	P_{sat} (kPa)	T_{sat} (^{o}C)	G (kg/m^2-s)	x (mean)
Bogart and Thors (1999)	18 50 15	R134a R22 R407c		4.44	25 – 275	0.10 – 0.95
Ebisu and Torikoshi (1998)	7	R407c	545.57		150 – 300	0.6
Eckels and Pate (1991)	16 21	R12 R134a		5, 10, 15	130 – 420	0.09 – 0.84
Eckels et al. (1998a)	11	R134a	330	1	100 – 370	0.10 – 0.83
Eckels et al. (1998b)	7	R134a	350	2	80 – 260	0.10 – 0.83
Hitachi Cable Ltd (1987)	9	R22		8	130 – 300	0.6
Kuo and Wang (1995)	14	R22		6	100, 200, 300	0.04 – 0.96
Kuo and Wang (1996)	14 19	R22 R407c	600	6	100, 200, 300	0.16 – 0.74
Morita et al. (1993)	32	R22		2.5	90 – 410	0.5
Muzzio et al. (1998)	23	R22		5	90 – 400	0.3
Niddeggar et al. (1997)	8	R134a	340		100, 200, 300	0.23 – 0.91
Schlager (1988)	25	R22	1.62 0.925	525.4 514.2	100 – 400	0.18 – 0.82
Schlager et al. (1989)	15	R22	500 – 600	0 – 6	180 – 420	0.15 – 0.85
Yasuda et al. (1990)	8	R22		0.6	150 – 300	0.60
Zurcher (1998)	40	R407c	645		200, 300	0.09 – 0.9

Table 3.2. Tube geometries for micro-fin tubes used in an evaporation environment.

Reference	Tube Material	d_o (mm)	th (mm)	e (mm)	n_f	γ (^{o})	L (m)
Bogart and Thors (1999)	Copper	15.88	0.51	0.3	75	23	4.88 3.66
Ebisu and Torikoshi (1998)	Copper	7	0.25	0.18 0.22	60 50	18 16	0.54
Eckels and Pate (1991)	Copper	9.52	0.40	0.2	60	17	3.67
Eckels et al. (1998a)	Copper	9.52	0.3	0.2	60	17	3.66
Eckels et al. (1998b)	Copper	12.7	0.4	0.2	60	17	3.66
Hitachi Cable Ltd (1987)	Copper	9.5 9.52 9.52	0.5 0.48 0.49	0.208 0.2 0.209	60	17 18 17	3
Kuo and Wang (1995)	Copper	7	0.25	0.15	60	18	1.2
Kuo and Wang (1996)	Copper	9.52	0.3	0.20	60	18	1.3
Morita et al. (1993)	Copper	4 – 9.52	0.3	0.1 – 0.2	34 – 60	0 – 18	0.018 – 0.0419
Muzzio et al. (1998)	Copper	9.52	0.3 0.3 0.34	0.23 0.20 0.15	54 60 65	18 18 25	2.6
Niddeggar et al. (1997	Copper	12.7	0.4	0.25	70	18	3
Schlager (1988)	Copper	9.52	0.4 0.505	0.20 0.38	60 21	18 30	3.67
Schlager et al. (1989)	Copper	9.52	0.3	0.20 0.16 0.15	60	18 15 25	3.67
Yasuda et al. (1990)	Copper	9.52	0.39	0.20 0.25	60	18 30	3.05
Zurcher (1998)	Copper	12.7	0.4	0.25	70	18	3.27

Table 3.3. Flow conditions for pure refrigerants and refrigerant mixtures flowing inside micro-fin tubes in a condensation environment.

Reference	Runs	Fluid	P_{sat} (kPa)	T_{sat} (^{o}C)	G (kg/m^2-s)	x (mean)
Ebisu and Torikoshi (1998)	8	R407c	1974		150 – 400	0.6
Eckels and Pate (1991)	19 16	R12 R134a		30, 40, 50	130 – 410	0.09 – 0.84
Eckels et al. (1994)	12	R134a	1010	40	130 – 370	0.07 – 0.84
Eckels et al. (1998a)	8	R134a	1010	40	130 – 370	0.07 – 0.84
Eckels et al. (1998b)	4	R134a	1000	40	80 – 300	0.07 – 0.84
Eckels et al. (1999)	19 13 11 11	R134a R22 R407c R410A		40	125 – 600	0.5
Morita et al. (1993)	33	R22		50	90 – 410	0.5
Muzzio et al. (1995)	16	R22		35	80 – 410	0.5
Muzzio et al. (1998)	24	R22		35	90 – 400	0.5
Choi et al. (1999)	60 43 31	R134a R32 R410A		42 – 46 30 – 39 27 – 32	100 – 500 80 – 340 100 – 500	0.3 – 0.9
Schlager (1988)	27	R22	1543, 1561	40.2, 40.7	120 – 410	0.09 – 0.85
Schlager et al. (1989)	11	R22	1550	40	180 – 530	0.15 – 0.85

Table 3.4. Tube geometries for micro-fin tubes used in a condensation environment.

Reference	Tube Material	d_o (mm)	th (mm)	e (mm)	n_f	γ (^{o})	L (m)
Ebisu and Torikoshi (1998)	Copper	7	0.25	0.18 0.22	60 50	18 16	0.54
Eckels and Pate (1991)	Copper	9.52	0.40	0.2	60	17	3.67
Eckels et al. (1994)	Copper	9.52	0.30	0.2	60	17	3.66
Eckels et al. (1998a)	Copper	9.52	0.30	0.2	60	17	3.66
Eckels et al. (1998a)	Copper	12.7	0.40	0.2	60	17	3.66
Eckels et al. (1999)	Copper	9.53 15.88 7.94	0.305 0.635 0.3	0.203 0.305 0.203	60 60 50	18 27 18	3.78 3.81 3.78
Morita et al. (1993)	Copper	4 – 9.52	0.3	0.1 – 0.2	34 – 60	0 – 18	0.018 – 0.0419
Muzzio et al. (1995)	Copper	9.52	0.3 0.3 0.34	0.23 0.20 0.15	54 60 65	18 18 25	2.6
Muzzio et al. (1998)	Copper	9.52	0.3 0.3 0.34	0.23 0.20 0.15	54 60 65	18 18 25	2.6
Choi et al. (1999)	Copper	9.52	0.3	0.2	60	18	1.587
Schlager (1988)	Copper	9.52	0.4 0.505	0.20 0.38	60 21	18 30	3.67
Schlager et al. (1989)	Copper	9.52	0.3	0.20 0.16 0.15	60	18 15 25	3.67

Most of the experimental datasets have pressure-drop values for varying mass fluxes with vapor quality held constant. Kuo and Wang (1995,1996), Niddeggar et al.(1997), and Zurcher (1998) report pressure-drop measurements for varying vapor qualities at constant mass fluxes of 100 kg/m^{2}s, 200 kg/m^{2}s, and 300 kg/m^{2}s. The

pressure-drop values are averaged over the length of the test section.

A data extraction software, DigXY Version 1.0, was used to extract experimental data from graphs collected from published papers. Graphs were scanned into a windows bitmap format before being transferred into DigXY for the data extraction process. The extracted data points were then saved into a text file and added to an experimental database that was created for this project.

REFPROP 6.01 computer software was used to obtain the thermodynamic and transport properties for pure refrigerants and refrigerant mixtures.

The mean absolute deviation, MAD, is used to determine the effectiveness of the pressure-drop models. The MAD is obtained by calculating the normalized percentage difference between the experimental pressure-drop values and the predictive pressure-drop values. A pressure-drop model is deemed acceptable if the achieved MAD has a value of less than 30%.

$$MAD = \frac{1}{N} \cdot \sum \frac{\left| \Delta P_{experiment} - \Delta P_{predicted} \right|}{\Delta P_{experiment}} \tag{3.1}$$

MathCAD 2001 computer software was used to perform all the mathematical calculations in this research. To compare pressure-drop models against the available experimental data, four different MathCAD files (model, data, property, and calculation) were generated. The model file contain the equations and parameters used for a particular pressure-drop model. The data file is where flow conditions, thermodynamic properties, transport properties and tube geometries are input. The property file is programmed with

an interpolation function (cubic spline function) to obtain the required refrigerant properties from the property tables (text files) generated from REFPROP 6.01. The accuracy of the interpolated property values is four decimal places. All three files are combined in a calculation file and the results are computed. A sample of all four MathCAD files is shown in the Appendix.

Cavallini et al. (1999) Pressure-Drop Model

Cavallini et al. (1999) used the separated flow model as the basis for their pressure-drop correlation. The smooth-tube Friedel (1979) correlation was used to obtain the frictional pressure gradient. Prediction of two-phase flow pressure-drops in micro-fin tubes were achieved by the modification of the calculation of single-phase friction factors, f_{GO} and f_{LO}, to include equivalent roughness factors for the micro-fin structures. The roughness-factor equation, shown in equation (2.14), has a constant *A*. Cavallini et al. (1999) recommended two different values for constant *A*: 0.18 in condensation and 0.30 in evaporation.

The Cavallini et al. (1999) model was validated with experimental datasets comprising pure refrigerants and refrigerant mixtures in both condensation and evaporation environments. The constant value of 0.18 was applied in the roughness-factor equation in the validation process for condensation. For every condensation dataset, both smooth-tube single-phase friction factors and micro-fin friction factors were computed, with the higher value chosen as the single-phase friction-factor multiplier for the frictional pressure gradient. The Cavallini et al. (1999) model was validated with 13

pure refrigerants experimental datasets. The datasets include refrigerants R12, R134a, R22 and R32.

Figure 3.1 shows the prediction results of the Cavallini et al. model (1999) on the condensation R12 experimental dataset by Eckels et al. (1991). Circular symbols are used to represent the experimental data points, and the diagonal solid line shows a perfect prediction by the pressure-drop model. The dashed lines present the ±30% mean absolute deviation lines. The model achieved a mean absolute deviation of around 20% for the R12 experimental dataset. Overall prediction was good, although some under-prediction occurred at mass fluxes of above 300 kg/m^{2}s.

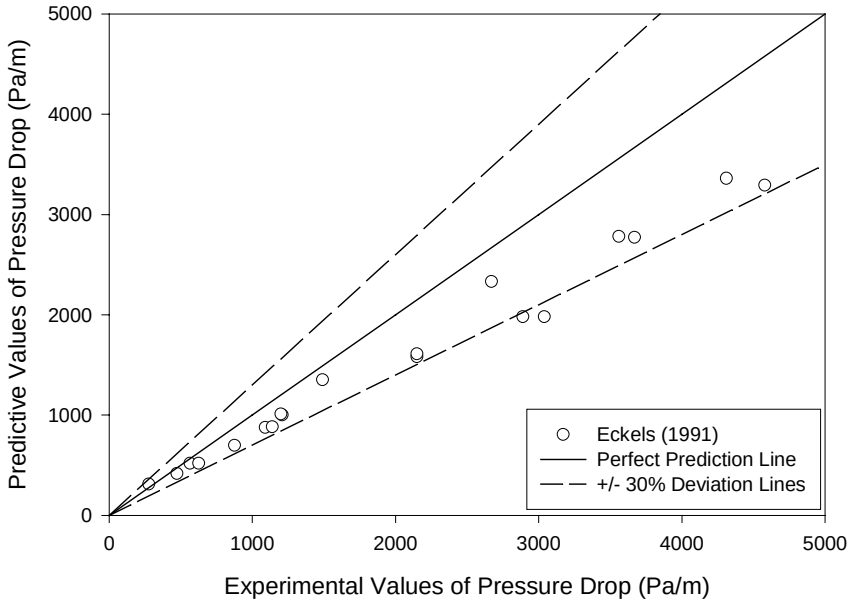

Figure 3.1. Cavallini et al. (1999) model for a condensation R12 experimental dataset

The Cavallini et al. (1999) model was then tested on evaporation R134a datasets. The mean absolute deviation achieved by the model was more than 30%. A major contributor to the high deviation was the experimental dataset from Choi et al. (1999). A deviation of more than 50% was consistently demonstrated by the prediction of the Cavallini et al. (1999) model for this dataset. Large deviations were observed at mass fluxes of 200 kg/m^{2}s and higher. The five datasets from Eckels (1991, 1994, 1998a, 1998b, 1999) provided a better match with the model as the mean absolute deviations achieved are around 30% or less. Figure 3.2 shows the comparison between the model and the R134a experimental datasets.

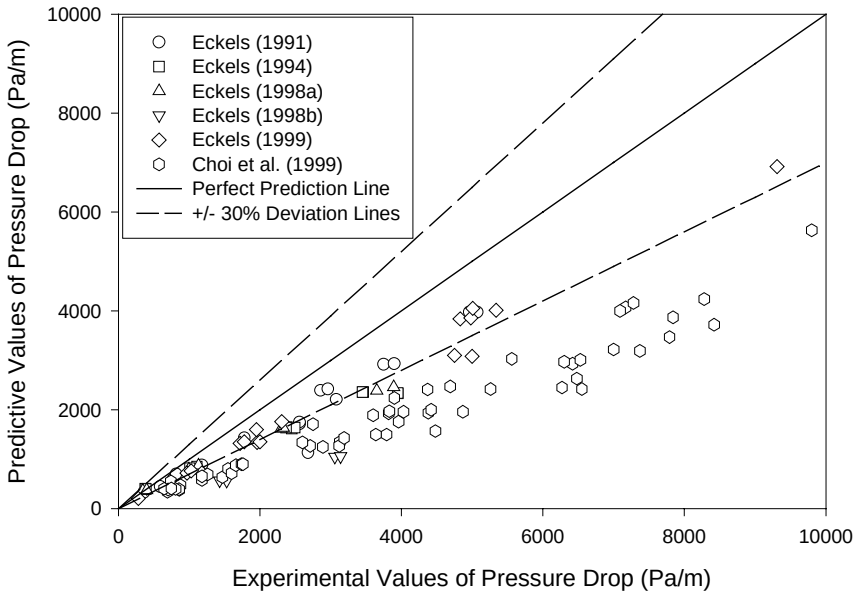

Figure 3.2. Cavallini et al. (1999) model for condensation R134a experimental datasets

Five R22 condensation datasets were tested with the Cavallini et al. (1999) model. Deviations from the experimental data were observed to be around 30%. Predictions from the model with the Schlager (1988, 1989) datasets are around 20% but higher deviations were observed with the other datasets. At lower mass fluxes of 200 kg/m^{2}s and less, a closer fit between the experimental data and the predictions from the model can be seen. Figure 3.3 shows the comparison between the model and the R22 experimental datasets.

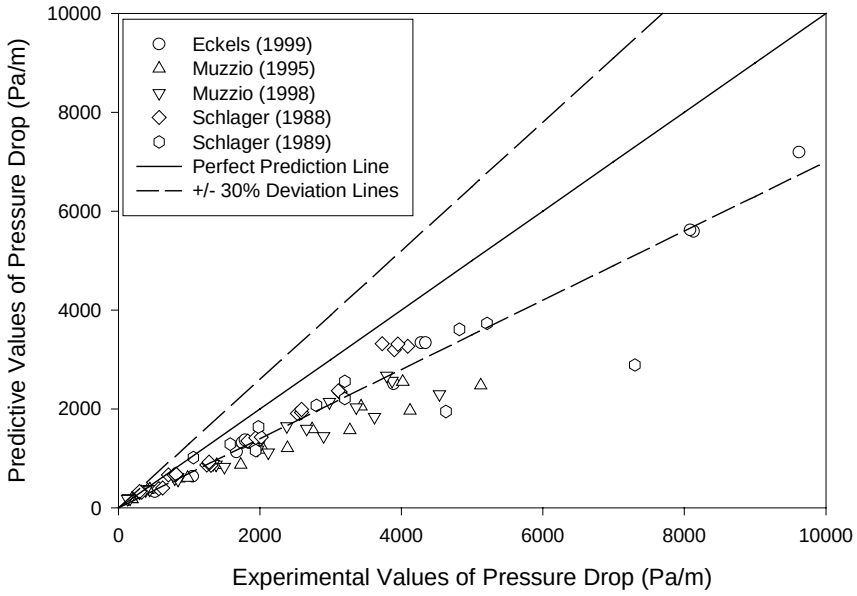

Figure 3.3. Cavallini et al. (1999) model for condensation R22 experimental datasets

A condensation dataset by Choi et al. (1999) for refrigerant R32 was used with the Cavallini et al. (1999) model. A high deviation of 50% was obtained with the model, and Figure 3.4 presents the results. The Cavallini et al. (1999) model was next tested on refrigerant mixtures consisting of two refrigerant R407c condensation datasets and two

refrigerant R410A condensation datasets. A mean absolute deviation of around 40% was obtained for all four datasets. Figure 3.5 and 3.6 show the results for refrigerants R407c and R401A, respectively.

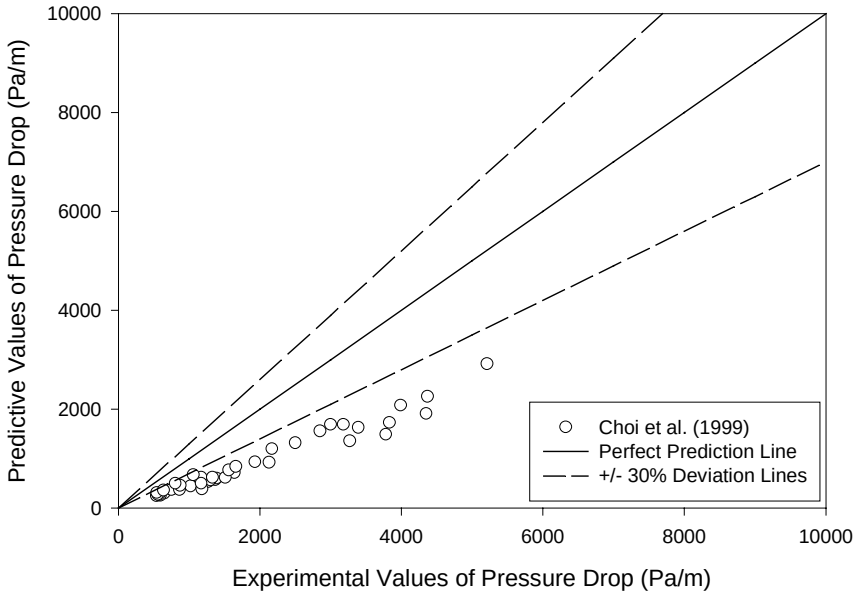

Figure 3.4. Cavallini et al. (1999) model for a condensation R32 experimental dataset

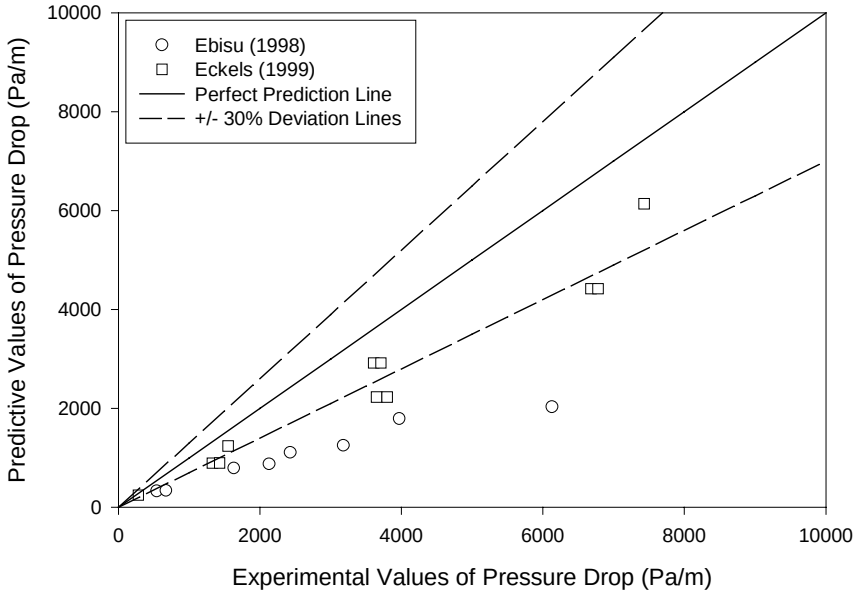

Figure 3.5. Cavallini et al. (1999) model for condensation R407c experimental datasets

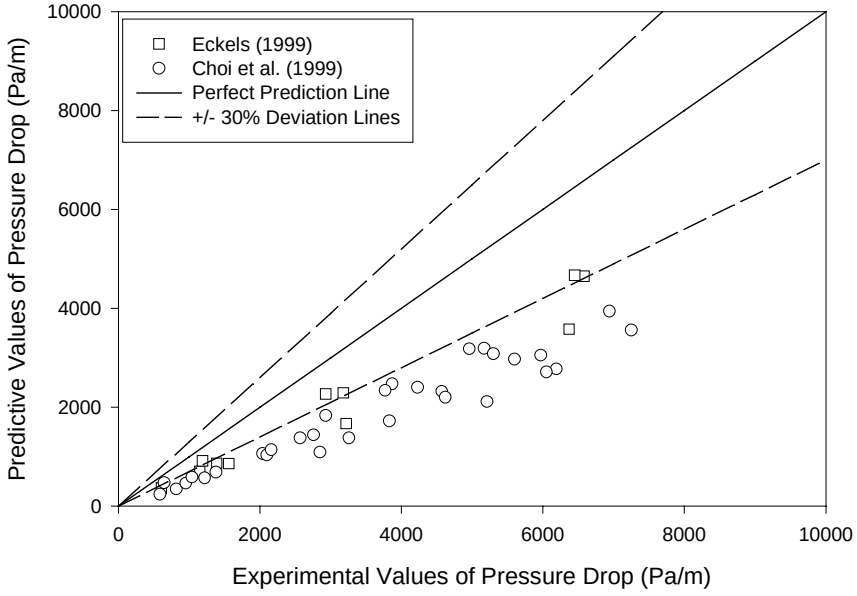

Figure 3.6. Cavallini et al. (1999) model for condensation R410A experimental datasets

Figure 3.7 presents all the predictions by the Cavallini et al. (1999) pressure-drop model on the condensation datasets. All total of 361 experimental data points were amassed. Predictions were inconsistent and an under-prediction trend can be observed from the graphs.

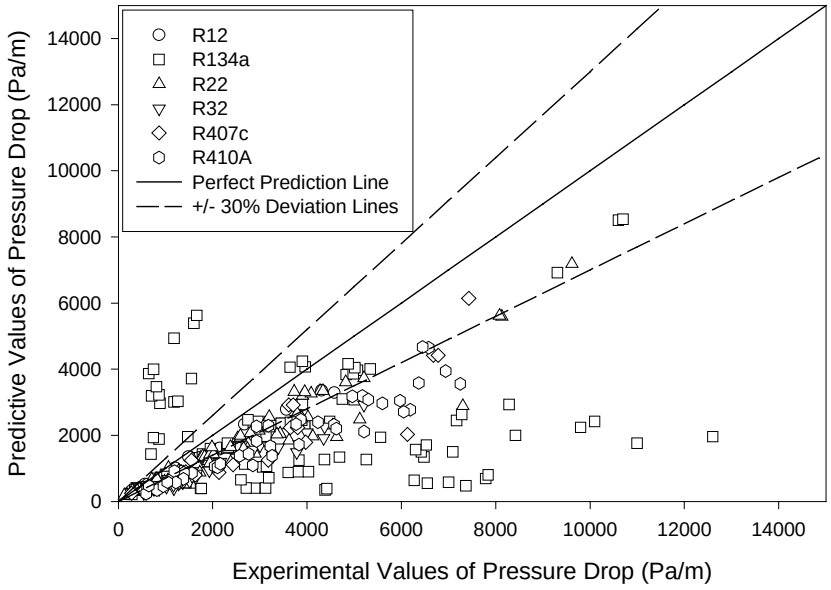

Figure 3.7. Cavallini et al. (1999) model for all condensation experimental datasets

The prediction method on evaporation datasets was similar to the Cavallini et al. (1999) model. However a different constant was used for the roughness-factor equation. A value of 0.30 was used for the constant *A*. Both smooth-tube single-phase friction factors and micro-fin friction factors were calculated, and the higher value was used in the calculation of the frictional pressure gradient. 13 evaporation datasets were tested with the model. Figures 3.8 and 3.9 show the prediction results for refrigerants R12 and

R134a, respectively. A mean absolute deviation of around 30% was achieved for both refrigerants.

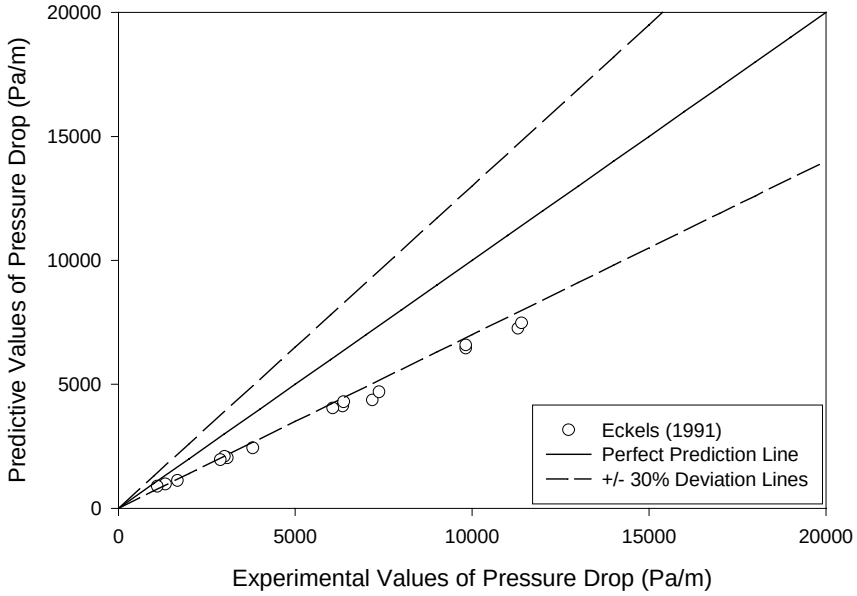

Figure 3.8. Cavallini et al. (1999) model for an evaporation R12 experimental dataset

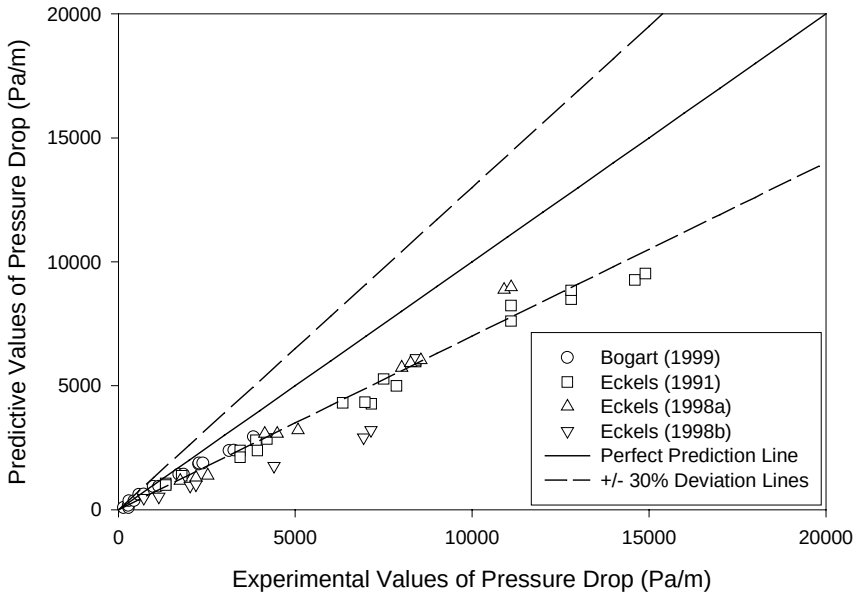

Figure 3.9. Cavallini et al. (1999) model for evaporation R134a experimental datasets

Refrigerant R22 produced a better fit with the model, particularly with the datasets from Schlager (1988), Schlager et al. (1989) and Muzzio et al. (1998). Comparisons with these datasets demonstrate deviations of around 20%. Overall the model deviates around 30% with most of the refrigerant R22 experimental datasets. Predictions for refrigerant mixtures have mixed results. The Bogart et al. (1999) dataset has deviations over 60% while predictions for the Ebisu et al. (1998) dataset has deviation of less than 30%. Figures 3.10 and 3.11 show the results for refrigerant R22 and R407c, respectively.

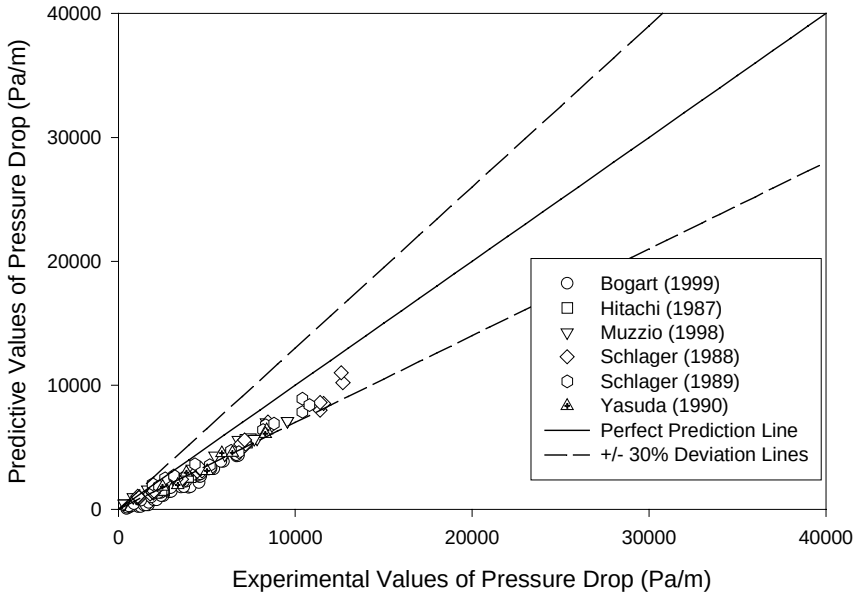

Figure 3.10. Cavallini et al. (1999) model for evaporation R22 experimental datasets

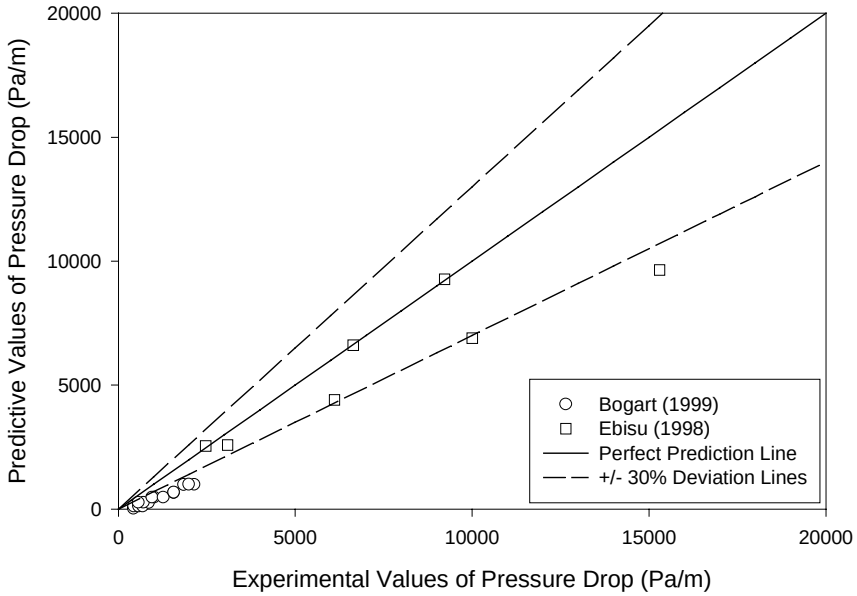

Figure 3.11. Cavallini et al. (1999) model for evaporation R407c experimental datasets

A total of 257 points were used for the prediction of evaporation pressure-drop. As illustrated in Figure 3.12, a slight under-prediction of the experimental values is observed. This follows a similar trend in the prediction of condensation pressure-drop. Pressure drops in micro-fin tubes generally increase by 20% or more (Newell, 2001) when compared with pressure drops in conventional smooth tubes. The Friedel (1979) correlation was originally developed for two-phase flow pressure drops in smooth tubes, and Cavallini et al. (1999) accounted for micro-fins by applying a roughness-factor equation. The roughness-factor equation calculates the micro-fin equivalent roughness height as approximately 16 to 19% of the actual fin height for helix angles ranging from 0 to 30^{o}. For fin heights greater than 0.25 mm and helix angles larger than 30^{o}, the model

may produce predictions that do not adequately account for the higher pressure drops in micro-fin tubes. Tables 3.5 and 3.6 present the mean absolute deviations achieved by the model on each condensation and evaporation dataset.

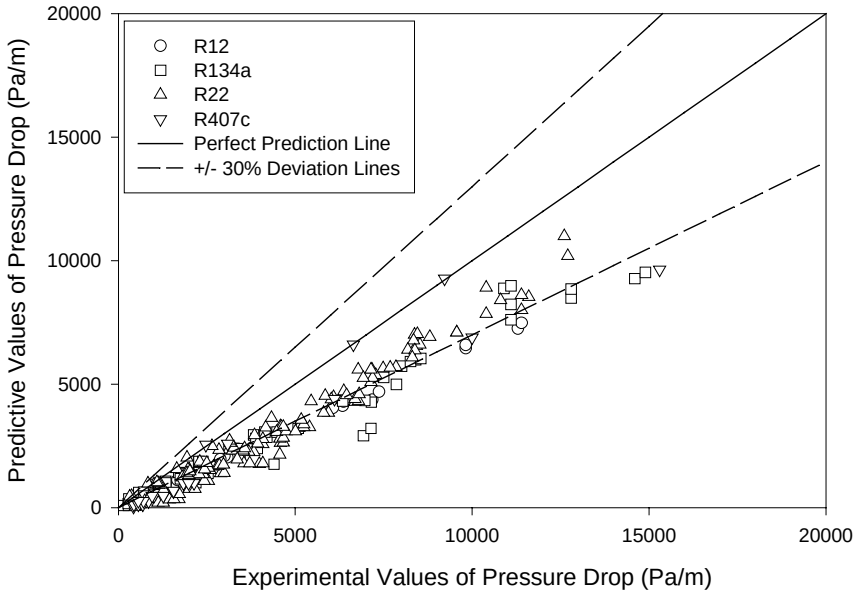

Figure 3.12. Cavallini et al. (1999) model for all evaporation experimental datasets

Table 3.5. Mean absolute deviations achieved by the Cavallini et al. (1999) model for condensation datasets.

Reference	Refrigerant	MAD (%)
Eckels and Pate (1991)	R12	19.16
Eckels and Pate (1991)	R134a	24.28
Eckels et al. (1994)	R134a	27.21
Eckels et al. (1998a)	R134a	23.07
Eckels et al. (1998b)	R134a	63.85
Eckels et al. (1999)	R134a	26.96
Choi et al. (1999)	R134a	51.23
Eckels et al. (1999)	R22	29.61
Muzzio et al. (1995)	R22	35.01
Muzzio et al. (1998)	R22	33.34
Schlager (1988)	R22	21.52
Schlager et al. (1989)	R22	31.79
Choi et al. (1999)	R32	45.82
Ebisu and Torikoshi (1998)	R407c	54.51
Eckels et al. (1999)	R407c	26.30
Eckels et al. (1999)	R410A	36.91
Choi et al. (1999)	R410A	48.81

Table 3.6. Mean absolute deviations achieved by the Cavallini et al. (1999) model for evaporation datasets

Reference	Refrigerant	MAD (%)
Eckels and Pate (1991)	R12	33.31
Bogart and Thors (1999)	R134a	24.22
Eckels and Pate (1991)	R134a	31.67
Eckels et al. (1998a)	R134a	30.66
Eckels et al. (1998b)	R134a	52.70
Bogart and Thors (1999)	R22	50.24
Hitachi Cable Ltd (1987)	R22	32.20
Muzzio et al. (1998)	R22	21.92
Schlager (1988)	R22	24.46

Schlager et al. (1989)	R22	18.63
Yasuda et al. (1990)	R22	29.24
Bogart and Thors (1999)	R407c	62.78
Ebisu and Torikoshi (1998)	R407c	14.60

Souza and Pimenta (1995) Pressure-Drop Model

Souza and Pimenta (1995) used the Lockhart-Martinelli (1949) parameter, X_{tt}, which is based on the separated-flow model, to develop their frictional pressure-drop correlation. The Lockhart-Martinelli (1949) parameter is the ratio between the frictional pressure gradient with liquid flowing alone in the pipe and the frictional pressure gradient with vapor flowing alone in the pipe. The frictional pressure gradient due to the single-phase flow of the liquid or vapor depends on the flow regime, laminar or turbulent, for each phase. For the parameter, X_{tt}, turbulent flow is assumed for both phases. Since Souza and Pimenta (1995) developed their pressure-drop correlation for flows in smooth tubes, Newell et al. (2001) suggested the usage of a pressure-drop penalty factor to account for the presence of micro-fins. Christoffersen et al. (1993) introduced a parameter, *PF*, as the pressure-drop penalty factor. The parameter *PF* is calculated as a function of the refrigerant properties and does not have a significant dependence on mass flux or quality. The tube used in the development of the PF parameter had an 18^o helix with a fin height of 0.19 mm.

The *PF* parameter was implemented into the Souza and Pimenta (1995) smooth-tube pressure-drop model. The model was first validated with condensation datasets. Figures 3.13 and 3.14 show the model's prediction results for refrigerants R12 and

R134a. The datasets were predicted within 20% and 25%, respectively. The pressure-drop model with the PF parameter also showed good predictions for refrigerants R22 and R32. The mean absolute deviations achieved were about 25% and 20% for refrigerants R22 and R32. Figures 3.15 and 3.16 presents the prediction results.

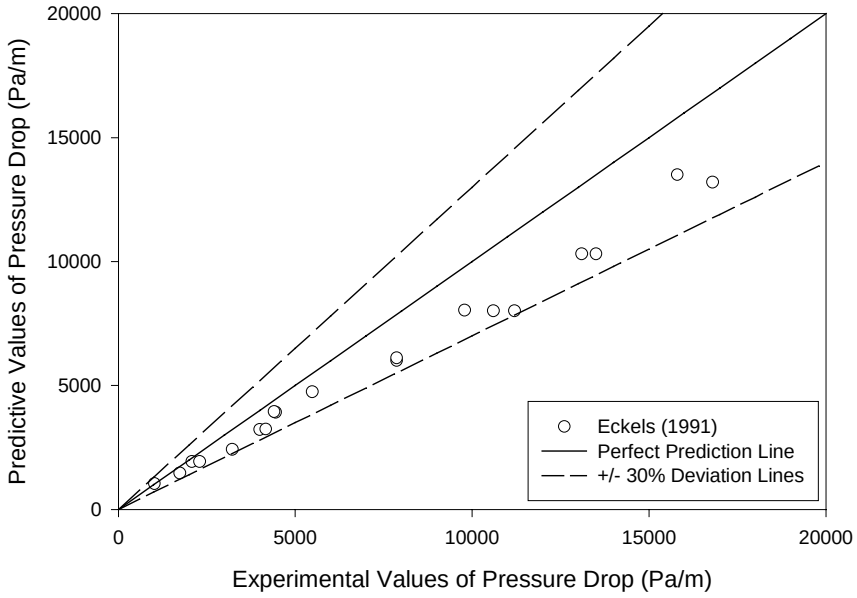

Figure 3.13. Souza and Pimenta (1995) model for a condensation R12 dataset

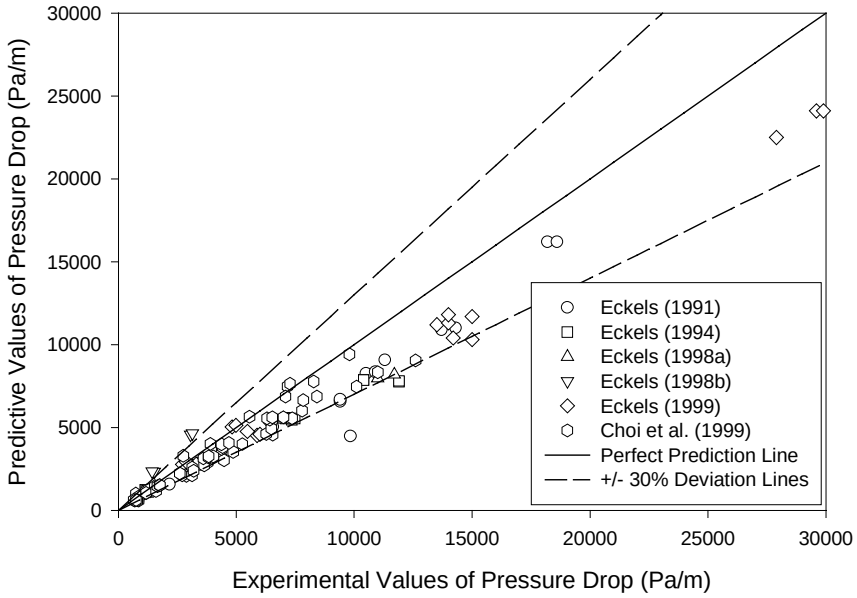

Figure 3.14. Souza and Pimenta (1995) model for condensation R134a datasets

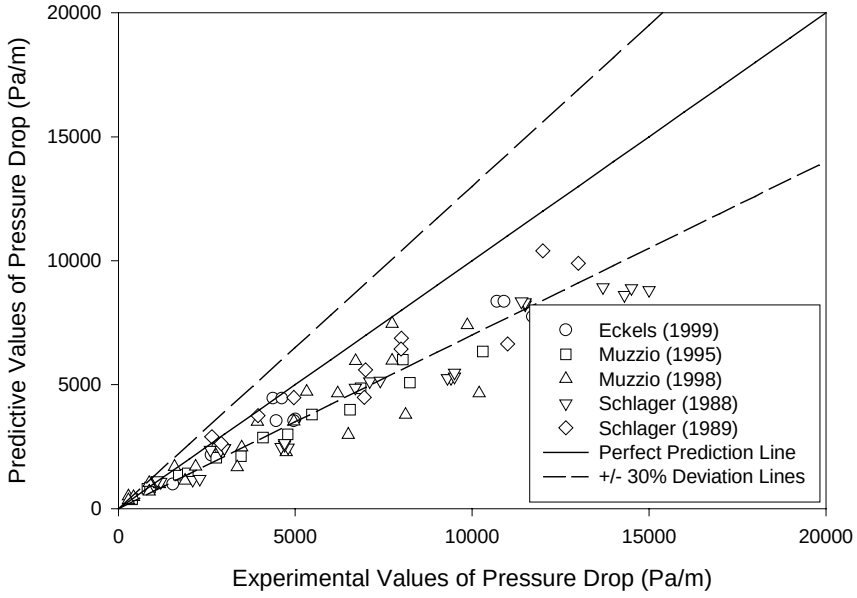

Figure 3.15. Souza and Pimenta (1995) model for condensation R22 datasets

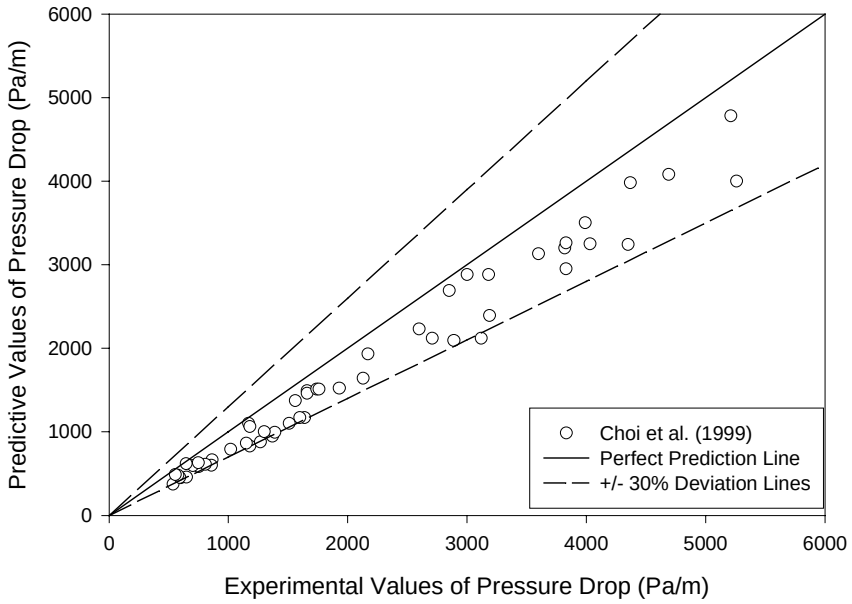

Figure 3.16. Souza and Pimenta (1995) model for a condensation R32 dataset

The predictions for refrigerant R407c had higher deviations, and the mean absolute deviation was about 45%. The dataset by Ebisu et al. (1998) was badly predicted by the model, as the deviations were more than 60%. The model, however, performed quite well with refrigerant R410A, with deviations less than 25%. Figures 3.17 and 3.18 illustrate the model's predictions for refrigerants R407c and R410A.

Figure 3.19 shows the model's prediction for all refrigerants in a condensation environment. The predictions were quite good overall, except for some slight under-predictions for refrigerant R22 and over-predictions for refrigerant R407c.

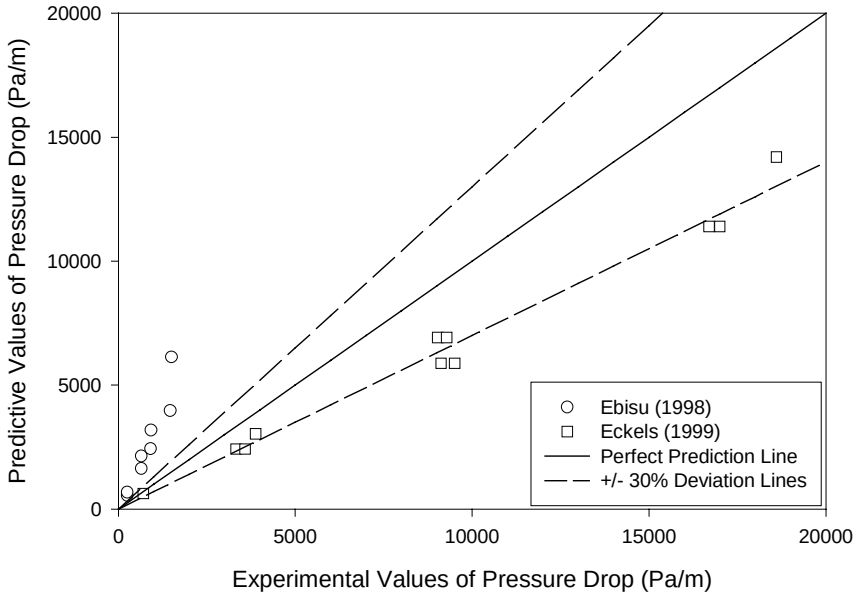

Figure 3.17. Souza and Pimenta (1995) model for condensation R407c datasets

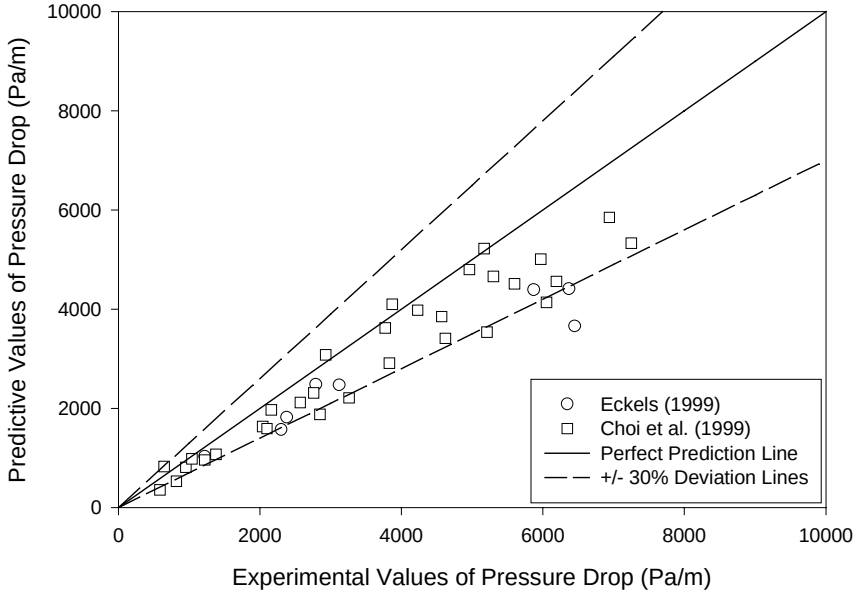

Figure 3.18. Souza and Pimenta (1995) model for condensation R410A datasets

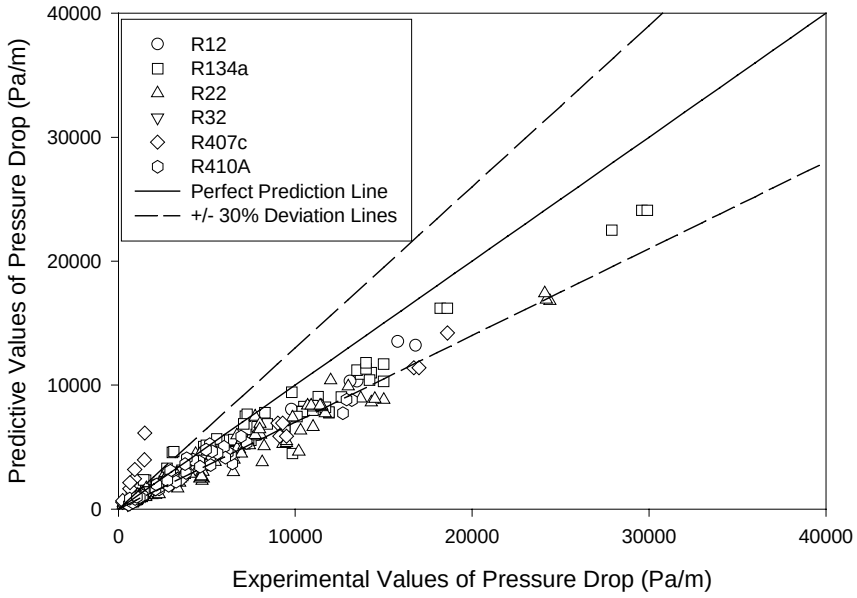

Figure 3.19. Souza and Pimenta (1995) model for all condensation datasets

The pressure-drop model by Souza and Pimenta (1995) is next validated with evaporation datasets. Figures 3.20, 3.21, and 3.22 illustrate the model's prediction for datasets for refrigerant R12, R134a, and R22, respectively. Some under-predictions can be observed for refrigerants R12 and R134a. The mean absolute deviations achieved for refrigerants R12, R134a, and R22 are about 45%, 30%, and 50%, respectively. The model was also used to predict datasets for refrigerant R407c, and the results are shown in Figure 3.23. The predictions deviate more than 60% from the experimental data. Most of the data were under-predicted by the model. Figure 3.24 summarizes all the predictions by the model for all evaporation datasets. Tables 3.7 and 3.8 tabulate the predictions results for each condensation and evaporation dataset.

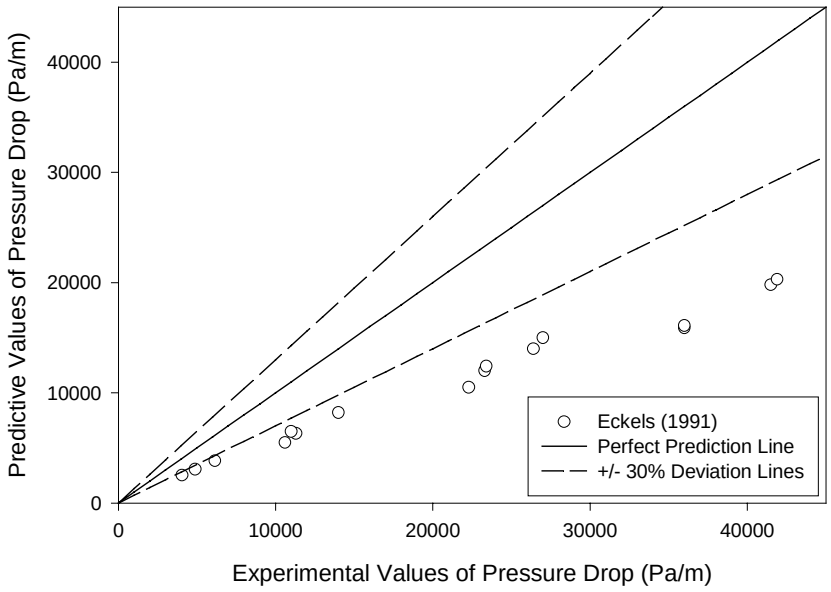

Figure 3.20. Souza and Pimenta (1995) model for an evaporation R12 dataset

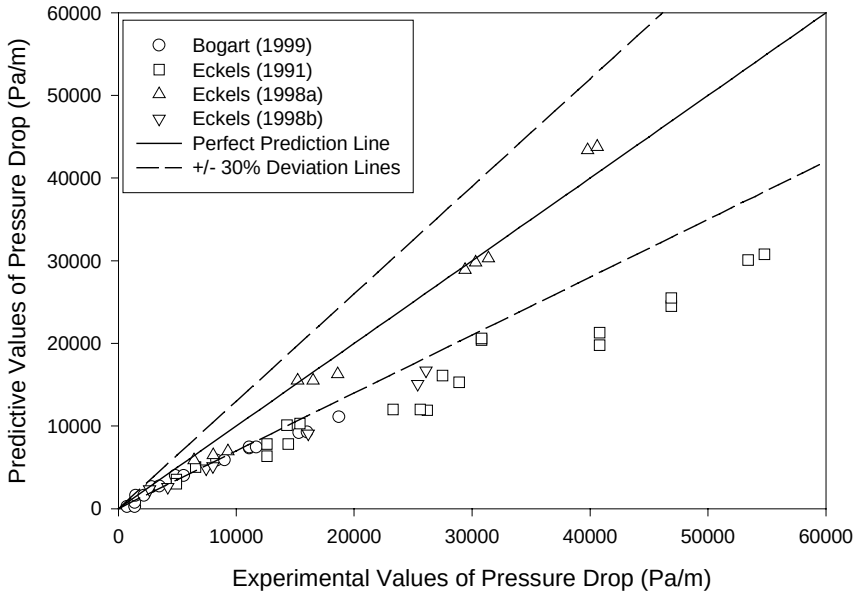

Figure 3.21. Souza and Pimenta (1995) model for evaporation R134a datasets

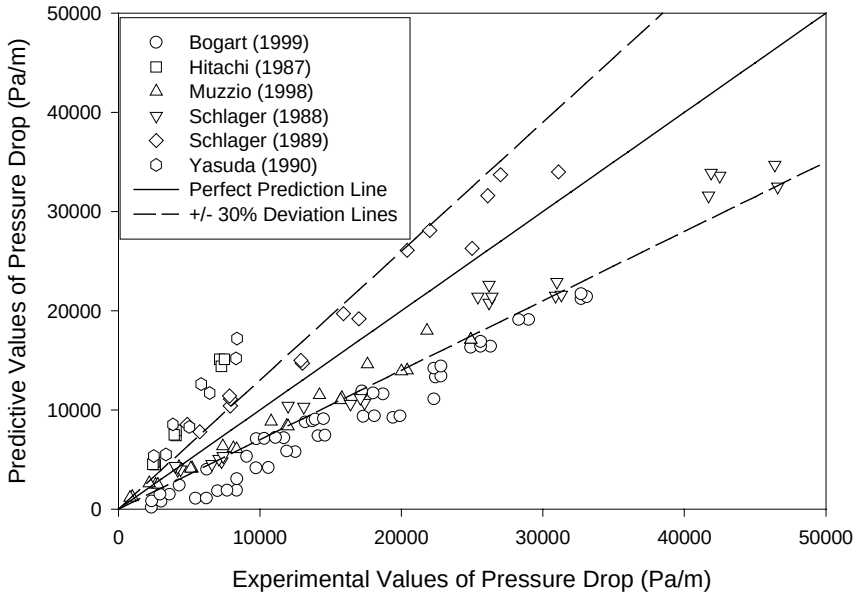

Figure 3.22. Souza and Pimenta (1995) model for evaporation R22 datasets

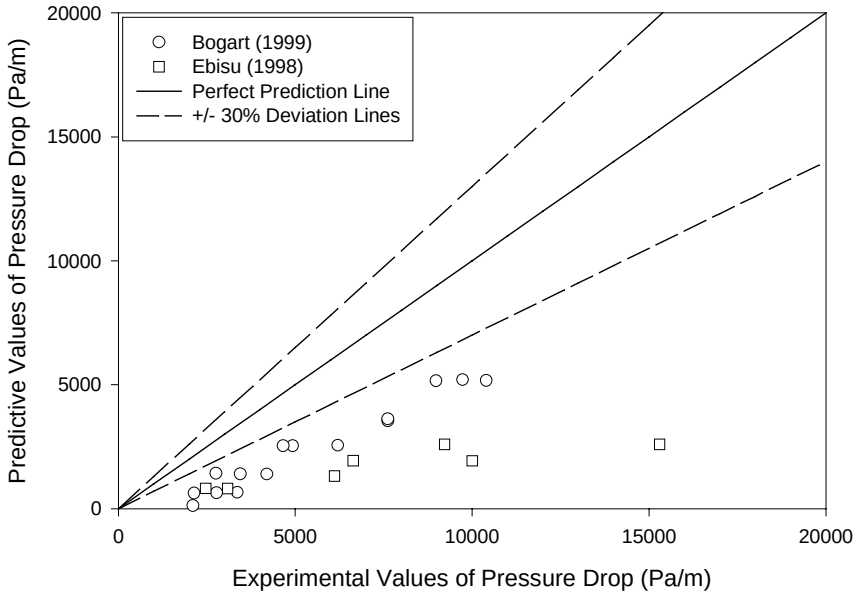

Figure 3.23. Souza and Pimenta (1995) model for evaporation R407c datasets

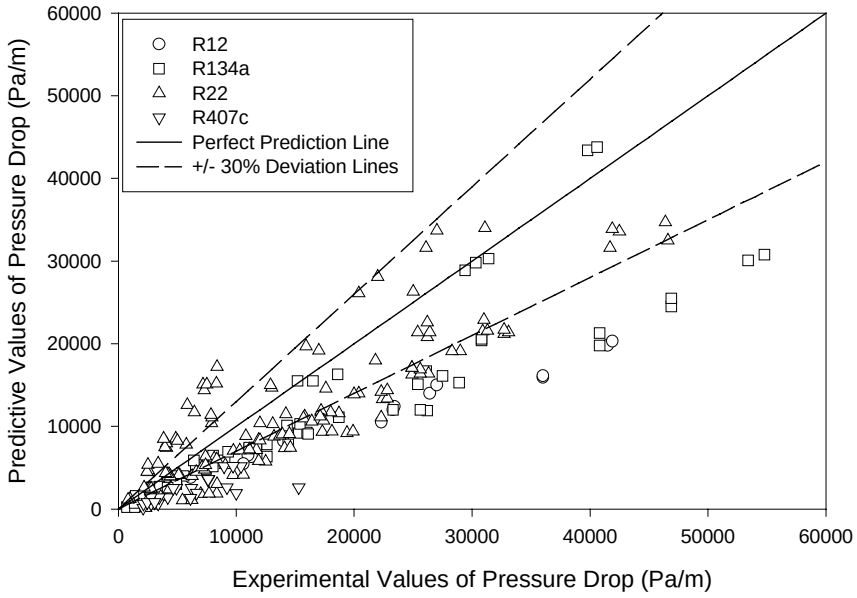

Figure 3.24. Souza and Pimenta (1995) model for all evaporation experimental datasets

Table 3.7. Mean absolute deviations achieved by the Souza and Pimenta (1995) model for condensation datasets.

Reference	Refrigerant	MAD (%)
Eckels and Pate (1991)	R12	17.45
Eckels and Pate (1991)	R134a	23.54
Eckels et al. (1994)	R134a	21.27
Eckels et al. (1998a)	R134a	17.52
Eckels et al. (1998b)	R134a	53.53
Eckels et al. (1999)	R134a	15.94
Choi et al. (1999)	R134a	16.98
Eckels et al. (1999)	R22	21.35
Muzzio et al. (1995)	R22	24.52
Muzzio et al. (1998)	R22	27.88
Schlager (1988)	R22	31.25
Schlager et al. (1989)	R22	19.28
Choi et al. (1999)	R32	20.11
Ebisu and Torikoshi (1998)	R407c	64.83
Eckels et al. (1999)	R407c	26.73
Eckels et al. (1999)	R410A	27.60

Choi et al. (1999)	R410A	20.41

Table 3.8. Mean absolute deviations achieved by the Souza and Pimenta (1995) model for evaporation datasets

Reference	Refrigerant	MAD (%)
Eckels and Pate (1991)	R12	46.24
Bogart and Thors (1999)	R134a	35.09
Eckels and Pate (1991)	R134a	41.85
Eckels et al. (1998a)	R134a	8.87
Eckels et al. (1998b)	R134a	34.28
Bogart and Thors (1999)	R22	46.68
Hitachi Cable Ltd (1987)	R22	91.01
Muzzio et al. (1998)	R22	22.43
Schlager (1988)	R22	23.08
Schlager et al. (1989)	R22	26.40
Yasuda et al. (1990)	R22	93.72
Bogart and Thors (1999)	R407c	59.76
Ebisu and Torikoshi (1998)	R407c	74.38

The Souza and Pimenta (1995) model predicted condensation datasets quite accurately, but under-predictions occured quite frequently for evaporation datasets. The PF parameter performed well, but some additional investigation needs to be performed to judge the usability of the PF parameter to smooth-tube pressure-drop correlations.

Choi et al. (1999) Pressure-Drop Model

Choi et al. (1999) developed a method based on the homogenous model for obtaining pressure drops in micro-fin tubes. Choi et al. (1999) modified the smooth-tube pressure-drop correlation of Pierre (1964) to obtain their pressure-drop model. The Pierre (1964) correlation was selected by Choi et al. (1999) because it produced pressure-drop

predictions that were the closest to the NIST micro-fin pressure-drop data, for convective evaporation and condensation. A new two-phase friction factor, $f_{N,}$ (Equation 1.32) was correlated to the NIST two-phase, micro-fin pressure-drop data. The Pierre (1964) correlation was further modified by using the hydraulic diameter, d_h, to account for micro-fins in tubes.

Choi et al. (1999) correlated the new pressure-drop model with experimental data from NIST and verified the model with experimental data from Eckels et al. (1991 and 1993). Choi et al. (1999) claimed predictions with less than 20% error for all the above-mentioned data with the new pressure-drop model.

The pressure-drop model by Choi et al. (1999) was evaluated with 17 condensation experimental datasets and 13 evaporation experimental datasets. Three Choi et al. (1999) condensation datasets comprising refrigerants R134a, R32, and R410A were also used in the validation process. Figures 3.25 and 3.26 shows the predictions results for refrigerants R12 and R134a. The prediction result are very good, with both refrigerant predictions having mean absolute deviations of less than 15%.

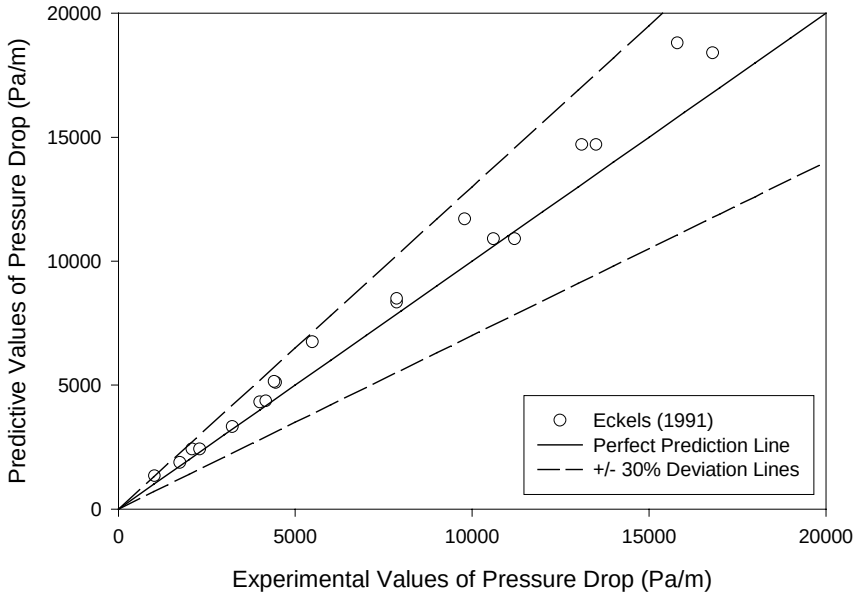

Figure 3.25. Choi et al. (1999) model for a condensation R12 experimental dataset

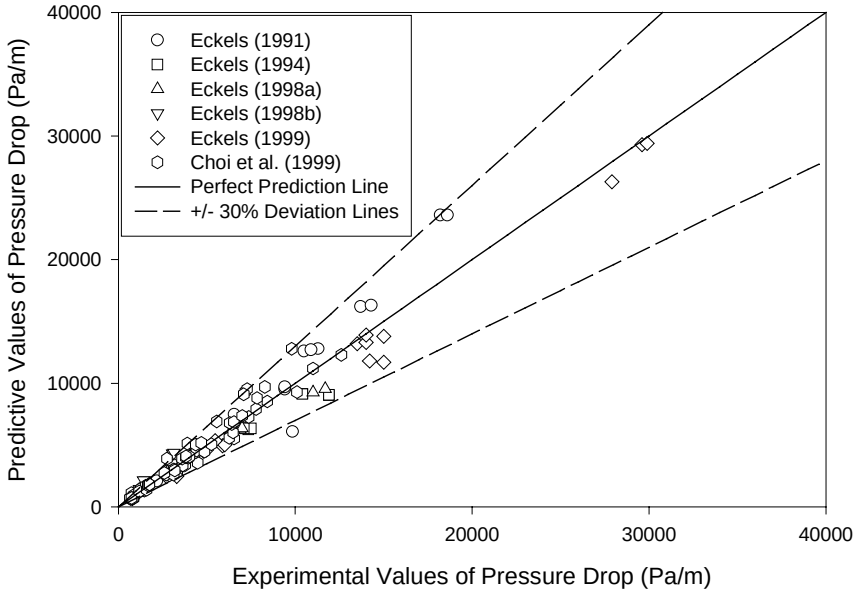

Figure 3.26. Choi et al. (1999) model for condensation R134a experimental datasets

The model was further validated with refrigerants R22 and R32. Figures 3.27 and

3.28 present the results. Predictions for the Choi et al. (1999) R32 dataset in Figure 3.28 were good, with mean absolute deviation of less than 15%. The R22 dataset predictions however, resulted in a deviation of almost 30%.

Two sets of refrigerant mixtures datasets were tested with the Choi et al. (1999) model, and the results are shown in Figures 3.29 and 3.30. The R407c dataset predictions demonstrated a mean absolute deviation of almost 40% while the dataset predictions for R410A achieved deviations of almost 30%. In both cases, the experimental data were slightly over-predicted by the model. Figure 3.31 presents the results by the model for each refrigerant.

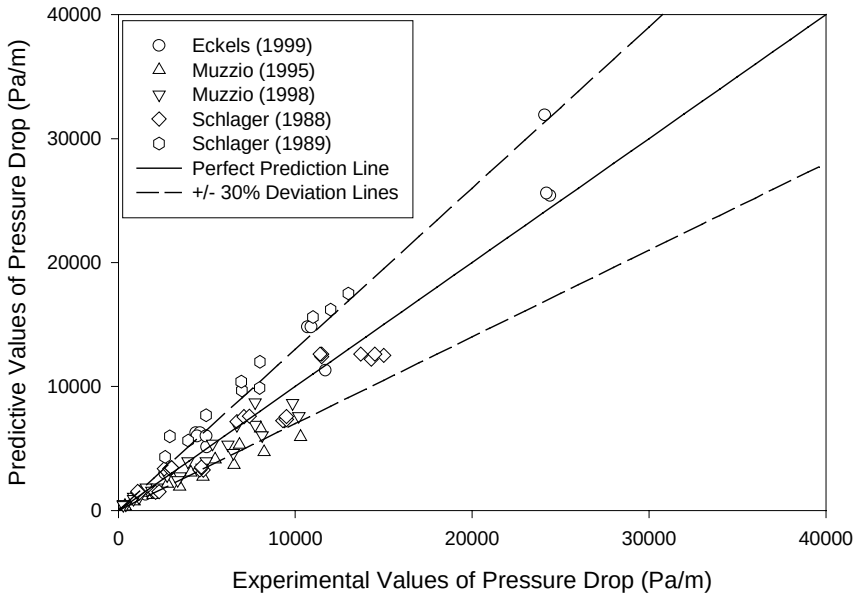

Figure 3.27. Choi et al. (1999) model for condensation R22 experimental datasets

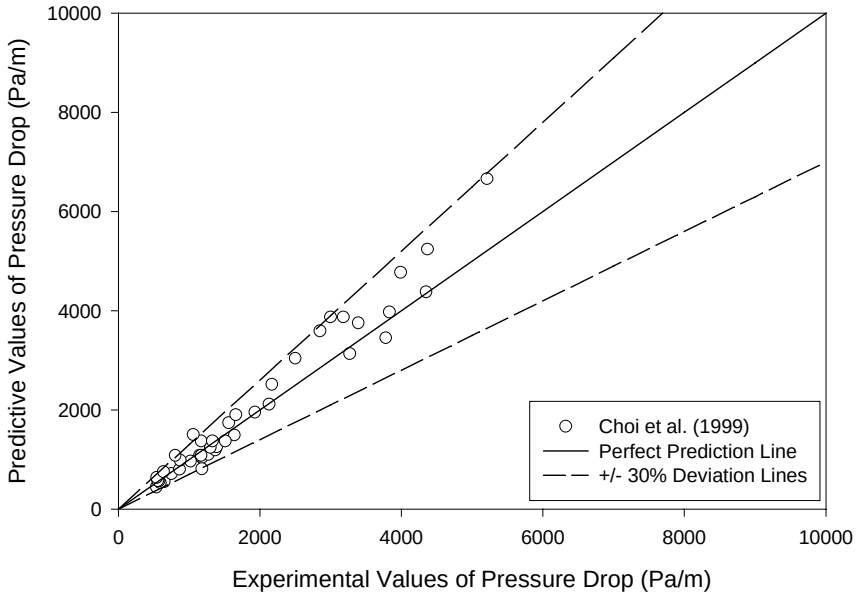

Figure 3.28. Choi et al. (1999) model for a condensation R32 experimental dataset

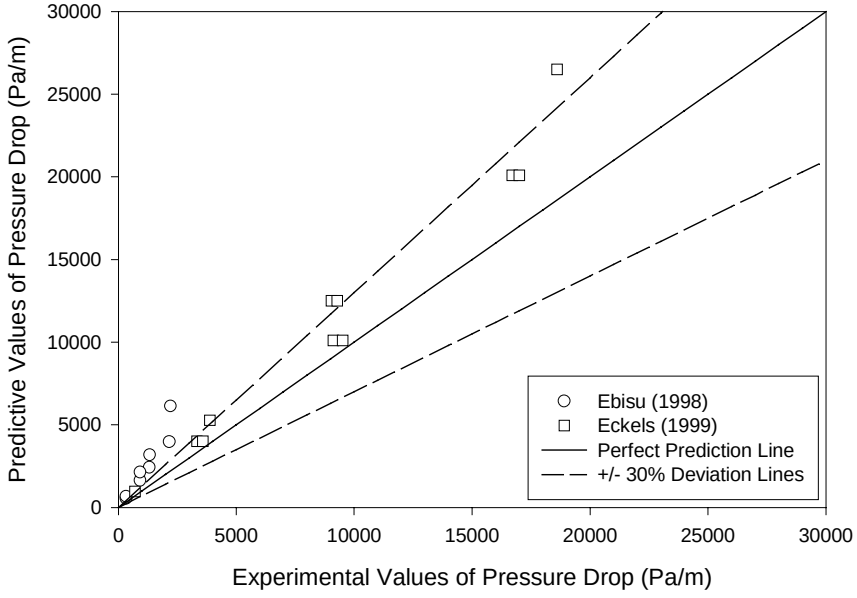

Figure 3.29. Choi et al. (1999) model for condensation R407c experimental datasets

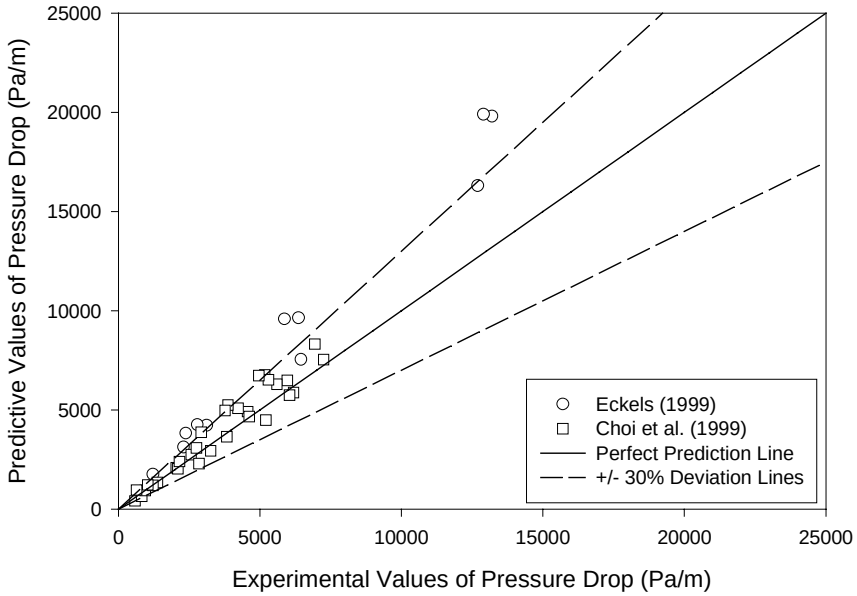

Figure 3.30. Choi et al. (1999) model for condensation R410A experimental datasets

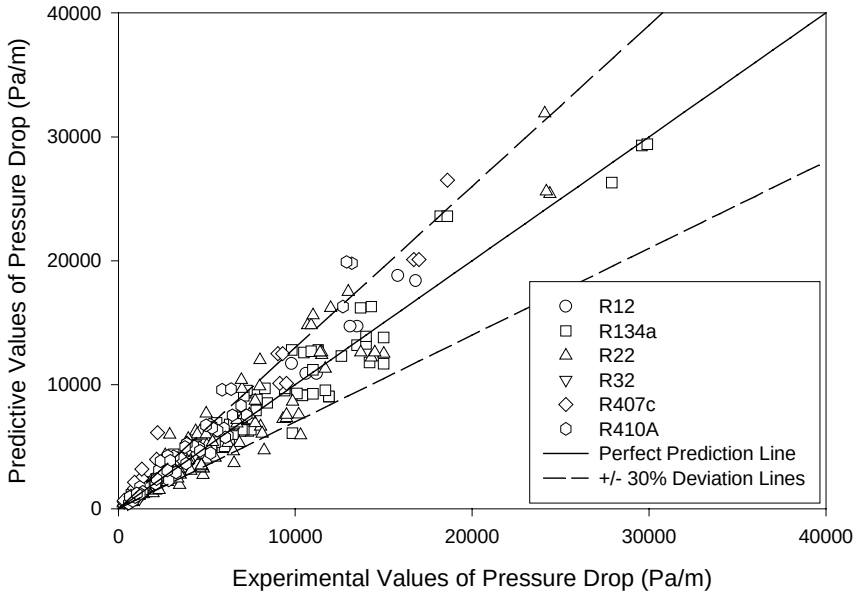

Figure 3.31. Choi et al. (1999) model for all condensation experimental datasets

Thirteen evaporation datasets comprising refrigerants R12, R134a, R22 and

R407c were tested with the Choi et al. (1999) pressure-drop model. Figure 3.32, 3.33 and 3.34 summarize the prediction results for refrigerants R12, R134a and R22. The model had an almost perfect fit with the R12 experimental dataset. The mean absolute deviation was less than 5%. The deviations were higher for refrigerant R134a, as the model predicted the data within 25%. The Bogart et al. (1999) data was over-predicted by the Choi et al. (1999) model. The model did not provide accurate predictions for refrigerant R22. The mean absolute deviation achieved was almost 50%. Data from Yasuda et al. (1990) and Schlager et al. (1989) were over-predicted and under-predicted by the model, respectively.

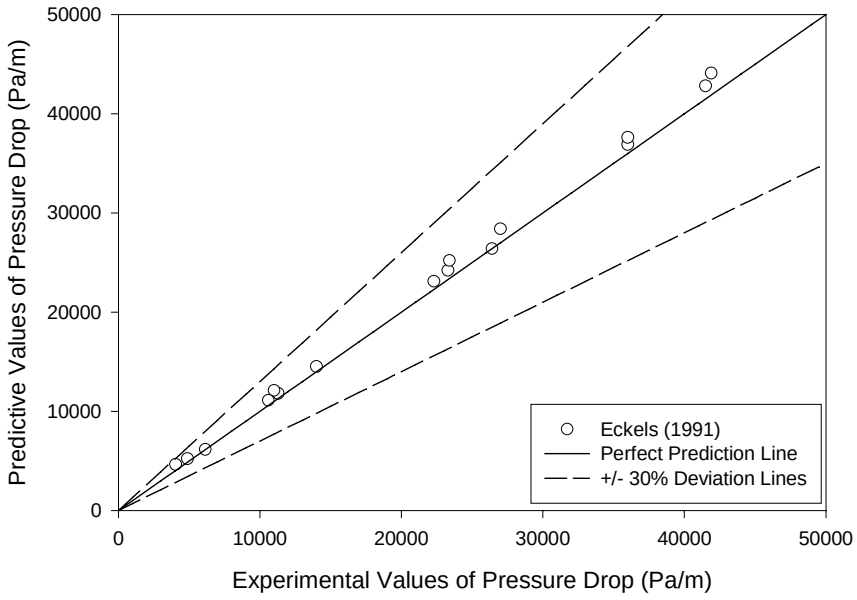

Figure 3.32. Choi et al. (1999) model for an evaporation R12 experimental dataset

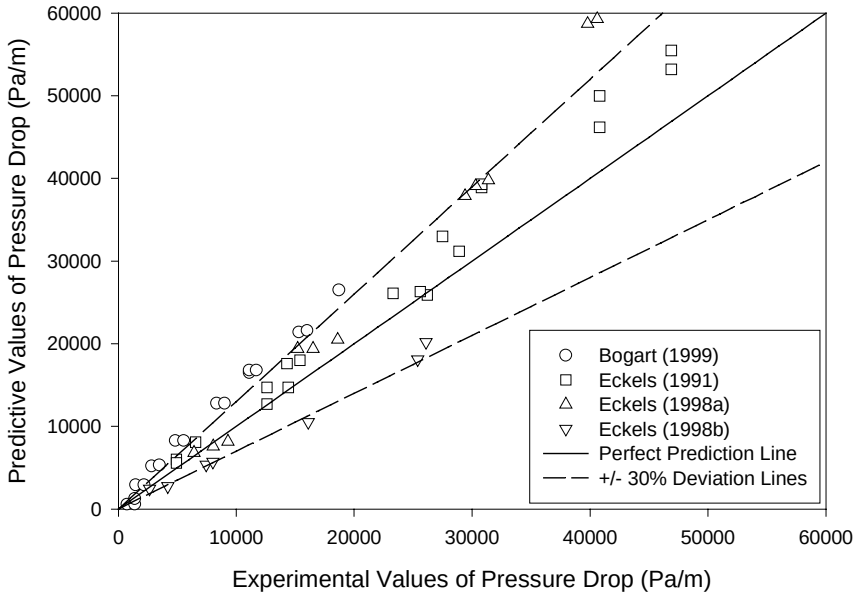

Figure 3.33. Choi et al. (1999) model for evaporation R134a experimental datasets

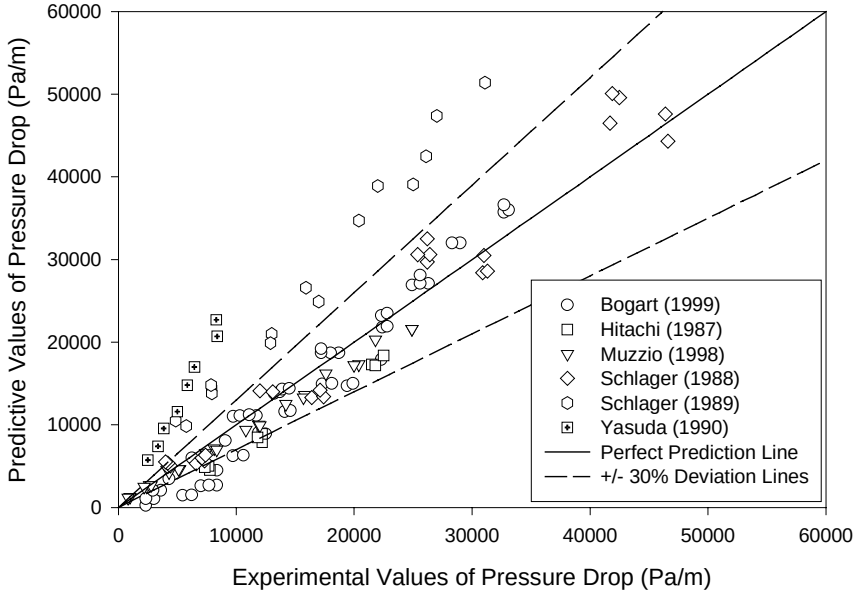

Figure 3.34. Choi et al. (1999) model for evaporation R22 experimental datasets

Figure 3.35 shows the prediction result for refrigerant R407c. Most of the data were under-predicted with the mean absolute deviation around 50%. Figure 3.36 shows the prediction results from the model for each evaporation dataset. Tables 3.7 and 3.8 summarize the prediction results for the condensation datasets and evaporation datasets. The Choi et al. (1999) pressure-drop model provided excellent predictions for datasets from NIST. These data from NIST were part of the data that were used by Choi et al. (1999) to calibrate the pressure-drop model. Datasets from Eckels and Pate (1991), Eckels et al. (1994), Eckels et al. (1998a), Eckels et al. (1998b), and Eckels and Tesene (1999), were also predicted quite well. Apart from the predictions for these data, however, inconsistencies were observed and there were large deviations, especially in the evaporation pressure-drop datasets. The evaporation and condensation datasets from Schlager et al. (1989) were over-predicted and the predictions for the evaporation dataset from Yasuda et al. (1990) demonstrated a mean absolute deviation of more than 100%.

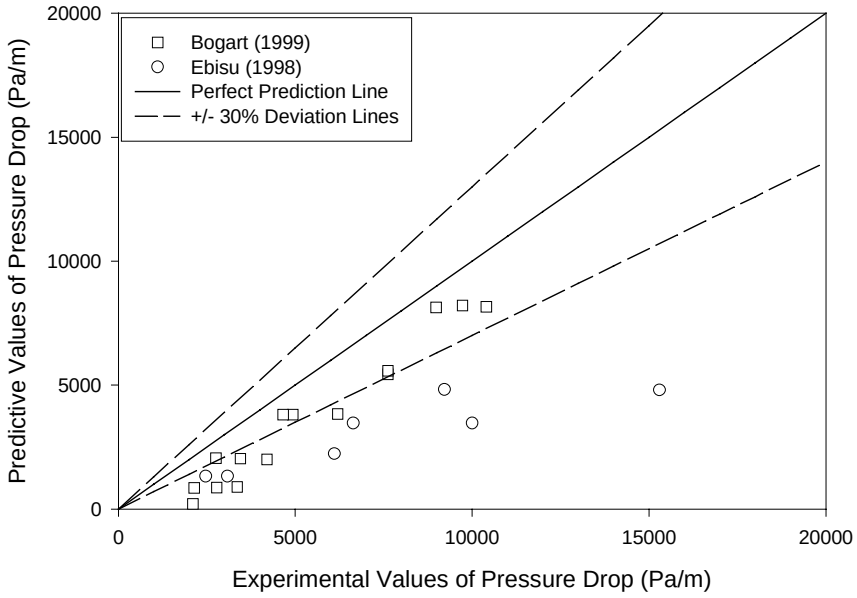

Figure 3.35. Choi et al. (1999) model for evaporation R407c experimental datasets

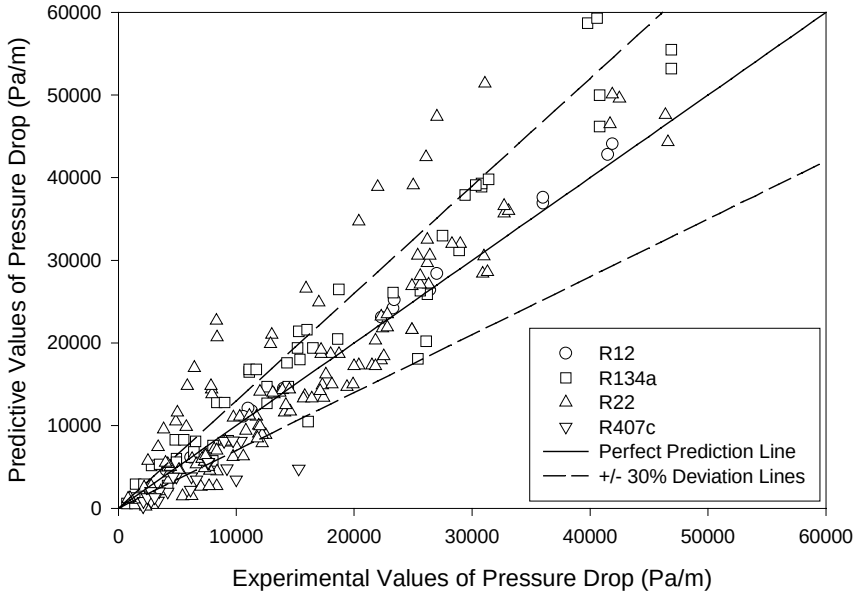

Figure 3.36. Choi et al. (1999) model for all evaporation experimental datasets

Table 3.9. Mean absolute deviations achieved by the Choi et al. (1999) model for condensation datasets

Reference	Refrigerant	MAD (%)
Eckels and Pate (1991)	R12	12.68
Eckels and Pate (1991)	R134a	15.10
Eckels et al. (1994)	R134a	13.40
Eckels et al. (1998a)	R134a	9.78
Eckels et al. (1998b)	R134a	42.97
Eckels et al. (1999)	R134a	10.44
Choi et al. (1999)	R134a	11.32
Eckels et al. (1999)	R22	23.07
Muzzio et al. (1995)	R22	26.42
Muzzio et al. (1998)	R22	19.06
Schlager (1988)	R22	19.47
Schlager et al. (1989)	R22	50.39
Choi et al. (1999)	R32	13.53
Ebisu and Torikoshi (1998)	R407c	50.39
Eckels et al. (1999)	R407c	27.97
Eckels et al. (1999)	R410A	42.15
Choi et al. (1999)	R410A	14.74

Table 3.10. Mean absolute deviations achieved by the Choi et al. (1999) model for evaporation datasets

Reference	Refrigerant	MAD (%)
Eckels and Pate (1991)	R12	4.70
Bogart and Thors (1999)	R134a	49.48
Eckels and Pate (1991)	R134a	14.66
Eckels et al. (1998a)	R134a	23.40
Eckels et al. (1998b)	R134a	26.25
Bogart and Thors (1999)	R22	22.08
Hitachi Cable Ltd (1987)	R22	28.87
Muzzio et al. (1998)	R22	13.15
Schlager (1988)	R22	15.92
Schlager et al. (1989)	R22	70.75
Yasuda et al. (1990)	R22	145.70
Bogart and Thors (1999)	R407c	39.52
Ebisu and Torikoshi (1998)	R407c	55.57

The three models exhibit good predictions on certain datasets, but the predictions were generally inconsistent. The Cavallini et al. (1999) model produced deviations of more than ±30% for many datasets while results obtained from the Souza and Pimenta (1995) model are more accurate for condensation datasets. The Choi et al. (1999) model produced very accurate predictions for condensation datasets, but was a little erratic with evaporation datasets. High deviations, larger than 50%, were observed when certain evaporation datasets were tested with the Choi et al. (1999) model.

The next chapter will focus on developing a new pressure-drop model that is built on correlations introduced in this chapter. The need for consistency and accuracy in predictions and wide applicability for different flow conditions are the key stimulus for

the development of a new model.

CHAPTER IV

THE NEW PRESSURE-DROP MODEL

The new pressure-drop model is based on the separated flow model and, thus, the addition of the frictional pressure-drop gradient and the acceleration pressure-drop gradient in the computation of the overall two-phase flow pressure-drop in horizontal tubes. The Friedel (1979) correlation is selected as the basis for a new two-phase multiplier, Φ_{LO}^2, for the single-phase (liquid) frictional pressure-drop, ΔP_{LO}. f_{LO} is evaluated as a smooth-tube single-phase friction factor calculated from the Blausius equation. The two-phase frictional pressure-drop gradient is then expressed as the single-phase frictional pressure-drop gradient multiplied by the two-phase multiplier, Φ_{LO}^2.

$$\Delta P_{LO} = 2 \cdot f_{LO} \cdot \frac{G^2}{d_i \cdot \rho_l} \tag{4.1}$$

$$\Delta P_f = \Phi_{LO}^{\ 2} \cdot \Delta P_{LO} \tag{4.2}$$

The Friedel (1979) correlation remains one of the more accurate frictional two-phase pressure-drop multiplierd for flows in smooth tubes. Its appeal lies in the simplicity of the correlation and the wide applicability it has in predicting two-phase pressure drops for different refrigerants in all regimes of flow.

The *PF* parameter introduced by Christoffersen et al. (1993) is used as a multiplier to equation (4.2). The experimental database discussed in Chapter III has several experimental datasets, with fin heights from 0.15 mm to 0.203 mm and with helix angles between 17^o and 25^o. Due to geometry similarities with the Christoffersen et al. (1993) model, equation (2.24) is used as the enhanced-tubes multiplier for the frictional pressure-drop smooth-tube correlation. The penalty factor, *PF*, is inserted into the frictional pressure-drop correlation as follows:

$$\Delta P_f = \Phi_{LO}^{\ 2} \cdot 2 \cdot f_{LO} \cdot \frac{G^2}{d_i \cdot \rho_l} \cdot PF \tag{4.3}$$

The computation of the acceleration component follows the procedure outlined by Cavallini et al. (1999). The void fraction, ε, is evaluated by the Rouhani (1969) model as suggested by Cavallini et al. (1999).

Friedel (1979) used a non-linear best-fit procedure to generate three empirical constants in the two-phase multiplier correlation. These empirical constants are needed in the mathematical model to provide prediction results that are reliable and consistent with experimental pressure-drop measurements. These empirical constants were, however, generated with smooth-tube pressure-drop data. To account for micro-fin pressure-drop data, the three empirical constants need to be regenerated. The three empirical constants are labeled *A1*, *A2*, and *A3* in equation (4.4).

$$\Phi_{LO}^{\ 2} = E + \frac{A1 \cdot Ff \cdot H}{Fr^{A2} \cdot We^{A3}} \tag{4.4}$$

The MathCAD 2001 mathematical function *Minimize* will be the focal point for this empirical constant regeneration process. The standard error of regression function (*SER*) introduced by Montgomery and Peck (1992) is selected as the reference minimum function.

$$SER = \left\{ \frac{\sum_{i=1}^{N} \left[\Delta P_{\exp} - function\left(\Delta P_{\exp} \right) \right]^2}{N - Coef} \right\}^{0.5} \tag{4.5}$$

Coef in equation (4.5) represents the number of empirical constants used in the function for two-phase pressure-drop $\Delta P_{exp.}$ A total number of 531 experimental data points were used in the empirical constant regeneration process. From that number, 268 data points are from 11 condensation datasets and 263 data points are from 15 evaporation datasets. Equation (4.6) is the expanded version of equation (4.5) and it is used in the computation of the *SER* function. This *SER* function is used as a reference function to achieve a minimum value with the new empirical constants.

$$SER(A) = \left\{ \frac{\sum_{i=1}^{N} \left[\Delta P_{\exp} - \left[\left(\left(E + \frac{A1 \cdot Ff \cdot H}{Fr^{A2} \cdot We^{A3}} \right) \cdot 2 \cdot f_{LO} \cdot \frac{G_{\exp}}{d_i \cdot \rho_l} \cdot PF \right) - \Delta P_{acc} \right] \right]^2}{N - 3} \right\}^{0.5} \tag{4.6}$$

Variables *A1*, *A2*, and *A3* are the new empirical constants. Since there are three coefficients to be determined in equation (4.6), 3 is subtracted from the total number of data points *N*. Initial guesses are made for the three unknown empirical constants *A1*, *A2*, and *A3* and the *Minimize* function in MathCAD 2001 determines the minimum value for

SER(A). A MathCAD calculation worksheet for the entire process is presented in the appendix.

The new empirical constants are shown in Table 4.1. With the new empirical constants, the new pressure-drop model has the form

$$\Delta P_{tp} = \left[\left[E + \frac{A1 \cdot Ff \cdot H}{Fr^{A2} \cdot We^{A3}}\right] \cdot 2 \cdot f_{LO} \cdot \frac{G^2}{d_i \cdot \rho_l} \cdot PF\right] + \left[\frac{G^2 \cdot \left[\frac{x^2}{\rho_v \cdot \varepsilon} + \frac{(1-x)^2}{[\rho_l \cdot (1-\varepsilon)]}\right]}{L}\right] \quad (4.7)$$

(ΔP_f) $*(\Delta P_a)$

$*\Delta P_a$ is subtracted in condensation environment.

Table 4.1: Empirical Constants in the New Pressure-Drop Model

Empirical Constants	Value
A1	3.5310
A2	0.0230
A3	0.0059

The acceleration component is added to the frictional component for the evaporation pressure-drop, but is subtracted in condensation pressure-drop because pressure recovery is involved in condensation.

The datasets used in the new empirical constants generation process are tested with the new pressure-drop model. Fifteen sets of evaporation pressure-drop experimental data and 11 sets of condensation pressure-drop experimental data from different authors were used in the development of the model. The predictions from the

pressure-drop model are compared with the experimental datasets by calculating the mean absolute deviation (*MAD*).

Figures 4.1 to 4.10 show the prediction results for all the experimental datasets used. Many of the experimental datasets have pressure-drop values measured in different micro-fin tubes or at slightly different environments. For summary purposes, all same-refrigerant pressure-drop measurements and model predictions are shown in a single graph. Tables 4.2 and 4.3 tabulate all the results and shows the calculated mean absolute deviations for each dataset.

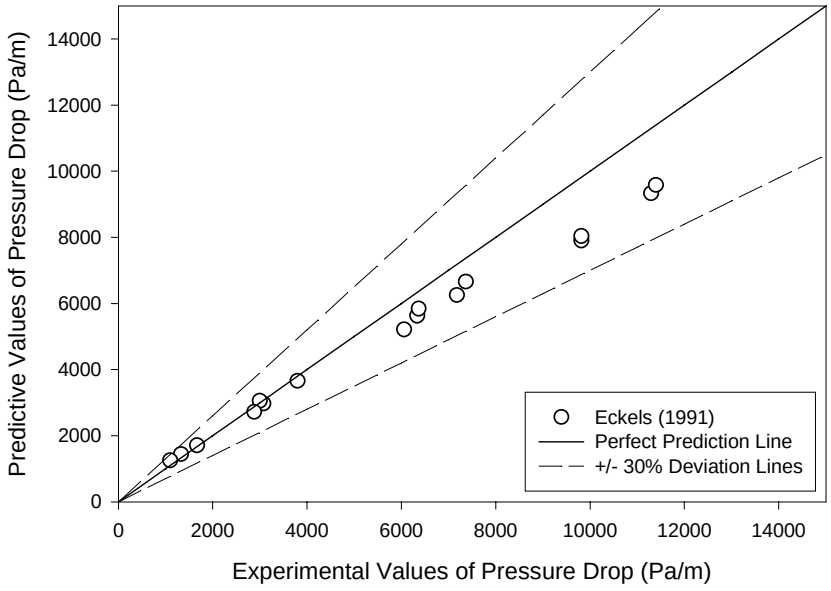

Figure 4.1. New pressure-drop model for an R12 evaporation dataset

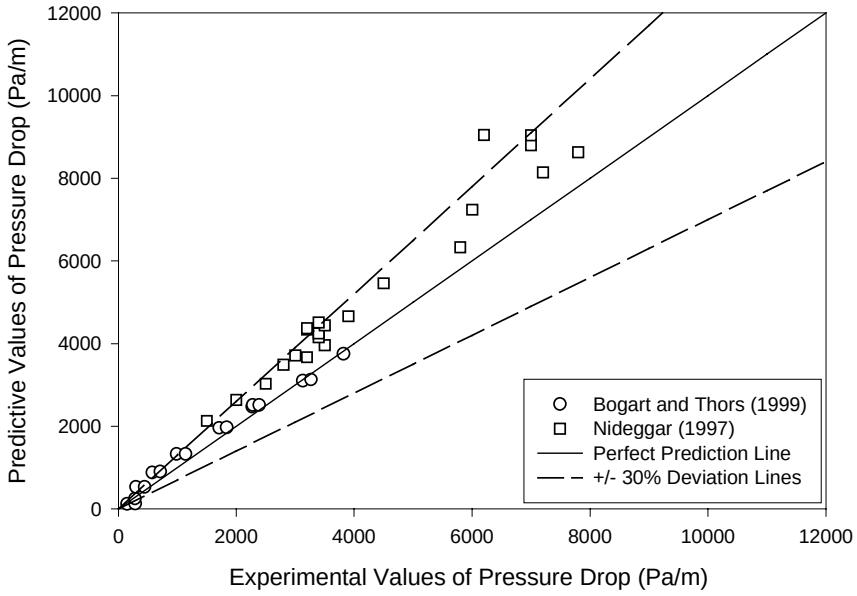

Figure 4.2. New pressure-drop model for R134a evaporation datasets

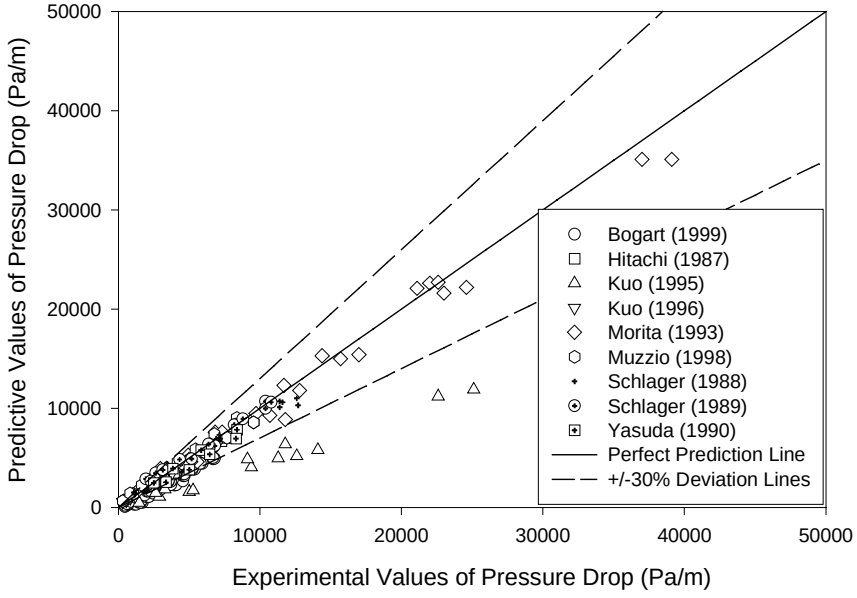

Figure 4.3. New pressure-drop model for R22 evaporation datasets

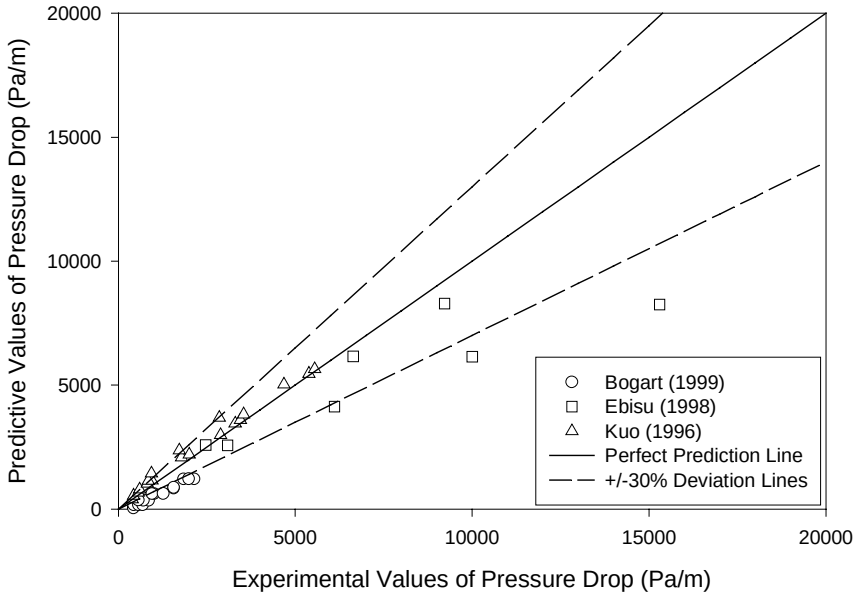

Figure 4.4. New pressure-drop model for R407C evaporation datasets

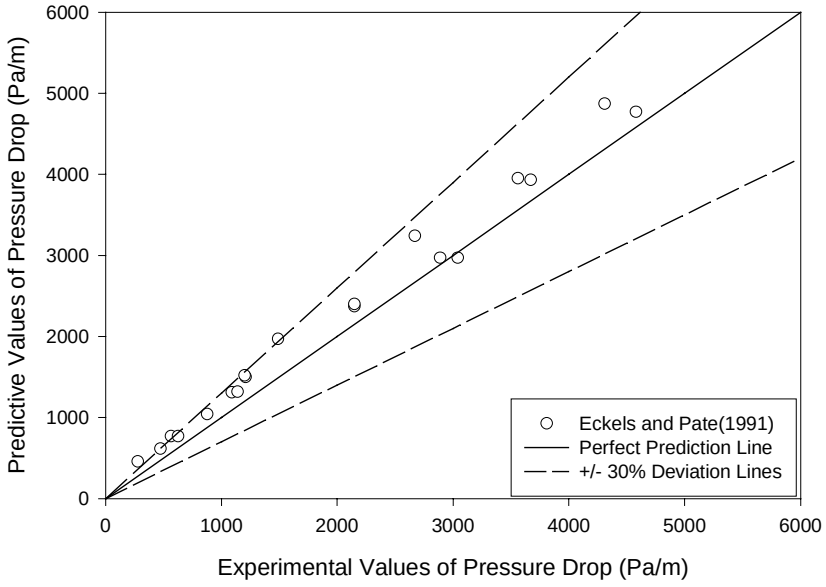

Figure 4.5. New pressure-drop model for an R12 condensation dataset

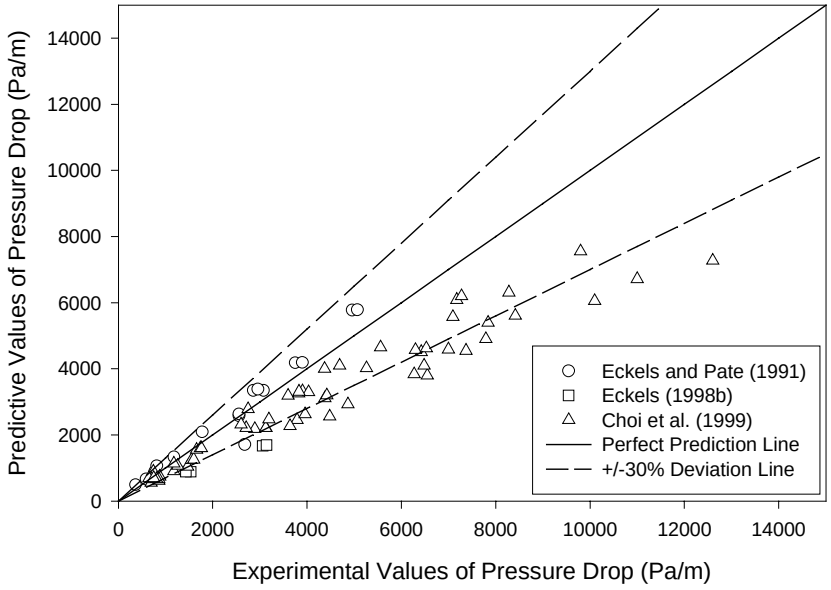

Figure 4.6. New pressure-drop model for R134a condensation datasets

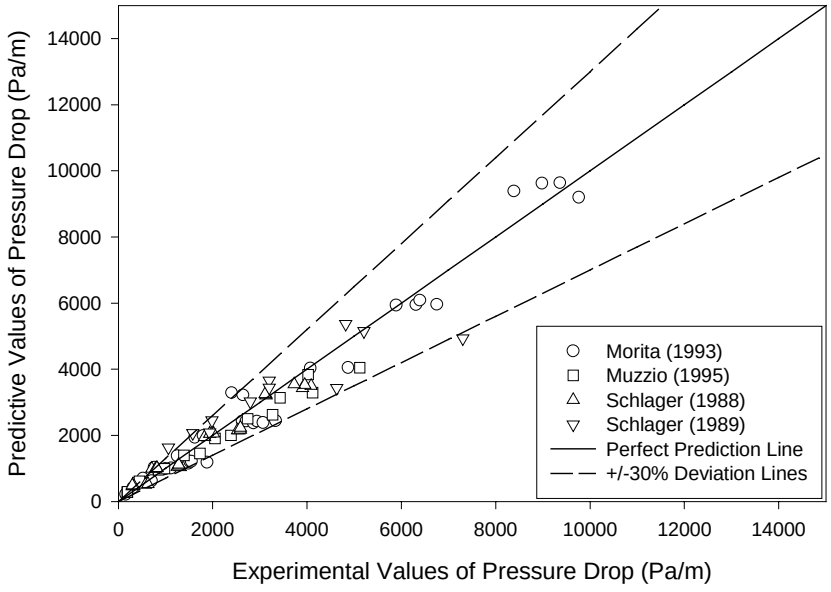

Figure 4.7. New pressure-drop model for R22 condensation datasets

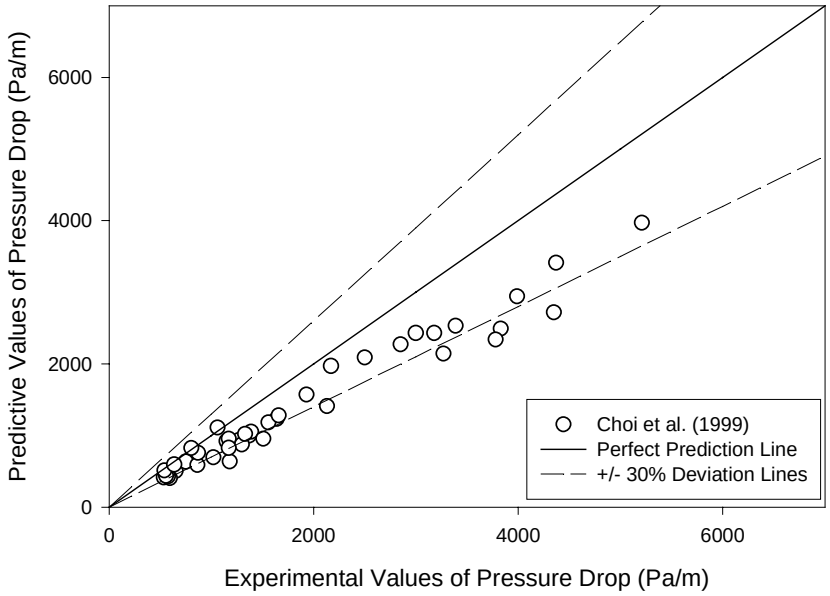

Figure 4.8. New pressure-drop model for a R32 condensation dataset

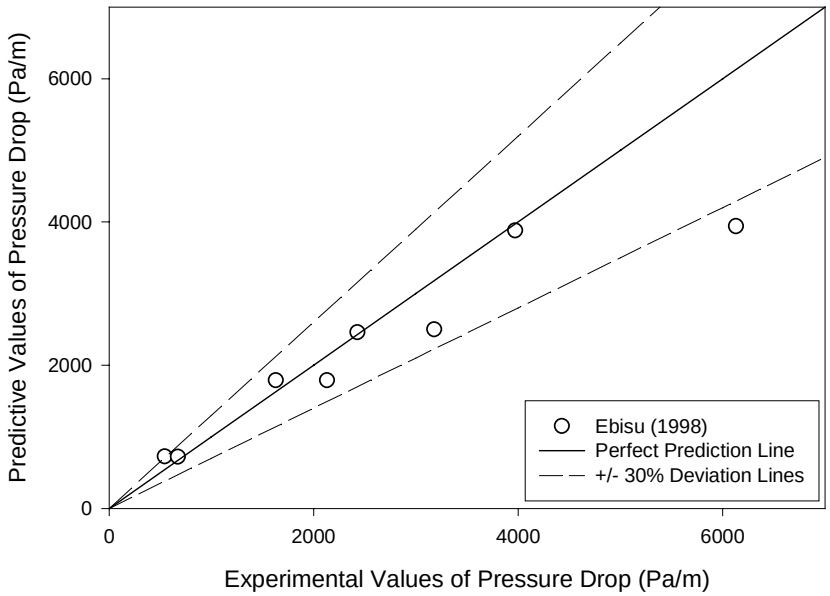

Figure 4.9. New pressure-drop model for a R407c condensation dataset

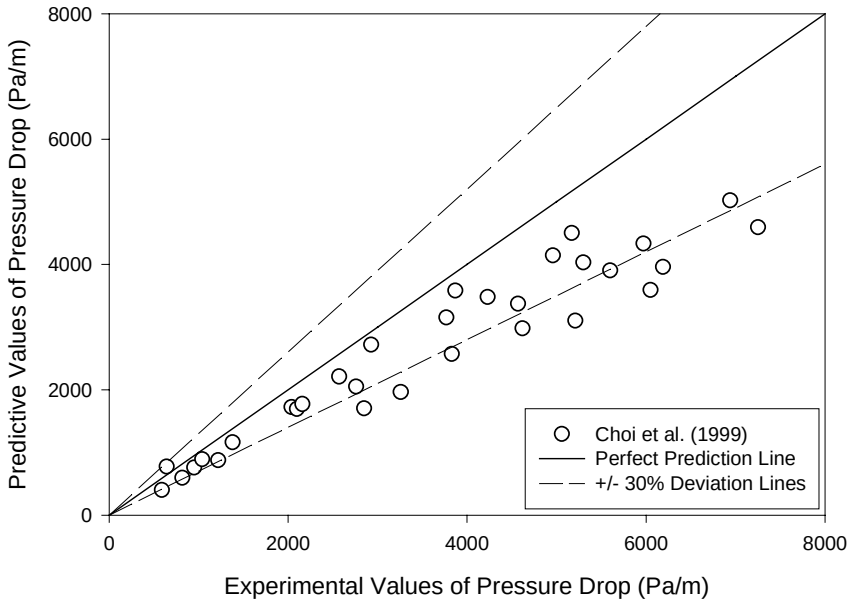

Figure 4.10. New pressure-drop model for a R410A condensation dataset

Table 4.2. New Pressure-Drop Model Prediction Results for Evaporation Datasets

Reference	Refrigerant	MAD (%)
Eckels 1991	R12	10.30
Bogart (1999)	R134a	21.51
Niddegar (1997)	R134a	35.85
Bogart (1999)	R22	39.27
Hitachi (1987)	R22	10.99
Kuo (1995)	R22	55.84
Kuo (1996)	R22	17.44
Morita (1993)	R22	11.89
Muzzio (1998)	R22	20.98
Schlager (1988)	R22	13.71
Schlager (1989)	R22	11.14
Yasuda (1990)	R22	11.63
Bogart (1999)	R407c	51.91
Ebisu (1998)	R407c	22.18
Kuo (1996)	R407c	17.89

Table 4.3. New Pressure-Drop Model Prediction Results for Condensation Datasets

Reference	Refrigerant	MAD (%)
Eckels (1991)	R12	19.75
Eckels (1991)	R134a	15.56
Eckels (1998b)	R134a	42.93
Choi et al. (1999)	R134a	23.17
Morita (1993)	R22	16.31
Muzzio (1995)	R22	19.24
Schlager (1988)	R22	18.10
Schlager (1989)	R22	19.64
Choi et al. (1999)	R32	23.78
Ebisu (1998)	R407c	15.81
Choi et al. (1999)	R410A	24.80

The new pressure-drop model results in less than ±30% mean absolute deviation between the predicted results and actual experimental data for 12 of the 15 evaporation datasets. This performance gives an 80% success rate for the predictive capabilities of the

model for evaporation datasets, and is a good number for the new model, as most pressure drop empirical models do not have the capability to predict all datasets accurately. The new model has a slightly higher success in predicting condensation datasets: 10 of the 11 condensation datasets are predicted with mean absolute deviations below ±30%. This gives a near 90% success rate for the new model in predicting the 11 condensation datasets. Datasets by Kuo et al. (1995), Bogart et al. (1999) and Eckels et al. (1998b) were predicted to have high deviations with the new model. Prediction errors may have occurred because of high uncertainty in pressure-drop measurements. Kuo et al. (1995) and Eckels et al. (1998b) reported uncertainties in pressure-drop measurements of more than 15% and 30%, respectively. The paper by Bogart et al. (1999) did not reveal the values of uncertainty for pressure-drop measurements. Refrigerant R134a was, however, reported to have lower pressure drops when compared to refrigerants R22 and R407c. The new model predicted the R134a dataset within 20% deviation while under-predicting the datasets for refrigerants R22 and R407c by more than 35% and 50%, respectively. Higher measured values of pressure-drop for refrigerants R22 and R407c may have caused the large deviations.

The new pressure-drop model was also tested on a few experimental datasets that were not included in the model development. Four evaporation datasets and 7 condensation datasets were tested. Figures 4.11 to 4.16 show the prediction results for the datasets and Tables 4.4 and 4.5 tabulates the results. Summary results for same-refrigerant datasets are also presented in one graph.

Table 4.4. New Pressure-Drop Model Prediction Results for Evaporation Datasets

Reference	Refrigerant	MAD (%)
Eckels (1991)	R134a	10.64
Eckels (1998a)	R134a	9.90
Eckels (1998b)	R134a	27.05
Zurcher (1998)	R407c	14.59

Table 4.5. New Pressure-Drop Model Prediction Results for Condensation Datasets

Reference	Refrigerant	MAD (%)
Eckels (1998a)	R134a	21.33
Eckels (1994)	R134a	17.36
Eckels (1999)	R134a	9.44
Eckels (1999)	R22	6.66
Muzzio (1998)	R22	23.53
Eckels (1999)	R407c	12.17
Eckels (1999)	R410A	12.12

The new model produced good prediction results for all 11 datasets used. All the datasets were predicted to well below the ±30% mean absolute deviation mark. Such accuracy augurs well for the new model since this indicate that the model has the capability to predict experimental data not included in its calibration process.

Based on the experimental data used this chapter, the new model can be applied on datasets for mass flux ranges up to 600 kg/m^{2}s. Data from micro-fin tubes with fin heights of 0.1 to 0.38 mm, and helix angles of 0 to 30^o, can also be applied to the new pressure-drop model.

The regression technique used in the empirical constants regeneration process for the new pressure-drop model was also applied to pressure drop models by Cavallini et al. (1999) and Choi et al. (1999). Poorer predictions with the above datasets were, however,

obtained with the new empirical constants when compared with the original constants proposed by the authors of both papers. The new pressure-drop model obtained more success in predictions with the new empirical constants when compared with the models from Cavallini et al. (1999) and Choi et al. (1999).

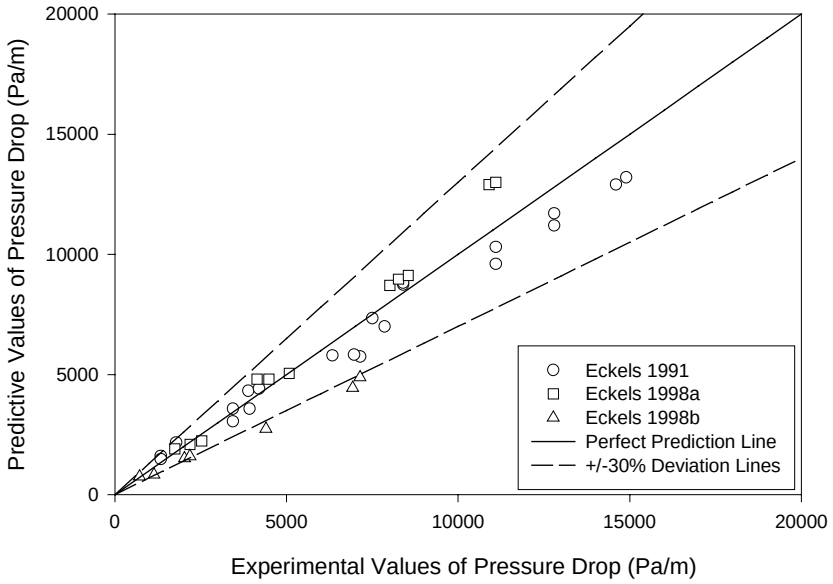

Figure 4.11. New pressure-drop model for evaporation R134a datasets

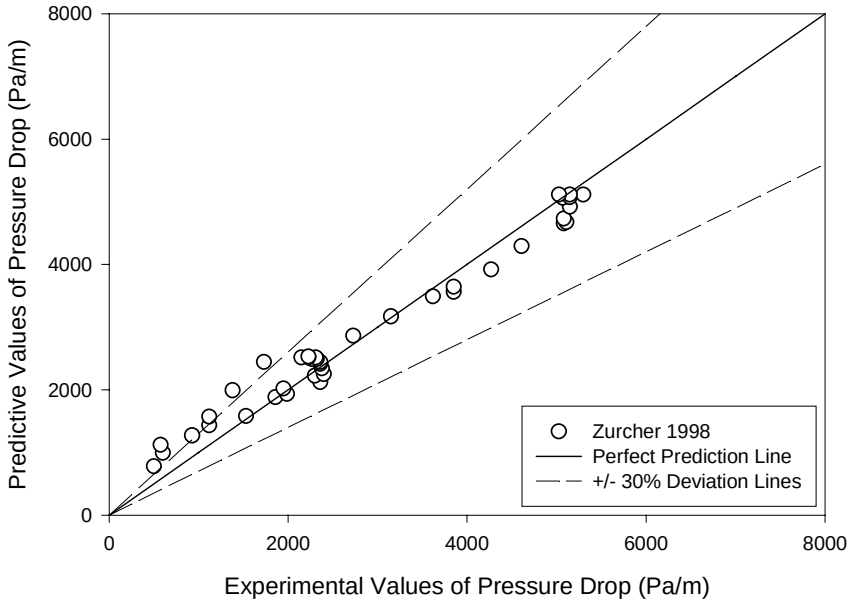

Figure 4.12. New pressure-drop model for an evaporation R407c dataset

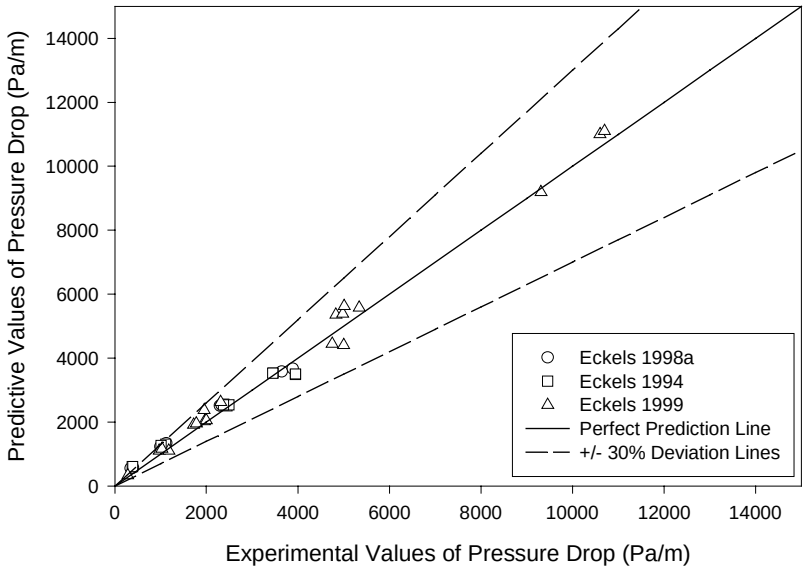

Figure 4.13. New pressure-drop model for condensation R134a datasets

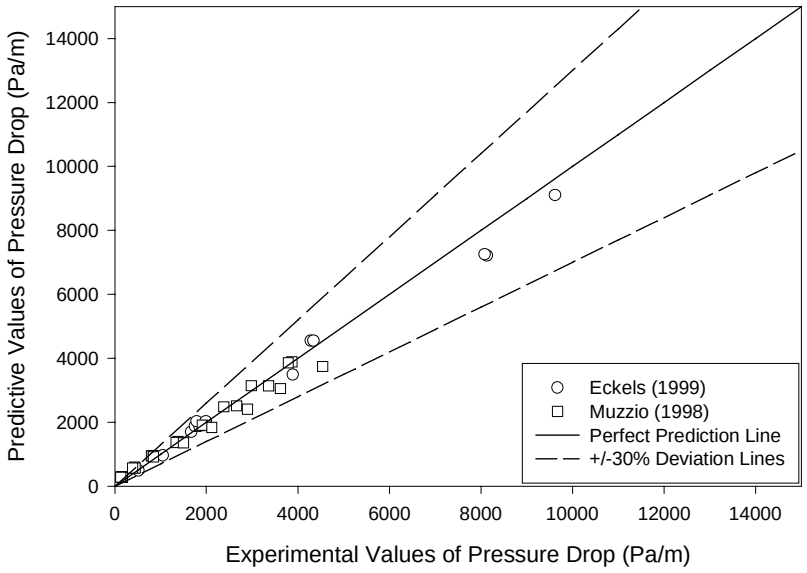

Figure 4.14. New pressure-drop model for condensation R22 datasets

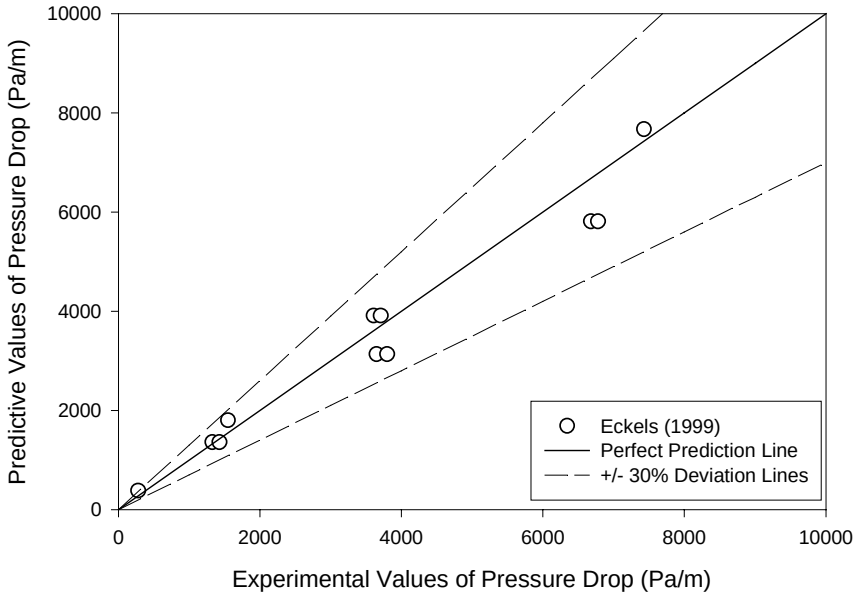

Figure 4.15. New pressure-drop model for a condensation R407c dataset

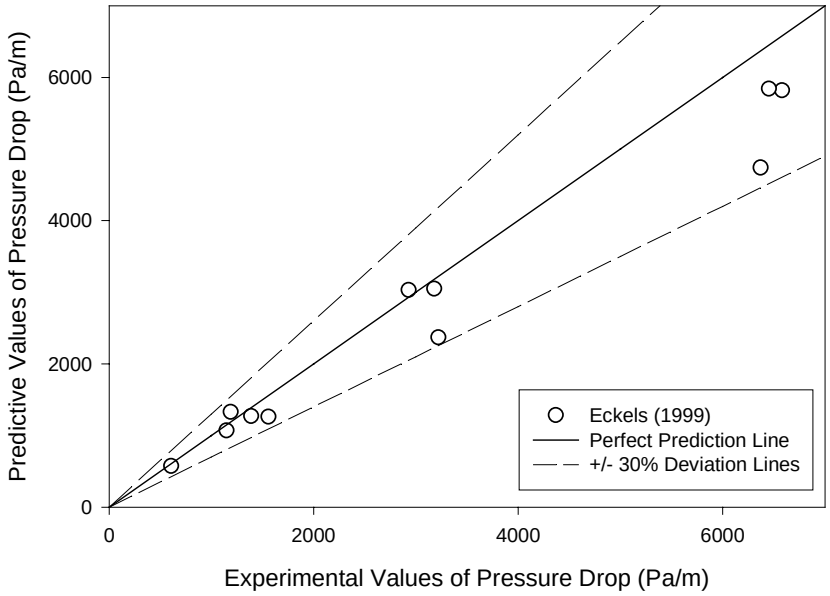

Figure 4.16. New pressure-drop model for a condensation R410A dataset

Further Analysis of the New Pressure-Drop Model

Wolverine Tube, Inc. provides many industries, including the refrigeration and the automotive industries, with copper and copper-alloy tubes. Micro-fin tubes are among the different variations of tubes that are produced by Wolverine Tube, Inc. The company provided five evaporation experimental datasets based on micro-fin tubes for analysis with the new pressure-drop model. These datasets were obtained from refrigerant flows in the Turbo-A micro-fin and the Turbo-A crosscut-fin environments. The Wolverine Tube, Inc. datasets were not used in the development of the new pressure-drop model.

The Turbo-A tube has a d_i of 8.865 mm, a d_o of 9.525 mm, a helix angle of 18^o, a fin height of 0.203 mm, and 60 internal micro-fins. The total length of the test section was 3.66 m. All five evaporation datasets had the saturation temperature and average

vapor quality of 1.67°C and 0.456, respectively. The Turbo-A crosscut tube had similar geometries, except it had a perpendicular cut across the micro-fins. The new pressure-drop model with the *PF* penalty factor does not reflect crosscut micro-fin tubes but, nevertheless, it was applied to experimental data from crosscut micro-fins. Table 4.6 summarizes the prediction results of the new model for the Wolverine Tube, Inc. datasets, and Figures 4.17 to 4.21 illustrate the prediction results on graphs.

Table 4.6. Prediction results for Wolverine Tube, Inc. evaporation datasets

Refrigerant	Tube Geometry	MAD (%)
R22	Turbo-A	5.95
R22	Turbo-A Crosscut	16.59
R410A	Turbo-A	17.05
R410A	Turbo-A Crosscut	25.28
R407c	Turbo-A Crosscut	25.61

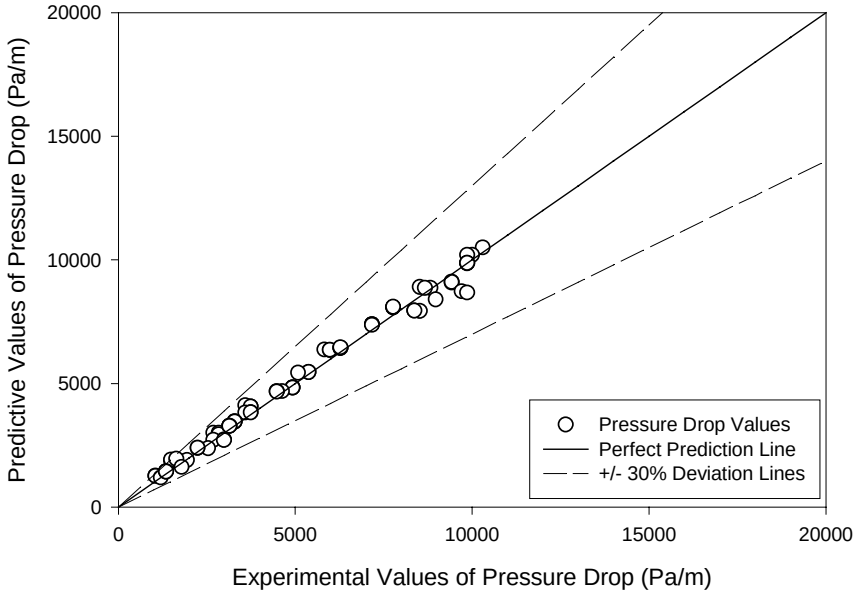

Figure 4.17. New pressure-drop model for an evaporation R22 Turbo-A dataset

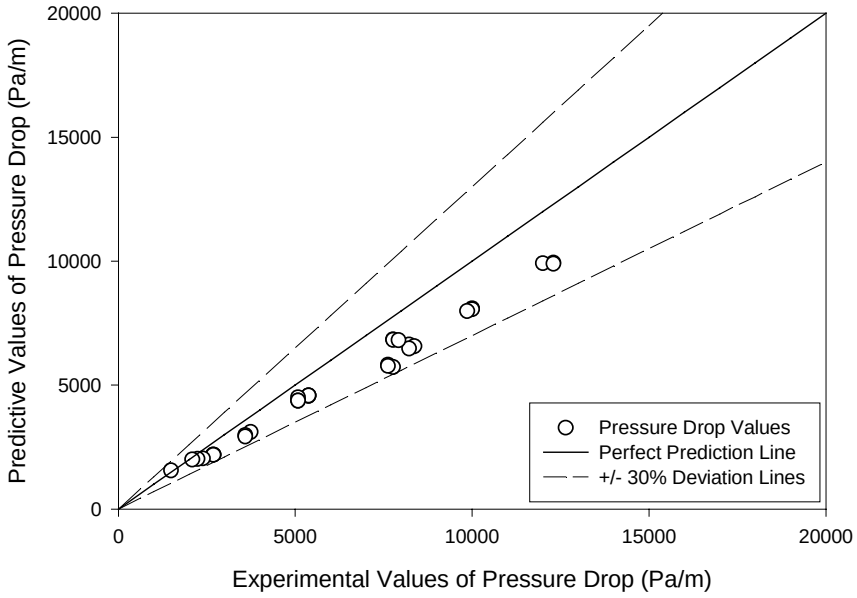

Figure 4.18. New pressure-drop model for an evaporation R22 Turbo-A crosscut dataset

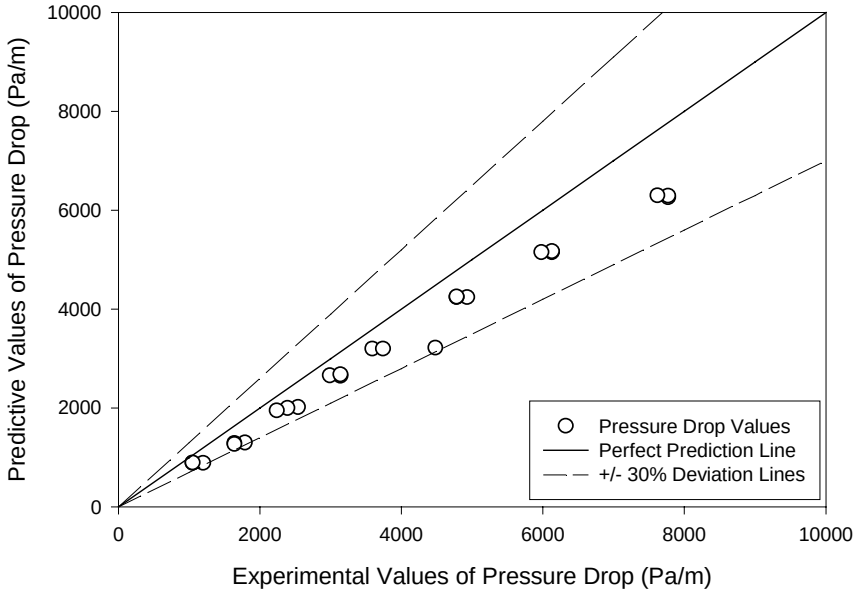

Figure 4.19. New pressure-drop model for an evaporation R410A Turbo-A dataset

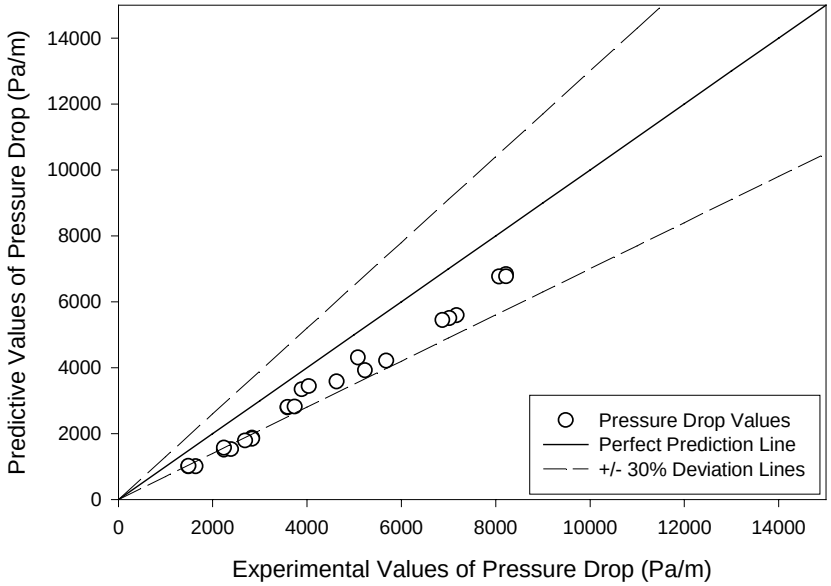

Figure 4.20. New pressure-drop model for an evaporation R410A Turbo-A crosscut dataset

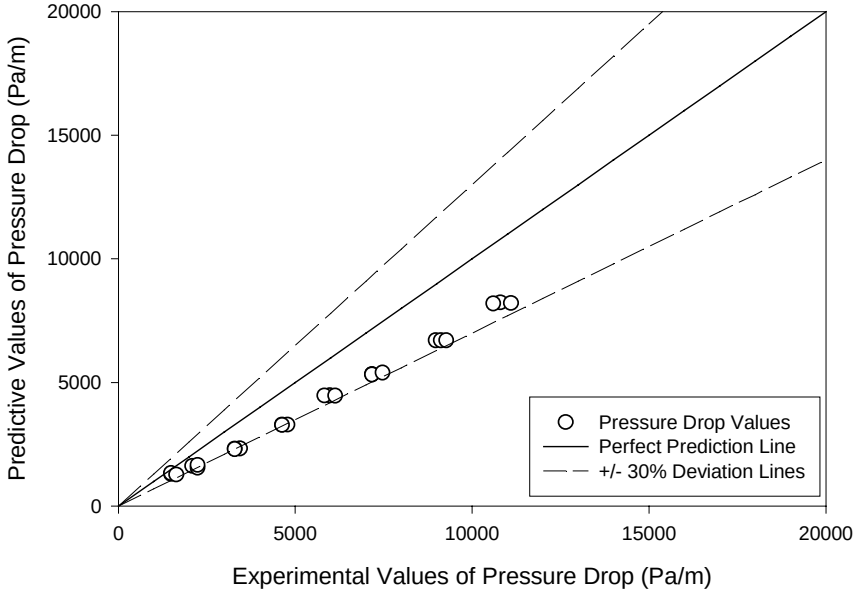

Figure 4.21. New pressure-drop model for an evaporation R407c Turbo-A crosscut dataset

Five condensation experimental datasets from Wolverine Tube, Inc. were also analyzed with the new pressure-drop model. These datasets were obtained from refrigerant flows in the Turbo-A micro-fin and the Turbo-A crosscut-fin environment.

The two tubes used in the condensation pressure-drop measurements were similar to the tubes used in the evaporation pressure-drop measurements. The Turbo-A tube has a d_i of 8.865 mm, a d_o of 9.525 mm, a helix angle of 18^o, a fin height of 0.203 mm, and 60 internal micro-fins. The total length of the test section was 3.66 m. All five evaporation datasets had the saturation temperature and average quality of 37.78^oC and 0.5, respectively. The Turbo-A crosscut tube had similar geometries except it now had a perpendicular cut across the micro-fins. Similar to the evaporation pressure-drop analysis discussed above, the pressure-drop model with the *PF* penalty factor was applied to experimental data from crosscut micro-fins. Table 4.7 tabulates the prediction results for the Wolverine Tube, Inc. datasets, and Figures 4.22 to 4.26 presents the prediction results on graphs.

Table 4.7. Prediction results for Wolverine Tube, Inc. condensation datasets

Refrigerant	Tube Geometry	MAD (%)
R22	Turbo-A	30.09
R22	Turbo-A Crosscut Dataset A	27.58
R22	Turbo-A Crosscut Dataset B	13.11
R410A	Turbo-A	28.25
R410A	Turbo-A Crosscut	28.36

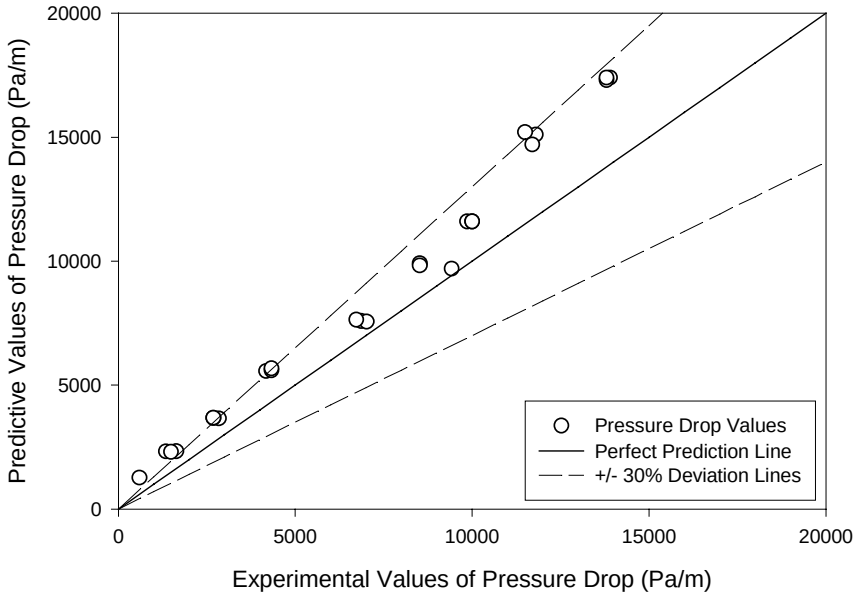

Figure 4.22. New pressure-drop model for a condensation R22 Turbo-A dataset

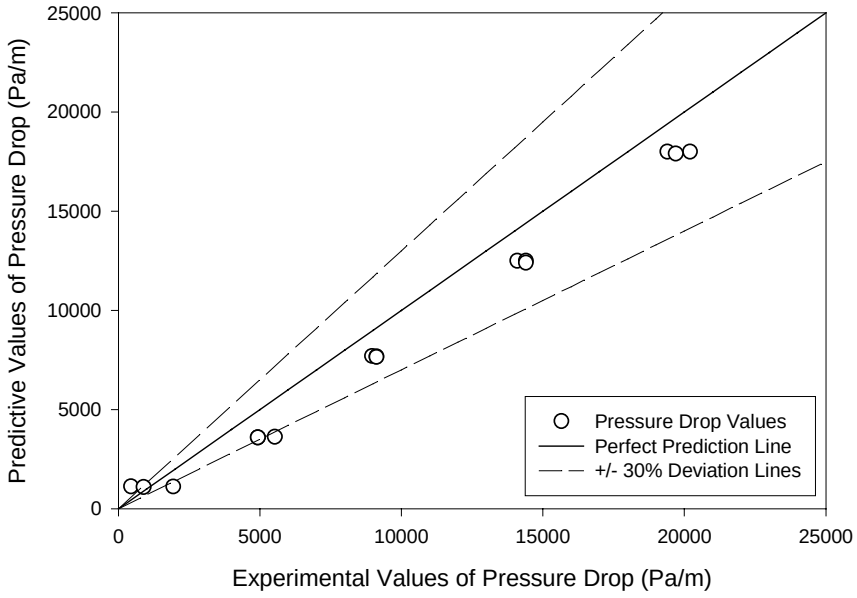

Figure 4.23. New pressure-drop model for condensation R22 Turbo-A crosscut dataset A

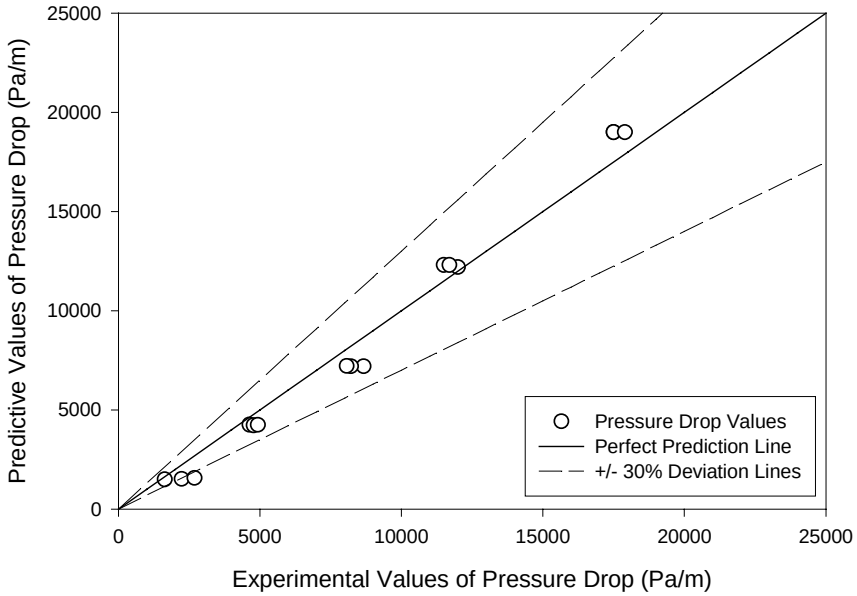

Figure 4.24. New pressure-drop model for condensation R22 Turbo-A crosscut dataset B

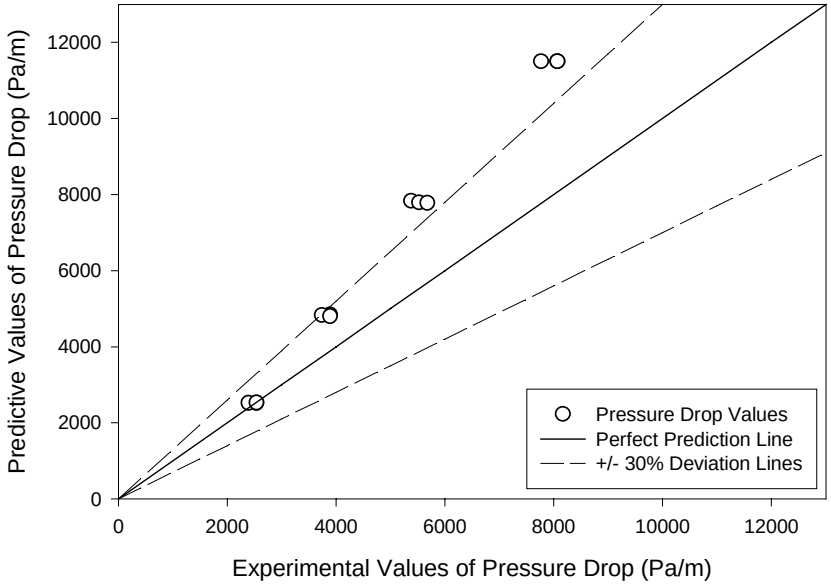

Figure 4.25. New pressure-drop model for a condensation R410A Turbo-A dataset

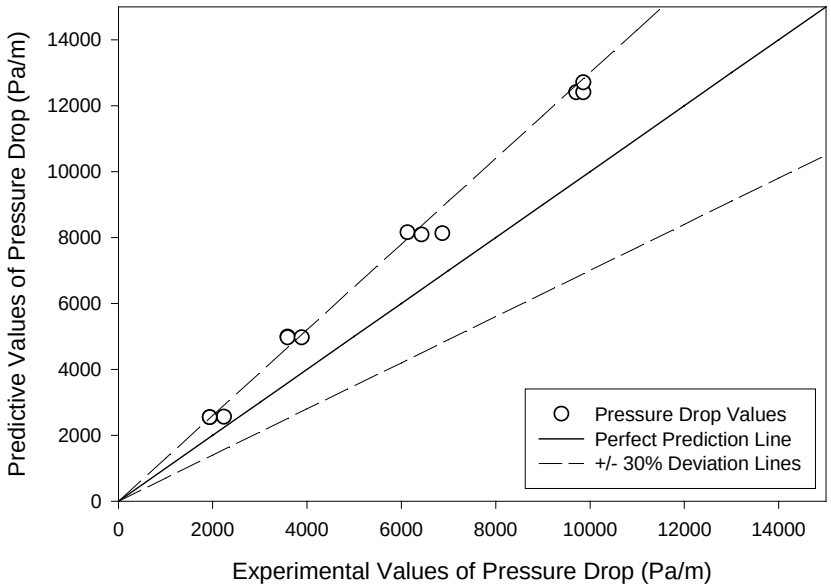

Figure 4.26. New pressure-drop model for a condensation R410A Turbo-A crosscut dataset

The new pressure-drop model produced mean absolute deviations of less than ±30% for all Wolverine Tube, Inc. experimental datasets. The results from the predictions are shown to be consistent and quite accurate. This shows that the model successfully predicts experimental data from Wolverine Tube, Inc.

CHAPTER V

CONCLUSIONS

The main purpose for this research was to obtain a pressure-drop model applicable to both pure refrigerants and refrigerant mixtures flowing in an evaporation or condensation environment inside horizontal micro-fin tubes. Three existing pressure-drop models were chosen for validation with experimental data for pressure-drop measurements, which were compiled from available literature. The three models were the Cavallini et al. (1999) model, the Souza and Pimenta (1995) model, and the Choi et al. (1999) model.

The results obtained from the validation process for the three existing models were fair with some inconsistent results. Thus, a new pressure-drop model based on an existing correlation was devised to obtain better and more consistent predictions with the existing experimental database. Tables 5.1 and 5.2 compare the prediction results of the new pressure-drop model with the other three existing models.

The results obtained from the new model shows a consistent trend of prediction results ranging from 10 to 25% mean absolute deviation. The other models exhibit high deviations with certain datasets and were more inconsistent. The Choi et al.

(1999) model produced good results with condensation datasets, but produced larger deviations with the evaporation datasets. The new model produces consistent predictions with both evaporation and condensation datasets. Additional datasets that were not included in the new model's development process were also tested, and the results obtained were good. This infers that the new model is capable of predicting pressure-drop measurements obtained from different sources. The new pressure-drop model has successfully achieve the preliminary objective of generating more reliable prediction results with lower mean absolute deviations and is capable of predicting pressure drops for different refrigerants, including pure refrigerants and refrigerant mixtures, flowing inside different configurations of micro-fin tubes for both condensation and evaporation.

Table 5.1. Comparison of Models for Condensation Datasets.

Reference	Refrigerant	New Pressure-Drop Model	Cavallini et al. (1999) Model	Souza and Pimenta (1995) Model	Choi et al. (1999) Model
		MAD (%)			
Eckels and Pate (1991)	R12	19.75	19.16	17.45	12.68
Eckels and Pate (1991)	R134a	15.56	24.28	23.54	15.10
Eckels et al. (1994)	R134a	17.36	27.21	21.27	13.40
Eckels et al. (1998a)	R134a	21.33	23.07	17.52	9.78
Eckels et al. (1998b)	R134a	42.93	63.85	53.53	42.97
Eckels et al. (1999)	R134a	9.44	26.96	15.94	10.44
Choi et al. (1999)	R134a	23.17	51.23	16.98	11.32
Eckels et al. (1999)	R22	6.66	29.61	21.35	23.07
Muzzio et al. (1995)	R22	19.24	35.01	24.52	26.42
Muzzio et al. (1998)	R22	23.53	33.34	27.88	19.06
Schlager (1988)	R22	18.10	21.52	31.25	19.47
Schlager et al. (1989)	R22	19.64	31.79	19.28	50.39
Choi et al. (1999)	R32	23.78	45.82	20.11	13.53
Ebisu and Torikoshi (1998)	R407c	15.81	54.51	64.83	50.39
Eckels et al. (1999)	R407c	12.17	26.30	26.73	27.97
Eckels et al. (1999)	R410A	12.12	36.91	27.60	42.15
Choi et al. (1999)	R410A	24.80	48.81	20.41	14.74

Table 5.2. Comparison of Models for Evaporation Datasets.

Reference	Refrigerant	New Pressure-Drop Model	Cavallini et al. (1999) Model	Souza and Pimenta (1995) Model	Choi et al. (1999) Model
		MAD (%)			
Eckels and Pate (1991)	R12	10.30	33.31	46.24	4.70
Bogart and Thors (1999)	R134a	21.51	24.22	35.09	49.48
Eckels and Pate (1991)	R134a	10.64	31.67	41.85	14.66
Eckels et al. (1998a)	R134a	9.90	30.66	8.87	23.40
Eckels et al. (1998b)	R134a	27.05	52.70	34.28	26.25
Bogart and Thors (1999)	R22	39.27	50.24	46.68	22.08
Hitachi Cable Ltd (1987)	R22	10.99	32.20	91.01	28.87
Muzzio et al. (1998)	R22	20.98	21.92	22.43	13.15
Schlager (1988)	R22	13.71	24.46	23.08	15.92
Schlager et al. (1989)	R22	11.14	18.63	26.40	70.75
Yasuda et al. (1990)	R22	11.63	29.24	93.72	145.70
Bogart and Thors (1999)	R407c	51.91	62.78	59.76	39.52
Ebisu and Torikoshi (1998)	R407c	22.18	14.60	74.38	55.57

REFERENCES CITED

[1] Bogart, J.; and Thors, P. In-tube evaporation of R-22 and three of its alternatives in a 15.88 mm internally enhanced tube, *Enhanced Heat Transfer,* 6, 1999, pp. 317-326.

[2] Cavallini A.; Del Col D.; Doretti L.; Longo G.A.; and Rossetto L. A new computational procedure for heat transfer and pressure-drop during refrigerant condensation inside enhanced tubes, *Enhanced Heat Transfer*, 6, 1999, pp. 441-456.

[3] Cavallini A.; Del Col D.; Doretti L.; Longo G.A.; and Rossetto L. Heat transfer and pressure-drop during condensation of refrigerants inside horizontal enhanced tubes, *International Journal of Refrigeration*, 23, 2000, pp. 4-25.

[4] Cavallini A.; Del Col D.; Doretti L.; Longo G.A.; and Rossetto L. Pressure-drop during condensation and vaporisation of refrigerants inside enhanced tubes, *Heat and Technology*, 15, no.1, 1997, pp. 3-10.

[5] Choi, J.; Kedzierski, M.A.; and Domanski, P.A. A generalized pressure-drop correlation for evaporation and condensation of alternative refrigerants in smooth and micro-fin tubes, *NISTIR 6333*, 1999.

[6] Collier, John G.; and Thome, John R. *Convective Boiling and Condensation*. 3rd Edition; Oxford University Press, 1996.

[7] Christoffersen, B.R.; J.C. Chato; J.P. Wattelet; and A.L. deSouza. Heat transfer and flow characteristics of R22, R32/R125 and R134a in smooth and micro-fin tubes. *ACRC Report TR-47*, Air-Conditioning and Refrigeration Center, University of Illinois, Urbana, 1993.

[8] Ebisu, T.; and Torikoshi, K. Experimental study on evaporation and condensation heat transfer enhancement for R-407C using herringbone heat transfer tube, *ASHRAE Transactions*, 104, no. 2 (1998), pp. 1044-1052.

[9] Eckels, S.J.; Doerr, T.M.; and Pate, M.B. A comparison of the heat transfer and pressure-drop performance of R-134a lubricant mixtures in different diameter smooth tubes and micro-fin tubes, *ASHRAE Transactions*, 104, no. 1 (1998), pp. 376-386.

[10] Eckels, S.J.; Doerr, T.M.; and Pate, M.B. Heat transfer coefficients and pressure-drops for R-134a and an ester lubricant mixture in a smooth tube and a micro-fin tube, *ASHRAE Transactions*, 104, no. 1 (1998), pp. 366-375.

[11] Eckels, S.J.; Doerr, T.M.; and Pate, M.B. In-tube heat transfer and pressure-drop of R-134a and ester lubricant mixtures in a smooth tube and a micro-fin tube: Part 2 – Condensation, *ASHRAE Transactions*, 100, no. 2, (1994), pp. 283-294.

[12] Eckels. S.J.; and Pate, M.B. Evaporation and condensation of HFC-134a and CFC-12 in a smooth tube and a micro-fin tube, *ASHRAE Transactions*, 97, no. 2 (1991), pp. 71-81.

[13] Eckels, S. J.; and Tesene, B.A. A comparison of R-22, R-134a, R-410a, and R-407c condensation performance in smooth and enhanced tubes: Part II, Pressure-drop, *ASHRAE Transactions*, 1999, pp. 442-452.

[14] Friedel, I. Improved friction pressure drop correlations for horizontal and vertical two-phase pipe flow, *European two-phase flow group meet*, Ispra, paper E2, 1979.

[15] Hitachi Cable Ltd. Effect on Performance of Expanding the Thermofin-EX and Thermofin-HEX Tube, *Hitachi Cable, Ltd.*: 14, no. 958 (1987).

[16] Ito, M.; and H. Kimura. Boiling and heat transfer and pressure drop in internal spiral-grooved tubes. *Bull. JSME (22) 171*, 1979, pp. 1251-57.

[17] Kedzierski, M.A.; and Goncalves, J.M. Horizontal convective condensation of alternative refrigerants within a micro-fin tube, *Journal of Enhanced Heat Transfer*, 6, 1999, pp. 161-178.

[18] Kuo, C.; and Wang, C. Evaporation of R-22 in a 7-mm micro-fin tube, *ASHRAE Transactions*, 101, no. 1 (1995), pp. 1055-1061.

[19] Kuo, C.; and Wang, C. Horizontal flow boiling of R22 and R407C in a 9.52 mm micro-fin tube, *Applied Thermal Engineering*, 16, no. 8/9 (1996), pp. 719-731.

[20] Lockhart, R.W.; and Martinelli, R.C. Proposed correlation of data for isothermal two-phase two-component flow in pipes, *Chem. Eng. Prog.*, 45, 1949, 39.

[21] Martinelli,R.C.; and Nelson, D.B. Prediction of pressure drop during forced circulation boiling of water, *Trans. ASME*, 70, 1948, 695.

[22] Montgomery, D. C.; Peck, E. A. *Introduction to Linear Regression Analysis*. 2nd ed.; John Wiley and Sons: New York, 1992.

[23] Morita, H.; Kito, Y.; and Satoh, Y. Recent improvements in small bore inner grooved copper tube, *International Tube Association*, Warwickshire, U.K., no. 9335 (1993).

[24] Muzzio, A.; Niro, A.; and Arosio, S. Heat transfer and pressure-drop during evaporation and condensation of R22 inside 9.52mm O.D. micro-fin tubes of different geometries, *ASHRAE Transactions*, 101, no. 1 (1995), pp. 1055-1061.

[25] Muzzio, A.; Niro, A.; and Arosio, S. Heat transfer and pressure-drop during evaporation and condensation of R22 inside 9.52 mm O.D. micro-fin tubes of different geometries, *Enhanced Heat Transfer*, 5, no.1 (1998), pp. 39-52.

[26] Newell, T.A.; and Shah R.K. An assessment of refrigerant heat transfer, pressure-drop, and void fraction effects in micro-fin tubes, *International Journal of HVAC&R Research*, 7, no. 2 (April 2001), pp. 125-153.

[27] Nidegger, E.; Thome, J.R.; and Favrat, D. Flow boiling and pressure-drop measurements for R-134a/Oil mixtures. Part 1: Evaporation in a micro-fin tube, *HVAC&R Research*, 3, no. 1 (1997), pp. 38-53.

[28] Pierre, B. Flow resistance with boiling refrigerants - Part 1, *ASHRAE Journal*, 6, no. 9, 1964, pp. 58-65.

[29] Rouhani, S.Z. Sub-cooled void fraction, *AB Atomenergi Sweden*, internal report, AE-RTV841, 1969.

[30] Schlager, L.M. The effect of oil on heat transfer and pressure-drop during evaporation and condensation of refrigerant inside augmented tubes. Ph. D. Dissertation, Iowa State University, Ames, Iowa, 1988.

[31] Schlager, L.M.; Pate, M.B.; and Bergles, A.E. Heat transfer and pressure-drop during evaporation and condensation of R22 in horizontal micro-fin tube, *International Journal of Refrigeration*, 12, 1989, pp. 6

[32] Souza, A.; and Pimenta, M. Prediction of pressure-drop during horizontal two-phase flow of pure and mixed refrigerants, *Cavitation and Multiphase Flow*, 210, 1995, pp. 161- 171.

[33] Tong, L.S. *Boiling heat transfer and two-phase flow.* John Wiley & Sons Inc., New York, 1967.

[34] Wallis, G.B. *One-dimensional two-phase flow.* McGraw Hill, Inc., New York, 1969.

[35] Yasuda, K.; Ohizumi, K.; Hori, M.; and Kawamata, O. Development of condensing "Thermofin-HEX-C Tube", *Hitachi Cable Review*, no. 9 (August 1990).

[36] Zivi, S.M. Estimation of steady-state steam void fraction by means of the principle of minimum entropy production, *Journal of Heat and Mass Transfer*, 86, 1964, pp. 247-252.

[37] Zurcher, O.; Thome, J.R.; and Favrat, D. In-tube flow boiling of R-407C and R-407C/oil mixtures. Part I: Micro-fin tube, *HVAC&R Research*, 4, no. 4 (1998), pp. 347-372.

APPENDIX A

MathCAD Files

Sample Data File

Experimental Data from
Yasuda 1990 R22
Thermofin-HEX

R22

Define flow condition

$T_{sat} := 0.6 + 273.15$ K $\qquad P_{sat} := 0.51 \cdot 10^{6}$ Pa

$G := 150..310$ $\quad kg \cdot m^{-2} \cdot s^{-1}$

$g := 9.807$ $\quad m \cdot s^{-2}$

Import property table generated by REFPROP.

TABLE

:=

C:\..\R22.TXT

Calculate thermodynamics and transport properties by Mathcad cubic spline interpolation:

Reference:C:\MFT Project\Pressure Drop\Correlation\Properties.mcd

Define tube configuration:

Tube Material ==> Copper

Tube properties,

$d_o := 9.52 \cdot 10^{-3}$ m $\qquad th := 0.39 \cdot 10^{-3}$ m

$d_i := d_o - 2 \cdot th$ $\qquad d_i = 8.74 \times 10^{-3}$ m

Micro-fin properties, (assumption: equal triangular micro-fin)

$\gamma := 18 \cdot deg$ $\qquad n_f := 60$ $\qquad p := \frac{\pi \cdot d_i}{n_f}$ m

$L := 3.05$ m $\qquad e := 0.2 \cdot 10^{-3}$ m

Experimental Data

$x_{in} := 0.8$

$x_{out} := 0.4$

$x := (x_{in} + x_{out}) \cdot 0.5$ $x = 0.6$

$\Delta x := |x_{out} - x_{in}|$ $\Delta x = 0.4$

$Data_{exp} :=$

	0	1
0	152.74	2497.16
1	200.1	3851.46
2	251.4	5845.08
3	300.29	8378.04

$\Delta P\_exp\_1 := Data_{exp}^{\langle 1 \rangle}$

$G_{exp\_1} := Data_{exp}^{\langle 0 \rangle}$

Sample Property File

Cubic Spline interpolation for all required properties.

$P := \text{TABLE}^{\langle 0 \rangle}$ $T_{l\_} := \text{TABLE}^{\langle 1 \rangle}$

$\rho_{l\_} := \text{TABLE}^{\langle 2 \rangle}$ $\rho_{v\_} := \text{TABLE}^{\langle 3 \rangle}$ $i_{l\_} := \text{TABLE}^{\langle 4 \rangle}$ $i_{v\_} := \text{TABLE}^{\langle 5 \rangle}$

$c_{p\_l\_} := \text{TABLE}^{\langle 6 \rangle}$ $c_{p\_v\_} := \text{TABLE}^{\langle 7 \rangle}$ $\mu_{l\_} := \text{TABLE}^{\langle 8 \rangle}$ $\mu_{v\_} := \text{TABLE}^{\langle 9 \rangle}$

$k_{l\_} := \text{TABLE}^{\langle 10 \rangle}$ $k_{v\_} := \text{TABLE}^{\langle 11 \rangle}$ $\sigma_{\_} := \text{TABLE}^{\langle 12 \rangle}$

$\rho_{l\_s} := \text{cspline}(P, \rho_{l\_})$ $\rho_{v\_s} := \text{cspline}(P, \rho_{v\_})$ $i_{l\_s} := \text{cspline}(P, i_{l\_})$ $i_{v\_s} := \text{cspline}(P, i_{v\_})$

$c_{p\_l\_s} := \text{cspline}(P, c_{p\_l\_})$ $c_{p\_v\_s} := \text{cspline}(P, c_{p\_v\_})$ $\mu_{l\_s} := \text{cspline}(P, \mu_{l\_})$ $\mu_{v\_s} := \text{cspline}(P, \mu_{v\_})$

$k_{l\_s} := \text{cspline}(P, k_{l\_})$ $k_{v\_s} := \text{cspline}(P, k_{v\_})$ $\sigma_s := \text{cspline}(P, \sigma_{\_})$

$T_{l\_s} := \text{cspline}(P, T_{l\_})$

$\rho_l(PP) := \text{interp}(\rho_{l\_s}, P, \rho_{l\_}, PP)$ $\rho_v(PP) := \text{interp}(\rho_{v\_s}, P, \rho_{v\_}, PP)$

$i_l(PP) := \text{interp}(i_{l\_s}, P, i_{l\_}, PP)$ $i_v(PP) := \text{interp}(i_{v\_s}, P, i_{v\_}, PP)$

$c_{p\_l}(PP) := \text{interp}(c_{p\_l\_s}, P, c_{p\_l\_}, PP)$ $c_{p\_v}(PP) := \text{interp}(c_{p\_v\_s}, P, c_{p\_v\_}, PP)$

$\mu_l(PP) := \text{interp}(\mu_{l\_s}, P, \mu_{l\_}, PP)$ $\mu_v(PP) := \text{interp}(\mu_{v\_s}, P, \mu_{v\_}, PP)$

$k_l(PP) := \text{interp}(k_{l\_s}, P, k_{l\_}, PP)$ $k_v(PP) := \text{interp}(k_{v\_s}, P, k_{v\_}, PP)$

$\sigma(PP) := \text{interp}(\sigma_s, P, \sigma_{\_}, PP)$

$T_l(PP) := \text{interp}(T_{l\_s}, P, T_{l\_}, PP)$

Define fluid properties: (Source: REFPROP 6.01)

$\rho_l := \rho_l\left(P_{sat}\cdot 10^{-6}\right)$ $\rho_l = 1279.016$ $kg\cdot m^{-3}$

$\rho_v := \rho_v\left(P_{sat}\cdot 10^{-6}\right)$ $\rho_v = 21.726$ $kg\cdot m^{-3}$

$c_{p\_l} := c_{p\_l}\left(P_{sat}\cdot 10^{-6}\right)\cdot 10^{3}$ $c_{p\_l} = 1.171\times 10^{3}$ $J\cdot kg^{-1}\cdot K^{-1}$

$c_{p\_v} := c_{p\_v}\left(P_{sat}\cdot 10^{-6}\right)\cdot 10^{3}$ $c_{p\_v} = 742.116$ $J\cdot kg^{-1}\cdot K^{-1}$

$\mu_l := \mu_l\left(P_{sat}\cdot 10^{-6}\right)\cdot 10^{-6}$ $\mu_l = 216.477\left(10^{-6}\right)$ $Pa\cdot s$

$\mu_v := \mu_v\left(P_{sat}\cdot 10^{-6}\right)\cdot 10^{-6}$ $\mu_v = 11.534\left(10^{-6}\right)$ $Pa\cdot s$

$k_l := k_l\left(P_{sat}\cdot 10^{-6}\right)$ $k_l = 0.095$ $W\cdot m^{-1}\cdot K^{-1}$

$k_v := k_v\left(P_{sat}\cdot 10^{-6}\right)$ $k_v = 0.009$ $W\cdot m^{-1}\cdot K^{-1}$

$i_{fg} := \left(i_v\left(P_{sat}\cdot 10^{-6}\right) - i_l\left(P_{sat}\cdot 10^{-6}\right)\right)\cdot 10^{3}$ $i_{fg} = 204.456\left(10^{3}\right)$ $J\cdot kg^{-1}$

$\sigma := \sigma\left(P_{sat}\cdot 10^{-6}\right)$ $\sigma = 0.012$ $N\cdot m^{-1}$

$Pr_l := \dfrac{\mu_l\cdot c_{p\_l}}{k_l}$ $Pr_l = 2.683$

$\nu_l := \rho_l^{-1}$ $\nu_l = 7.819\times 10^{-4}$ $m^{3}\cdot kg^{-1}$

$\nu_v := \rho_v^{-1}$ $\nu_v = 0.046$ $m^{3}\cdot kg^{-1}$

$\nu := \left(\nu_l + \nu_v\right)\cdot 0.5$ $\nu = 0.023$ $m^{3}\cdot kg^{-1}$

Sample Calculation

Correlation for Refrigerant flowing inside Micro-fin Tubes

R22

Source of Correlations:
1. Friedel

Source of Experimental Data:
1. Yasuda 1990 R22
Thermofin HEX OD 9.52

Import experimental data:

Define flow condition, fluid properties (REFPROP 6.01), tube configuration:

Reference:C:\MFT Project\Pressure Drop\Data Evaporation R22 Yasuda 1990 HEX-C Tube 1.mcc

Import Friedel model:

Reference:C:\MFT Project\Pressure Drop\Friedel Correlation\Friedel Model with PF.mcd

Define range of mass flux, $G := 150..310$ $kg \cdot m^{-2} \cdot s^{-1}$

Define average quality, $x = 0.6$ $\Delta x = 0.4$

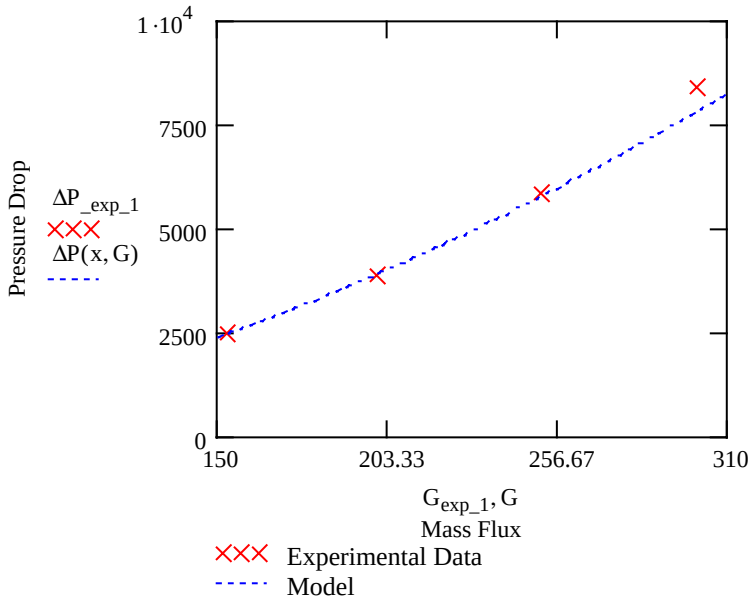

$N := \text{length}(\Delta P\_exp\_1)$ $N = 4$

$$MAD := \frac{1}{N} \cdot \sum \overrightarrow{\frac{\left|\Delta P\_exp\_1 - \Delta P(x, G_{exp\_1})\right|}{\Delta P\_exp\_1}}$$

MAD = 2.661%

File $WRITEPRN("temp1.dat") := \overrightarrow{\Delta P(x, G_{exp\_1})}$ $WRITEPRN("temp2.dat") := \Delta P\_exp\_1$

Plot for $\Delta P_{predicted}$ versus $\Delta P_{experiment}$

$\Delta P_{predicted} := READPRN("temp1.dat")$

$\Delta P_{experiment} := READPRN("temp2.dat")$

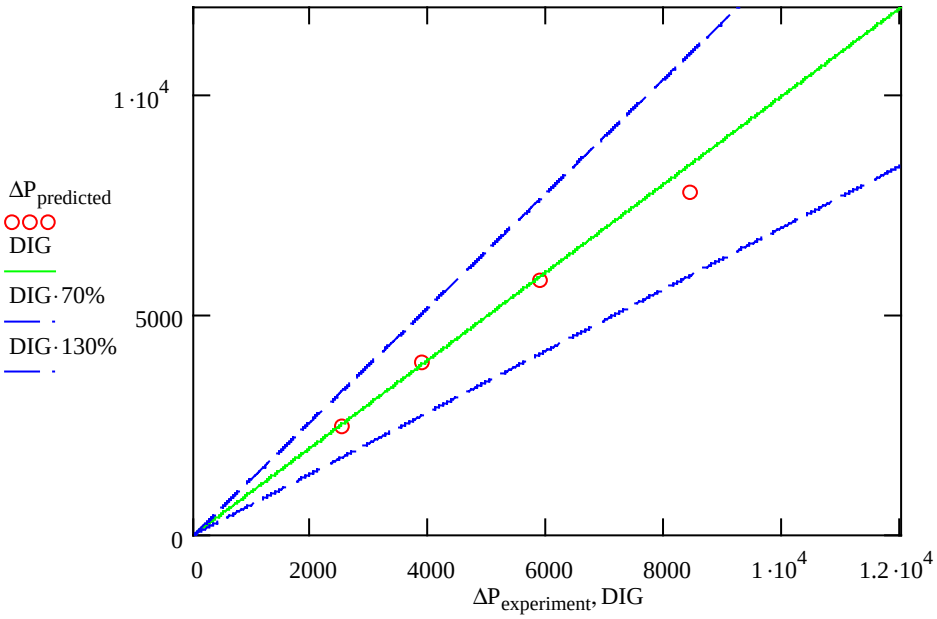

$N := length(\Delta P_{predicted})$

$N = 4$

$$MAD := \frac{1}{N} \cdot \sum \overrightarrow{\frac{|\Delta P_{experiment} - \Delta P_{predicted}|}{\Delta P_{experiment}}}$$

MAD = 2.658%

APPENDIX B

MathCAD Model File for the Cavallini et al. (1999) Pressure-Drop Model

Define Roughness Factor:

$$e_{over\_d} := \frac{A \cdot \left(\frac{e}{d_i}\right)}{0.1 + \cos(\gamma)}$$

A = 0.18 for condensation
A = 0.30 for evaporation

Define single-phase friction factors:

$$f_{LO1}(G) := \begin{cases} 0.079\left(\frac{G \cdot d_i}{\mu_l}\right)^{-0.25} & \text{if } \frac{G \cdot d_i}{\mu_v} > 2000 \\ \frac{16}{\left(\frac{G \cdot d_i}{\mu_l}\right)} & \text{if } \frac{G \cdot d_i}{\mu_v} \le 2000 \end{cases} \qquad f_{LO2} := \frac{\left(1.74 - 2 \cdot \log\left(2 \cdot e_{over\_d}\right)\right)^{-2}}{4}$$

$$f_{GO1}(G) := \begin{cases} 0.079\left(\frac{G \cdot d_i}{\mu_v}\right)^{-0.25} & \text{if } \frac{G \cdot d_i}{\mu_v} > 2000 \\ \frac{16}{\left(\frac{G \cdot d_i}{\mu_v}\right)} & \text{if } \frac{G \cdot d_i}{\mu_v} \le 2000 \end{cases} \qquad f_{GO2} := \frac{\left(1.74 - 2 \cdot \log\left(2 \cdot e_{over\_d}\right)\right)^{-2}}{4}$$

Choose higher value for f_{LO} and f_{GO}:

$$f_{LO}(G) := \begin{cases} f_{LO1}(G) & \text{if } f_{LO1}(G) > f_{LO2} \\ f_{LO2} & \text{otherwise} \end{cases}$$

$$f_{GO}(G) := \begin{cases} f_{GO1}(G) & \text{if } f_{GO1}(G) > f_{GO2} \\ f_{GO2} & \text{otherwise} \end{cases}$$

Evaluate Friedel Correlation:

$$E(x, G) := (1 - x)^2 + x^2 \cdot \frac{\left(\rho_l \cdot f_{GO}(G)\right)}{\left(\rho_v \cdot f_{LO}(G)\right)}$$

$$Ff(x) := x^{0.78} \cdot (1 - x)^{0.224}$$

Define phase change number:

$$H := \left(\frac{\rho_l}{\rho_v}\right)^{0.91} \cdot \left(\frac{\mu_v}{\mu_l}\right)^{0.19} \cdot \left(1 - \frac{\mu_v}{\mu_l}\right)^{0.7}$$

Define homogenous density:

$$\rho_m(x) := \frac{\rho_l \cdot \rho_v}{\left[x \cdot \rho_l + (1 - x) \cdot \rho_v\right]}$$

Define Weber Number:

$$We(x, G) := \frac{G^2 \cdot d_i}{\rho_m(x) \cdot \sigma}$$

Define Froude Number:

$$Fr(x, G) := \frac{G^2}{g \cdot d_i \cdot \rho_m(x)^2}$$

Define the Friedel two-phase multiplier:

$$\Phi_{LO}(x, G)^2 = E(x, G) + \frac{(3.24\, Ff(x) \cdot H)}{\left(Fr(x, G)^{0.045} \cdot We(x, G)^{0.035}\right)}$$

Define frictional component of pressure drop:

$$\Delta P_f(x, G) := \left[E(x, G) + \frac{(3.24 Ff(x) \cdot H)}{\left(Fr(x, G)^{0.045} \cdot We(x, G)^{0.035}\right)}\right] \cdot 2 \cdot f_{LO}(G) \cdot \frac{G^2}{d_i \cdot \rho_l}$$

Define Rouhani's Model (void fraction):

$$C_{o1}(x,G) := 1 + 0.2\cdot(1-x)\cdot\left(\frac{g\cdot d_i\cdot \rho_l^{\,2}}{G^2}\right)^{\frac{1}{4}}$$

$$\mu_{g1}(x) := 1.18\cdot(1-x)\cdot\left[\sigma\cdot g\cdot\frac{(\rho_l-\rho_v)}{\rho_l^{\,2}}\right]^{\frac{1}{4}}$$

$$\varepsilon(x,G) := \frac{(x\cdot\rho_l)}{\left[\left(C_{o1}(x,G)\right)\cdot\left[x\cdot\rho_l + (1-x)\cdot\rho_v\right] + \left(\frac{\rho_l\cdot\rho_v\cdot\mu_{g1}(x)}{G}\right)\right]}$$

$$C_o(x,G) := \begin{cases} 0 & \text{if } \varepsilon(x,G) < 0.1 \\ C_{o1}(x,G) & \text{otherwise} \end{cases}$$

$$\varepsilon(x,G) := \frac{(x\cdot\rho_l)}{\left[\left(C_o(x,G)\right)\cdot\left[x\cdot\rho_l + (1-x)\cdot\rho_v\right] + \left(\frac{\rho_l\cdot\rho_v\cdot\mu_{g1}(x)}{G}\right)\right]}$$

Define acceleration pressure drop:

$$\Delta P_a(x,G) := G^2\cdot\frac{\left[\frac{x^2}{\rho_v\cdot\varepsilon(x,G)} + \frac{(1-x)^2}{\rho_l\cdot(1-\varepsilon(x,G))}\right]}{L}$$

Compute total pressure drop:

$$\Delta P(x,G) := \Delta P_f(x,G) - \Delta P_a(x,G)$$

(ΔP_a is added to frictional component in evaporation pressure drop)

APPENDIX C

MathCAD Model File for the Souza and Pimenta (1995) Pressure-Drop Model

Define single-phase liquid friction factor:

$$f_{LO}(G) := \begin{cases} 0.079\left(\frac{G \cdot d_i}{\mu_l}\right)^{-0.25} & \text{if } \frac{G \cdot d_i}{\mu_l} > 2000 \\ \frac{16}{\left(\frac{G \cdot d_i}{\mu_l}\right)} & \text{if } \frac{G \cdot d_i}{\mu_l} \le 2000 \end{cases}$$

Define Christoffersen (1993) PF Multiplier:

$$PF := \begin{cases} 1.55 & \text{if } \frac{\rho_v}{\rho_l} < 0.01 \\ \left[1.71 - 17.5 \cdot \left(\frac{\rho_v}{\rho_l}\right)\right] & \text{if } 0.01 \le \left(\frac{\rho_v}{\rho_l}\right) < 0.03 \\ 1.19 & \text{otherwise} \end{cases}$$

Define Martinelli Parameter:

$$Xtt(x) := \left(\frac{1-x}{x}\right)^{0.875} \cdot \left(\frac{\rho_v}{\rho_l}\right)^{0.5} \cdot \left(\frac{\mu_l}{\mu_v}\right)^{0.125}$$

Define Property Index:

$$\Gamma := \left(\frac{\rho_l}{\rho_v}\right)^{0.5} \cdot \left(\frac{\mu_v}{\mu_l}\right)^{0.125}$$

Define Souza and Pimenta two-phase multiplier:

$$\phi_{LO}(x) := \left[1 + \left(\Gamma^2 - 1\right) \cdot x^{1.75} \cdot \left(1 + 0.9524 \cdot \Gamma \cdot Xtt(x)^{0.4126}\right)\right]^{0.5}$$

Define two-phase frictional pressure drop component:

$$\Delta P_f(x, G) := \phi_{LO}(x)^2 \cdot \frac{2 \cdot f_{LO}(G) \cdot G^2 \cdot L}{\rho_l \cdot d_i} \cdot PF$$

Evaluate void fraction:

$$\alpha_{out} := \frac{1}{1 + \left(\frac{1 - x_{out}}{x_{out}}\right) \cdot \left(\frac{\rho_v}{\rho_l}\right)^{0.67}} \qquad \alpha_{in} := \frac{1}{1 + \left(\frac{1 - x_{in}}{x_{in}}\right) \cdot \left(\frac{\rho_v}{\rho_l}\right)^{0.67}}$$

Define acceleration pressure drop:

$$\Delta P_a(G) := G^2 \cdot \left[\left| \frac{x_{out}^{\,2}}{\rho_v \cdot \alpha_{out}} + \frac{(1 - x_{out})^2}{\rho_l \cdot (1 - \alpha_{out})} \right| - \left| \frac{x_{in}^{\,2}}{\rho_v \cdot \alpha_{in}} + \frac{(1 - x_{in})^2}{\rho_l \cdot (1 - \alpha_{in})} \right| \right]$$

Define total pressure drop:

$$\Delta P(x, G) := \Delta P_f(x, G) - \Delta P_a(G)$$

(ΔP_a is added to frictional component in evaporation pressure drop)

APPENDIX D

MathCAD Files for the Choi et al. (1999) Pressure-Drop Model

Sample Data File

R22

Experimental Data from
Yasuda 1990 R22
Thermofin-HEX

Define flow condition

$T_{sat} := 0.6 + 273.15$ K $\qquad P_{sat} := 0.51 \cdot 10^{6}$ Pa

$G := 150..310$ $\quad kg \cdot m^{-2} \cdot s^{-1}$

$g := 9.807 \quad m \cdot s^{-2}$

Import property table generated by REFPROP.

TABLE

:=

C:\..\R22.TXT

Calculate thermodynamics and transport properties by Mathcad cubic spline interpolation:

Reference:C:\MFT Project\Pressure Drop\Correlation\Properties.mcd

Define tube configuration:

Tube Material ==> Copper

Tube properties,

$d_o := 9.52 \cdot 10^{-3}$ m $\qquad th := 0.39 \cdot 10^{-3}$ m

$d_i := d_o - 2 \cdot th \qquad d_i = 8.74 \times 10^{-3}$ m

Micro-fin properties, (assumption: equal triangular micro-fin)

$\gamma := 18 \cdot deg \qquad n_f := 60 \qquad p := \frac{\pi \cdot d_i}{n_f}$ m

$L := 3.05$ m $\qquad e := 0.2 \cdot 10^{-3}$ m

Evaluate hydraulic diameter:

$$b := \frac{\pi \cdot d_i}{n_f} - 2 \cdot e \cdot \tan\left(\frac{\beta}{2}\right) \qquad b = 3.152 \times 10^{-4} \quad m$$

$$A_c := \frac{\pi \cdot d_i^{\,2}}{4} - n_f \cdot e \cdot \tan\left(\frac{\beta}{2}\right) \cdot e \qquad A_c = 0.0610^{-3} \quad m^2$$

$$S_p := b + 2 \cdot \frac{e}{\cos\left(\frac{\beta}{2}\right)} \qquad S_p = 0.74110^{-3} \quad m$$

$$d_h := \frac{4 \cdot A_c \cdot \cos(\gamma)}{n_f \cdot S_p} \qquad d_h = 5.1310^{-3} \quad m$$

Experimental Data

$x_{in} := 0.8$

$x_{out} := 0.4$

$x := (x_{in} + x_{out}) \cdot 0.5 \qquad x = 0.6$

$\Delta x := |x_{out} - x_{in}| \qquad \Delta x = 0.4$

$Data_{exp} :=$

	0	1
0	152.74	2497.16
1	200.1	3851.46
2	251.4	5845.08
3	300.29	8378.04

$\Delta P_{\_exp\_1} := Data_{exp}^{\langle 1 \rangle}$

$G_{exp\_1} := Data_{exp}^{\langle 0 \rangle}$

Sample Model File

Define inlet and outlet specific volume:

$$\nu_{in} := x_{in} \cdot \nu_v + \left(1 - x_{in}\right) \cdot \nu_l$$

$$\nu_{out} := x_{out} \cdot \nu_v + \left(1 - x_{out}\right) \cdot \nu_l$$

Define liquid Reynold's Number:

$$Re_{fo}(G) := \frac{G \cdot d_h}{\mu_l}$$

Define two-phase number:

$$K_f := \frac{\Delta x \cdot i_{fg}}{L \cdot g}$$

Define two-phase friction factor:

$$f_N(G) := 0.00506 \cdot Re_{fo}(G)^{-0.0951} \cdot K_f^{0.1554}$$

Define Choi et al. (1999) Pressure Drop Model:

$$\Delta P(x, G) := \left[\frac{\left[f_N(G) \cdot L \cdot \left(\nu_{out} + \nu_{in}\right)\right]}{d_h} + \left(\nu_{out} - \nu_{in}\right)\right] \cdot G^2$$

APPENDIX E

MathCAD Model File for the New Pressure-Drop Model

Define single-phase friction factor for liquid and gas Phases:

$$f_{LO}(G) := \begin{cases} 0.079\left(\frac{G \cdot d_i}{\mu_l}\right)^{-0.25} & \text{if } \frac{G \cdot d_i}{\mu_v} > 2000 \\ \frac{16}{\left(\frac{G \cdot d_i}{\mu_l}\right)} & \text{if } \frac{G \cdot d_i}{\mu_v} \le 2000 \end{cases}$$

$$f_{GO}(G) := \begin{cases} 0.079\left(\frac{G \cdot d_i}{\mu_v}\right)^{-0.25} & \text{if } \frac{G \cdot d_i}{\mu_v} > 2000 \\ \frac{16}{\left(\frac{G \cdot d_i}{\mu_v}\right)} & \text{if } \frac{G \cdot d_i}{\mu_v} \le 2000 \end{cases}$$

Define phase change number:

$$H := \left(\frac{\rho_l}{\rho_v}\right)^{0.91} \cdot \left(\frac{\mu_v}{\mu_l}\right)^{0.19} \cdot \left(1 - \frac{\mu_v}{\mu_l}\right)^{0.7}$$

Define homogenous density:

$$\rho_m(x) := \frac{\rho_l \cdot \rho_v}{\left[x \cdot \rho_l + (1 - x) \cdot \rho_v\right]}$$

Define Weber Number:

$$We(x, G) := \frac{G^2 \cdot d_i}{\rho_m(x) \cdot \sigma}$$

Define Froude Number:

$$Fr(x, G) := \frac{G^2}{g \cdot d_i \cdot \rho_m(x)^2}$$

Define the Friedel (1979) two-phase multiplier:

$$E(x,G) := (1-x)^2 + x^2 \cdot \frac{\left(\rho_l \cdot f_{GO}(G)\right)}{\left(\rho_v \cdot f_{LO}(G)\right)}$$

$$Ff(x) := x^{0.78} \cdot (1-x)^{0.224}$$

$$\Phi_{LO}(x,G)^2 = E(x,G) + \frac{(3.24 Ff(x) \cdot H)}{\left(Fr(x,G)^{0.045} \cdot We(x,G)^{0.035}\right)}$$

Define the Christoffersen (1993) PF Multiplier:

$$PF := \begin{cases} 1.55 \text{ if } \frac{\rho_v}{\rho_l} < 0.01 \\ \left[1.71 - 17.5\left(\frac{\rho_v}{\rho_l}\right)\right] \text{ if } 0.01 \le \left(\frac{\rho_v}{\rho_l}\right) < 0.03 \\ 1.19 \text{ otherwise} \end{cases}$$

Define frictional component of pressure drop:

$$\Delta P_f(x,G) := \left[E(x,G) + \frac{(3.531 Ff(x) \cdot H)}{\left(Fr(x,G)^{0.023} \cdot We(x,G)^{0.005874}\right)}\right] \cdot 2 \cdot f_{LO}(G) \cdot \frac{G^2}{d_i \cdot \rho_l} \cdot PF$$

Define Rouhani's Model (1969) for evaluating void fraction:

$$C_{o1}(x,G) := 1 + 0.2 \cdot (1-x) \cdot \left(\frac{g \cdot d_i \cdot \rho_l^2}{G^2}\right)^{\frac{1}{4}}$$

$$\mu_{g1}(x) := 1.18 \cdot (1-x) \cdot \left[\sigma \cdot g \cdot \frac{\left(\rho_l - \rho_v\right)}{\rho_l^2}\right]^{\frac{1}{4}}$$

$$\varepsilon(x,G) := \frac{\left(x \cdot \rho_l\right)}{\left[\left(C_{o1}(x,G)\right) \cdot \left[x \cdot \rho_l + (1-x) \cdot \rho_v\right] + \left(\frac{\rho_l \cdot \rho_v \cdot \mu_{g1}(x)}{G}\right)\right]}$$

$$C_o(x,G) := \begin{cases} 0 & \text{if } \varepsilon(x,G) < 0.1 \\ C_{o1}(x,G) & \text{otherwise} \end{cases}$$

$$\varepsilon(x,G) := \frac{\left(x \cdot \rho_l\right)}{\left[\left(C_o(x,G)\right) \cdot \left[x \cdot \rho_l + (1-x) \cdot \rho_v\right] + \left(\frac{\rho_l \cdot \rho_v \cdot \mu_{g1}(x)}{G}\right)\right]}$$

Define acceleration pressure drop:

$$\Delta P_a(x,G) := G^2 \cdot \frac{\left[\frac{x^2}{\rho_v \cdot \varepsilon(x,G)} + \frac{(1-x)^2}{\rho_l \cdot \left(1-\varepsilon(x,G)\right)}\right]}{L}$$

Define total pressure drop:

$$\Delta P(x,G) := \Delta P_f(x,G) - \Delta P_a(x,G)$$

(ΔP_a is added to frictional component in evaporation pressure drop)